In presenting the dissertation as a partial fulfillment of the requirements for an advanced degree from the Georgia Institute of Technology, I agree that the Library of the Institution shall make it available for inspection and circulation in accordance with its regulations governing materials of this type. I agree that permission to copy from, or to publish from, this dissertation may be granted by the professor under whose direction it was written, or, in his absence, by the Dean of the Graduate Division when such copying or publication is solely for scholarly purposes and does not involve potential financial gain. It is understood that any copying from, or publication of, this dissertation which involves potential financial gain will not be allowed without written permission.

PHASE EQUILIBRIA IN THE ARGON-HELIUM AND ARGON-HYDROGEN SYSTEMS

A THESIS

Presented to

The Faculty of the Graduate Division

by

Joseph Chester Mullins

In Partial Fulfillment

of the Requirements for the Degree

Doctor of Philosophy in the School of Chemical Engineering

Georgia Institute of Technology

May, 1965

PHASE EQUILIBRIA IN THE ARGON-HELIUM

AND ARGON-HYDROGEN SYSTEMS

Approved:

Chairman

Date Approved by Chairman: May 26, 1961

ACKNOWLEDGMENTS

Two persons were primarily responsible for directing the author's attention to the original problem as well as for the accomplishment of much of the work presented here: my thesis advisor, Dr. W. T. Ziegler, and my good friend and co-worker, Dr. B. S. Kirk. To Dr. Ziegler the author is indebted for teaching the many things required to accomplish a research project, as well as for providing employment on other projects which also contributed to his research training.

Many of the ideas presented here stem from Dr. Kirk, who built the phase equilibrium apparatus used in this work. Many of the computer programs used in this research were programmed jointly with Dr. Kirk or by him. Particular gratitude is expressed to Dr. Kirk for aiding in the development of the method and for writing the computer program used in this work to predict phase equilibria directly from the Benedict-Webb-Rubin equation of state.

The assistance of the Engineering Experiment Station of the Georgia Institute of Technology is gratefully acknowledged for providing a portion of the funds used in this research, as well as for the use of many of its facilities, and for providing funds to enable the author to attend the Cryogenic Engineering Conference for the past three years.

Part of the funds for this research were provided by the Chemical Engineering Department of the Georgia Institute of Technology. For making available these funds thanks are due Dr. Homer V. Grubb.

The financial help of the Standard Reference Data Center of the National Bureau of Standards in the form of a project to correlate the available argon-helium phase equilibrium data is gratefully acknowledged.

Many people associated with the Rich Electronic Computer Center of the Engineering Experiment Station contributed to this work, but particular gratitude is expressed to Mr. John Gwynn and Mr. Jerry Head for helping with many phases of the computational work.

To his wife, Diane, the author is indebted for her devotion and encouragement during trying times.

TABLE OF CONTENTS

Page

LIST OF TABLES

LIST OF FIGURES

Figure Page

Figure Page

LIST OF SYMBOLS AND ABBREVIATIONS

$\bar{A}$ = matrix in least squares fit of BWR constants.

A_o = empirical parameter in BWR equation.

A_o^L = constant in Eq. (I-18).

A_i^S = constants in Eq. (I-19).

a = empirical parameter in BWR equation; also used as a constant in Eq. (I-3).

a_{ij} = element of matrix $\bar{A}$.

B = second virial coefficient; see Eq. (IV-4).

$\bar{B}$ = vector in least squares fit of BWR constants.

B_o = empirical parameter in BWR equation.

B_o^L, B_o^S = constants defined by Eq. (I-16) and (I-17).

B_K = second virial coefficient calculated from classical Kihara (6-12) core model; see Eq. (IV-23).

B_{RP}^o = second virial coefficient for "simple fluids" reduced by P_c and T_c (also written $B_{RP}^o(T_R)$); see Eq. (IV-30).

B_{RV}^o = second virial coefficient for "simple fluids" reduced by V_c and T_c; see Eq. (IV-33).

B'_{RP} = acentric correction term for second virial coefficient reduced by P_c and T_c (also written $B'_{RP}(T_R)$); see Eq. (IV-31).

B_{CL}^* = reduced classical second virial coefficient from LJ (6-12) intermolecular potential function (also written $B_{CL}^*(T^*)$); see Eq. (IV-9).

B_I^*, B_{II}^*, B_{III}^* = first, second, and third reduced translational quantum corrections for the second virial coefficient from LJ (6-12) intermolecular potential function; see Eq. (IV-17).

B_o^* = reduced translational quantum second virial coefficient for an ideal gas; see Eq. (IV-21).

BWR = Benedict-Webb-Rubin; also see Table 11.

b = empirical parameter in BWR equation; also used as a constant in Eq. (I-3).

b_i = elements in vector $\overline{B}$.

b' = modified BWR constant; see Eq. (A-30).

b_o = volumetric parameter in LJ (6-12) intermolecular potential function; see Eq. (IV-11).

$b_s^{(j)}$ = coefficients for series representation of F_s; see Eq. (IV-25).

C = third virial coefficient; see Eq. (IV-4).

C_j = weighting factors in least squares fit; see Eq. (H-2).

$\overline{C}$ = vector in least squares fit of BWR constants.

C' = see Eq. (IV-48).

C_o = empirical parameter in BWR equation.

C_{RV}^o = third virial coefficient for "simple fluids" reduced by V_c (also written $C_{RV}^o(T_R)$); see Eq. (IV-40).

C_{CL}^* = reduced classical third virial coefficient from LJ (6-12) intermolecular potential function (also written $C_{CL}^*(T^*)$); see Eq. (IV-12).

c = empirical parameter in BWR equation; also used as a constant in Eq. (I-3).

c_j = elements of vector $\overline{C}$.

c_s = molal heat capacity of the saturated condensed phase.

D = fourth virial coefficient; see Eq. (IV-4).

e = energy parameter in LJ (6-12) intermolecular potential function; see Eq. (IV-8).

e/k = energy parameter in LJ (6-12) intermolecular potential function; units are ^oK.

F_1, F_2, F_3 = reduced functions for second virial coefficient from Kihara (6-12) core model; see Eq. (IV-24).

f = fugacity.

$\bar{f}_i$ = fugacity of component i in gas or condensed phase.

G = Gibb's free energy.

g = Gibb's molal free energy.

g^o = Gibb's molal free energy of an ideal gas at 1 atmosphere pressure.

H = Henry's law constant defined by Eq. (F-2).

H^o = Henry's law constant at infinite dilution defined by Eq. (I-8).

$\bar{H}_i$ = partial molal enthalpy of component i.

h = molal enthalpy; also used as peak height on chromatogram.

h_2^o = molal enthalpy of component 2 in the ideal gas state.

Δh_f = heat of fusion.

j = summation index integer.

K_i = constants in BWR equation; see Eq. (A-1); also used as K factor defined by Eq. (E-1).

$\bar{K}$ = Henry's law constant defined by Eq. (I-9).

$\bar{K}^o$ = Henry's law constant at infinite dilution defined by Eq. (F-25).

$\hat{K}$ = Henry's law constant defined by Eq. (F-26).

$\hat{K}^o$ = Henry's law constant at infinite dilution defined by Eq. (F-27).

k_j = constants in BWR equation.

KIHA = Kihara (6-12) core model with an adjusted mixture rule for $(U_o/k)_{12}$; see Table 11.

k = Boltzmann constant = 1.380308×10^{-16} erg/°K molecule.

LJ = Lennard-Jones.

ln = natural (base e) logarithm.

log = common (base 10) logarithm.

LJCL = Lennard-Jones, classical; see Table 11.

LJ3Q = Lennard-Jones with 3 translational quantum correction terms.

LJ2Q = Lennard-Jones with two translational quantum correction terms.

M = molecular weight.

M_o = core parameter in Kihara core model.

m = mass of molecule, M/N_A.

N = a dummy quantity used to represent various equation of state parameters in writing mixture rules; also used as number of points in data set.

N_A = Avogadro's number = 6.0238×10^{23} molecules/gm mole.

n = number of gm moles;

P = total absolute pressure.

P_c = critical pressure.

P_R = P/P_c.

PPG = Pitzer-Prausnitz-Gunn; also see Table 11.

PPGL = see Table 11.

p_{01} = vapor pressure of component 1.

p^o_{01} = triple point pressure of component 1.

R = gas constant = 0.0820574 liter-atm/gm mole-^{o} K.

r = intermolecular distance measured between centers of molecules.

S = entropy.

$\overline{S}_i$ = partial molal entropy of component i.

S_o = core parameter in Kihara core model.

s_1^o = entropy of component 1 in the ideal gas state at one atm pressure.

s = summation index integer; also dummy variable in Eq. (IV-24) and attenuation factor on chromatograph.

T = temperature (^oK).

T^o = triple point temperature.

T_c = critical temperature.

T_R = T/T_c.

T^* = kT/e.

T_{mp}^o = melting temperature of pure argon.

U_o/k = energy parameter in Kihara (6-12) core model; units are ^oK.

U = intermolecular potential energy.

$\overline{U}_7$ = column vector consisting of a_{i7} for i = 1, 2, ..., 6.

V = total volume of gas.

V^∞ = molal volume of gas at pressure sufficiently low to behave ideally.

V_m = molal volume of gas mixture.

V_1 = molal volume of component 1 gas.

V_2 = molal volume of component 2 gas.

$\overline{V}_7$ = row vector consisting of a_{7i} for i = 1, 2, ..., 6.

V_c = critical molal volume.

$\overline{V}_i$ = partial molal volume of component i.

V_o = core parameter in Kihara core model.

V_{01} = molal volume of component 1 gas at its vapor pressure, p_{01}.

v = molal volume of a condensed phase.

X = sum of the squares of the residuals in BWR least squares fit; see Eq. (A-2).

x = mole fraction in condensed phase; also independent variable in general least squares fit.

y = mole fraction in gas phase; also independent variable in general least squares fit.

z = mole fraction in either phase; also dependent variable in general least squares fit.

Z = compressibility factor, PV/nRT; also (U_o/kT) in Kihara core model.

Z_c = $P_c V_c / RT_c$.

GREEK LETTERS

α = empirical parameter in BWR equation.

β = undetermined multiplier in Eq. (A-17).

γ = empirical parameter in BWR equations.

γ_1' = activity coefficient of component 1 in liquid solutions referred to the pure component at the system pressure and temperature.

γ_2' = activity coefficient of component 2 in liquid solutions referred to the infinitely dilute state at the system temperature and pressure.

θ_i = variables in BWR equation; see Eq. (A-1).

Λ = undetermined multiplier in Eq. (A-17).

Λ^* = translational quantum mechanical parameter; see Eq. (IV-18).

λ = undetermined multiplier in Eq. (A-17).

μ = chemical potential.

μ^o = chemical potential of ideal gas at 1 atmosphere pressure.

μ^* = chemical potential of pure liquid.

ρ = molal density; also used as shortest distance between molecular cores in Kihara core model.

ρ_o = shortest distance between molecular cores at minimum potential energy. Parameter in Kihara core model.

σ = length parameter in LJ (6-12) intermolecular potential; see Eq. (IV-8); also standard error of estimate.

Φ = enchancement factor = Py_1/p_{01}.

χ_i = fugacity coefficient of component i; see Eq. (F-28).

Ψ_j = orthogonal functions in least squares fit; see Eq. (H-5).

ω = acentric factor in PPG equations, defined by Eq. (IV-28).

SUBSCRIPTS

1 = argon.

01 = gas at its normal vapor pressure.

2 = helium or hydrogen.

c = critical.

G = gas.

L = liquid.

m = gas mixture.

max = maximum value of variable in data set.

mp = melting point.

i,j,k = 1, 2, or m.

q = 1 or 12.

SUPERSCRIPTS

G = gas.

L = liquid.

S = solid.

C = condensed.

$-\infty$ = infinite dilution.

SUMMARY

This work is concerned with the experimental determination of phase equilibria in the two binary systems, argon-helium and argon-hydrogen, between 68° and 108° K at pressures up to 120 atmospheres, and the examination of a number of methods used to predict or correlate the data.

Determinations of the equilibrium gas phase and liquid phase compositions were carried out in a single-pass, flow type, equilibrium apparatus previously described by Kirk.[42,43] No determination was made of the solid phase composition, though thermodynamic arguments based on the measured locus of the three-phase lines of the two systems and the melting curve of pure argon indicated that the solid phase was essentially pure argon.

In the argon-helium system, gas phase compositions were determined at 68.07°, 74.05°, 77.90°, and 80.06° K at pressures up to 120 atmospheres for the gas-solid region; in the gas-liquid region, compositions are reported for both phases at 86.02°, 91.98°, 97.51° and 108.02° K at pressures up to 120 atmospheres. In the argon-hydrogen system gas compositions are reported at 68.04°, 73.05°, and 79.01° K at pressures up to 110 atmospheres, and compositions for the liquid and gas phases were determined at 86.95°, 94.21°, 99.95° and 105.01° K at pressures up to 120 atmospheres. In the argon-helium system, the gas phase compositions are estimated to be accurate to ± 3 per cent of

the mole fraction of argon; in the argon-hydrogen system the gas phase compositions are estimated to be accurate to ± 2 per cent of the mole fraction of argon. The solubility of helium or hydrogen in liquid argon is estimated to be accurate to ± 2 per cent of the mole fraction. Temperatures are accurate to ± 0.03° K and pressures to ± 1/2 per cent for each point. The three-phase line for each of the two binary systems has been determined for pressures up to 120 atmospheres with an estimated uncertainty of ± 0.05° K and 1/2 per cent of the reported pressure. Four points were determined for the melting curve of pure argon up to 120 atmospheres.

A total of 357 different samples were analyzed for the equilibrium phase compositions; based on these, a selected value is reported at each different pressure measured on an isotherm. These selected experimental phase equilibrium data are represented by analytical functions derived from a least squares surface fit. This method, which utilizes functions made orthogonal with respect to the data sets, was adapted from Bain.[1] The independent variables chosen to represent the thermodynamic surfaces are the difference between the total pressure and the vapor pressure of argon, $(P-p_{01})$, and the reciprocal absolute temperature, $(1/T)$. For the gas phase compositions the dependent variable is $(\text{Log } \Phi)/(P-p_{01})$ where Φ is the enhancement factor, (Py_1/p_{01}), and y_1 is the mole fraction of argon in the gas phase. For the liquid phase compositions, the dependent variable is $\text{Log}(\overline{K})-2$, where $\overline{K}$ is a Henry's law constant, $((P-p_{01})/x_2)$, and x_2 is the mole fraction of either helium or hydrogen in the liquid phase. The average

deviation of (Log Φ)/(P-p_{01}) from the experimental values is 5.3 x 10^{-5} for argon-helium and 2.9 x 10^{-5} for argon-hydrogen. The corresponding values of the standard error of estimate are 6.5 x 10^{-5} for the 47 argon-helium points and 3.7 x 10^{-5} for the 43 argon-hydrogen points. The average deviations of Log $\overline{K}$ from the experimental values is 0.0016 for the 23 helium-argon points and 0.0011 for the 23 hydrogen-argon points. The corresponding values of the standard error of estimates are 0.0021 and 0.0017.

The value of the Henry's law constant at infinite dilution is reported based on the values calculated from the least squares surface fit. In addition, values are reported for the infinitely dilute Henry's law constant defined by $\hat{K} = (Py_2/x_2)$.

A comparison is made of the experimentally determined gas and liquid phase compositions with the results of previous investigators. The data for the solubility of helium in argon found in the present work agree within ± 5 per cent of the data of McCain[51] below 120° K with the exception of his lowest point at 99.92° K which appears to be in error. The Henry's law constants extrapolated to low pressure do not agree with the results of Karasz[36,37] between 84.05° and 87.53° K being about two to three times greater. The gas phase compositions for the argon-helium system do not agree with the dew-point data of McCain which appear to be in error by as much as 40 per cent in the region of overlap (99.74°-108.02° K). The solubility of hydrogen in liquid argon determined in the present work agrees well with the data of Volk and Halsey[78] at low pressures, but differs by as much

as 15 per cent at 101 atm, the highest pressure reported by Volk and Halsey. There appears to be no published data for the equilibrium gas phase composition in the argon-hydrogen system.

The experimentally determined three-phase lines, and liquid phase compositions are used in conjunction with reported values of solid and liquid heat capacity, heat of fusion, and the normal melting curve of pure argon to determine the activity coefficient of argon in the liquid phase along the three-phase line. These values assume that the equilibrium solid consisted of pure argon.

The prediction of gas phase compositions is examined for the Benedict-Webb-Rubin and the virial equations of state assuming that the condensed phase is an ideal solution, and in the solid-gas region that the solid is pure argon. For the argon-helium system the predictions are limited to the virial equation of state.

For the virial equation of state, the second virial coefficients, B_{11} and B_{22}, and the second virial interaction coefficient, B_{12}, are calculated utilizing two theoretical models, the Lennard-Jones (6-12) intermolecular potential function and the Kihara core model with a (6-12) intermolecular potential function. For the Lennard-Jones (6-12) model the second virial coefficient of helium and hydrogen and the interaction coefficient, B_{12}, are calculated from parameters fitted both without and with translational quantum corrections. Translational quantum corrections are made for the second virial coefficient of helium, hydrogen and the second virial interaction coefficient, B_{12}, calculated from the Kihara core model. The third virial coefficient

and all interaction coefficients are calculated from the Lennard-Jones (6-12) classical model.

In addition to the theoretical methods of calculating the second and third virial coefficients, one generalized method attributed to Pitzer and coworkers[60] and later extended by Prausnitz and Gunn[64] for mixtures, is examined. This generalized approach, based on the principle of corresponding states, uses as reducing parameters the critical temperature, critical volume, and the acentric factor. The acentric factor, which is a measure of the deviation from a "simple" fluid, is taken to be zero for hydrogen and helium and a set of pseudo critical values is used for the critical temperature and volume.

Kirk[42] had previously found that the best methods of predicting the enhancement factor of methane in hydrogen were ones which utilized the theoretical methods of determining the second virial coefficients and the second virial interaction coefficient and the Benedict-Webb-Rubin equation for predicting the remaining terms. A number of these "hybrid" methods are examined here for the argon-hydrogen system and found to be in good agreement with the experimental data at all pressures up to 120 atm.

Constants for the Benedict-Webb-Rubin equation of state were evaluated for hydrogen and argon. No previous values have been reported for argon, and none have been previously reported for hydrogen utilizing the recent PVT data of Goodwin and co-workers[31] for para-hydrogen. The constants for argon were obtained by a least squares fit of the compressibility factor, (PV/RT), to the PVT data of Michels et al.,[54] restricted to fit the experimental critical data of

Michels. One of the constants, C_o, is adjusted such that the vapor pressure of argon is predicted by the equation of state down to the triple point (83.81° K). The constants for hydrogen were not restricted to fit the critical point nor adjusted to fit vapor pressure data.

The feasibility of using the Benedict-Webb-Rubin equation of state to predict both the gas and liquid phase equilibrium compositions is examined. It was found that by adjusting slightly the value of γ, one of the equation of state parameters for hydrogen, the equation of state would predict the gas compositions within ± 15 per cent of the mole fraction of argon and the liquid compositions within ± 8 per cent of the mole fraction of hydrogen between 86.95° and 105.01° K and pressures up to 110 atmospheres.

From the experimental values of the enhancement factor and the liquid compositions, the values of the second virial interaction parameter B_{12} were determined for argon-helium and argon-hydrogen. These values are presented at the temperatures of the experimental isotherms and are essentially independent of the values of B_{11} and B_{22}. The values of B_{12} obtained are compared with the various methods used to predict B_{12} and other limited experimental data.

A method of correlating the gas phase compositions of the argon-helium system developed by Mullins and Ziegler[59] is examined and found to predict the gas phase compositions within ± 5 per cent of the mole fraction of argon over the range of temperatures and pressures measured in the present work. This method utilizes the virial equation of state

with the second virial coefficients calculated from the Kihara core model, but with an adjusted mixture rule to obtain the second virial interaction coefficient, B_{12}.

CHAPTER I

INTRODUCTION

Background and Statement of Problem

This work is a continuation of an investigation begun in 1958 in this laboratory of phase equilibria in binary systems in which one component, hereafter referred to as component 1, is well below its critical temperature and the other component, hereafter referred to as component 2, is above its critical temperature. Such a system usually results in very low concentrations of the gas dissolved in the condensed phase, and for many purposes the condensed phase may be considered to be pure component 1. A summary of a number of methods of predicting the gas phase composition in systems in which the condensed phase could be considered pure was presented by Kirk, Ziegler and Mullins[44] at the 1961 Cryogenic Engineering Conference with particular application to the methane-hydrogen system. The results of this investigation pointed out the need for better experimental data in the methane-hydrogen system before an unambiguous choice could be made between the several prediction methods. As a result of this conclusion, Kirk constructed an apparatus for the determination of phase equilibria in binary systems of this type and reported the results for the methane-hydrogen system from about 67° to 116.5° K, at pressures up to 125 atmospheres.[42] His results and the results of Hiza and Herring,[35] done concurrently, agree well. As a result of this agreement, phase equilibria in the methane-hydrogen

system appears to present now a reasonable test for methods of prediction. This agreement also lends confidence to results obtained from the apparatus of Kirk.[42]

The availability of an apparatus which could be used to determine phase equilibria in binary systems with an accuracy of about ± 2 per cent of the mole fraction of the minor component in the liquid and gas phase led quite naturally to a continuation of an experimental program as well as to the program to predict phase equilibria.

Selection of Systems to Study

An ideal system to study would be one with technical, as well as theoretical importance, and one which might be suitable for generalization to other similar systems and ultimately to ternary and multicomponent systems. For example, a study of the binary system argon-hydrogen might lead to an attempt to predict the argon-methane-hydrogen system utilizing the hydrogen-methane data of Kirk.[42] Before predicting phase equilibria in multicomponent systems with much success, one must necessarily be able to describe the binary combinations.

Perhaps more for theoretical than for technical reasons, the two binary systems argon-helium and argon-hydrogen were selected for study. In addition to their theoretical importance, the choice of these two systems was influenced by a number of practical considerations such as the availability of the gases with very high purity at low cost, and the ease with which analyses of the gas samples could be made on the available, existing, analytical apparatus. Several systems of technical as well as theoretical interest, such as the helium-methane, hydrogen-nitro-

gen and helium-nitrogen were discarded because either existing data seemed adequate or else measurements were in progress by other investigators.

The range of the measurements in this work was also based primarily on a number of practical considerations. The argon-helium system was measured along 8 isotherms between 68° and 108° K, and the argon-hydrogen system was measured along 7 isotherms from 68° to 105° K. The maximum pressure, 120 atmospheres was the upper limit which could be easily reached using gas or gas mixtures prepared from commercial cylinders. The upper temperatures were dictated by the ease with which the apparatus could be operated without an additional modification in the form of a recirculating pump. The lower temperature was just slightly higher than the minimum temperature obtainable using liquid nitrogen as the cryogen.

Work Done by Other Investigators

There have been no direct measurements of phase equilibria for the two systems over the temperature and pressure range studied here. McCain[51] in this laboratory, has measured the dew and bubble points for a number of argon-helium mixtures from 99.74° to 150.62° K at pressures up to 70 atmospheres. Karasz, [36,37] has indirectly determined values for the solubility of helium in argon from 84.05° to 87.53° K at partial pressures of helium less than 1 atmosphere. This method involved adding measured quantities of helium to a cell containing a known quantity of argon and agitating until equilibrium was reached. From a material balance, and the assumed ability to accurately calculate

the liquid volume, gas volume and the composition of the gas phase, Karasz calculated the amount of helium dissolved in the liquid argon. Volk and Halsey[78] have determined the solubility of hydrogen in liquid argon from 87° to 140° K at pressures up to 101 atmospheres using a method similar in principle to that of Karasz described above. The agreement of these various reported values with the results of this work are discussed in Chapter III.

General Thermodynamic Relations

Gas-Condensed Phase Enhancement Factor Relations

A useful term for describing the gas phase composition in equilibrium with a condensed phase, in the type of system considered here, is the enhancement factor. The enhancement factor is here defined as

$$\Phi = \frac{Py_1}{p_{01}} \tag{I-1}$$

An exact thermodynamic relation for predicting the enhancement factor is given by Equation (I-2).

$$\ln \Phi = \frac{1}{RT}\int_{p_{01}}^{P} v_1 dP + \frac{1}{RT}\int_{V_{01}}^{\infty}(P-\frac{RT}{V_1})dV_1 + Z_{01} - \ln Z_{01} - 1$$

$$- \frac{1}{RT}\int_{V_m}^{\infty}\left[\left(\frac{\partial P}{\partial n_1}\right)_{V_m,T,n_2} - \frac{RT}{V_m}\right]dV_m + \ln Z_m + \ln \gamma_1' x_1 \tag{I-2}$$

The derivation of this equation is included in Appendix G. This equation has been reported in similar form by a number of authors. Dokoupil et al.[25] have given a similar equation, although they did not show the derivation and also did not include the term $\ln \gamma_1' x_1$, which

accounts for the solubility of the gas in the condensed phase. The derivation of the equation of Dokoupil et al. is given by Kirk.[42] Another similar equation which does include the term $\ln \gamma_1' x_1$ is given by Beattie and Stockmayer.[4] In that equation pressure is the independent variable rather than volume. A derivation of the pressure implicit equation has also been given by Dokoupil et al.[25] except that the condensed phase was assumed to be pure.

Evaluation of Equation (I-2) requires an equation of state for the pure condensed phase, an equation of state for the pure component 1 gas, an equation of state for the gas mixture and a knowledge of the composition and activity of component 1 in the condensed phase. The first integral in Equation (I-2) refers to the molal volume of the pure condensed phase. Here the molal volume of solid argon is assumed incompressible, and the molal volume of pure liquid argon is represented by the following polynomial.

$$v_1 = a + b(P-p_{01}) + c(P-p_{01})^2 \qquad \text{(I-3)}$$

Evaluation of the first integral in Equation (I-2) is then given by

$$\frac{1}{RT}\int_{p_{01}}^{P} v_1 dP = \frac{1}{RT}\left[a(P-p_{01}) + \frac{b}{2}(P-p_{01})^2 + \frac{c}{3}(P-p_{01})^3\right] \qquad \text{(I-4)}$$

The second integral, which involves only pure component 1 gas, and the value of Z_{01}, the compressibility of pure component 1 gas at its normal vapor pressure, p_{01}, were evaluated in all cases considered in this work by a virial equation of state truncated after the third virial coefficient.

$$\frac{PV_1}{RT} = 1 + \frac{B_{11}}{V_1} + \frac{C_{111}}{V_1^2} \qquad \text{(I-5)}$$

Evaluation of the second integral leads to the following result.

$$\frac{1}{RT} \int_{V_{01}}^{\infty} \left(P - \frac{RT}{V_1}\right) dV_1 = \frac{B_{11}}{V_{01}} + \frac{C_{111}}{2V_{01}^2} \qquad \text{(I-6)}$$

Substitution of Equations (I-4) and I-6) into Equation (I-2) yields the following result.

$$\ln \Phi = \frac{1}{RT}\left[a(P-p_{01}) + \frac{b}{2}(P-p_{01})^2 + \frac{c}{3}(P-p_{01})^3\right] + \frac{2B_{11}}{V_{01}} + \frac{3C_{111}}{2V_{01}^2} - \ln Z_{01}$$

$$- \frac{1}{RT} \int_{V_m}^{\infty} \left[\left(\frac{\partial P'}{\partial n_1}\right)_{V_m,T,n_2} - \frac{RT}{V_m}\right] dV_m + \ln Z_m + \ln \gamma_1' x_1 \qquad \text{(I-7)}$$

Values of the second and third virial coefficient of component 1 were calculated from the same equation of state used to compute the properties of the gas mixture.

The evaluation of the integral, involving the properties of the gas mixture, is accomplished using various equations of state in Chapter VI. The correct evaluation of this integral is one of the primary objectives of this work. All of the other terms combined probably produce less than five per cent error in the enhancement factor except possibly at the highest temperatures and pressures in the argon-hydrogen system.

The last term, $\ln \gamma_1' x_1$, was evaluated from experimental data for the liquid phase composition and the assumption that $\gamma_1' = 1$, i.e., that

the solution is ideal. Information gained from freezing point studies indicated that γ_1' probably did not vary by more than 3 per cent from unity at concentrations of dissolved hydrogen up to about 11 per cent and much less than 1 per cent at all concentrations of helium in argon encountered in this work.

Henry's Law Constant

The enhancement factor described in the previous section is a relatively new parameter for describing the gas phase composition, but the solubility of component 2, in the liquid phase has for a number of years been widely expressed in terms of Henry's law. The more exact definition of a Henry's law constant is usually given by

$$H^{o} = \lim_{x_2 \to 0} \left(\frac{\bar{f}_2^{G}}{x_2}\right) \tag{I-8}$$

In this work the Henry's law constant is more conveniently expressed as

$$\bar{K} = \frac{P - p_{01}}{x_2} \tag{I-9}$$

This parameter given by Equation (I-9) can be more conveniently used to correlate liquid phase data since it requires no knowledge of the gas composition. A number of relations involving H^{o} and $\bar{K}$ and other forms of Henry's law are given in Appendix E.

Prediction of Phase Equilibria Using a Single Equation of State to Represent Both Phases

Rather than treating the gas phase and liquid phase separately, a single equation of state that is capable of representing the properties of both phases may be used. Historically, the van der Waals equation of state was the first equation of state used to predict the

properties of both liquid and gas phases. This simple two-parameter equation does give qualitative results for the gas and liquid phases of a pure substance. An equation of state which was developed to predict phase equilibria in hydrocarbon systems is the Benedict-Webb-Rubin equation of state.[6] If an equation of state can be written as a function of density, temperature and composition, the following equations must be satisfied to predict phase equilibria at constant temperature in a binary system.

$$P(\rho_m^L, x_1) = P(\rho_m^G, y_1) \tag{I-10}$$

$$\bar{f}_1^L(\rho_m^L, x_1) = \bar{f}_1^G(\rho_m^G, y_1) \tag{I-11}$$

$$\bar{f}_2^L(\rho_m^L, x_1) = \bar{f}_2^G(\rho_m^G, y_1) \tag{I-12}$$

Since there are three equations with four independent variables, it is necessary to specify one additional condition. In Chapter IV and in Appendix E the method of solution used in the present work is described. After initially calculating the vapor pressure of pure argon, the values of the liquid and gas phase compositions were calculated at selected even pressures greater than the vapor pressure of argon.

Activity Coefficient of Argon in the Liquid Phase from Freezing Point Depression

If the solid phase in equilibrium with a solution of liquid argon and helium or hydrogen is assumed to be pure argon, the activity of the argon in the liquid phase may be calculated from the freezing point depression at constant pressure.

From Prigogine and Defay,[68]

$$\ln \gamma_1' x_1 = \int_{T_{mp}^o}^{T_{mp}} \left(\frac{h_1^L - h_1^S}{RT^2}\right) dT \qquad \text{(I-13)}$$

where

T_{mp}^o = melting point of pure argon,

T_{mp} = observed melting point of the solution,

h_1^L = enthalpy of pure liquid argon at T,

and h_1^S = enthalpy of pure solid argon at T.

If the enthalpy of argon is referred to the solid at the triple point (T_o, p_{o1}^o), the following expressions result for the enthalpies of the liquid and solid at T and P.

$$h_1^L(T,P) = \Delta h_f(T_o, p_{o1}^o) + \int_{T_o, p_{o1}^o}^{T, p_{o1}} c_s^L \, dT + \int_{p_{o1}}^{P} \left(\frac{\partial h^L}{\partial P}\right) dP$$

$$+ \int_{T_o, p_{o1}^o}^{T, p_{o1}} v_1^L \, dP \qquad \text{(I-14)}$$

$$h_1^S(T,P) = \int_{T_o, p_{o1}^o}^{T, p_{o1}} c_s^S \, dT + \int_{p_{o1}, T}^{P, T} \left(\frac{\partial h^S}{\partial P}\right) dP + \int_{T_o, p_{o1}^o}^{T, p_{o1}} v_1^S \, dP \qquad \text{(I-15)}$$

Let

$$\left(\frac{\partial h^L}{\partial P}\right)_T = B_o^L \qquad \text{(I-16)}$$

$$\left(\frac{\partial h^S}{\partial P}\right)_T = B_o^S \qquad \text{(I-17)}$$

$$c_s^L = A_o^L \qquad \text{(I-18)}$$

$$c_c^S = A_o^S + A_1^S T + A_2^S T^2 + A_3^S T^3 \qquad \text{(I-19)}$$

The last term of Equations (I-14) and (I-15) are extremely small and may be neglected. The values of B_o^L and B_o^S are assumed constant over the range of interest. Integration of Equation (I-13) then results in the following expression for the activity coefficient of argon in the liquid solution.

$$R \ln \gamma_1' x_1 = \Delta h_f(T_o, p_{o1}^o)\left(\frac{1}{T_{mp}^o} - \frac{1}{T_{mp}}\right) + A_o^L \ln\left(\frac{T_{mp}}{T_{mp}^o}\right) - A_o^L T_o \left(\frac{1}{T_{mp}^o} - \frac{1}{T_{mp}}\right)$$

$$+ (B_o^L - B_o^S)(P - p_{o1})\left(\frac{1}{T_{mp}^o} - \frac{1}{T_{mp}}\right) - A_o^S \ln\left(\frac{T_{mp}}{T_{mp}^o}\right) + A_o^S T_o \left(\frac{1}{T_{mp}^o} - \frac{1}{T_{mp}}\right)$$

$$- \frac{A_1^S}{2}(T_{mp} - T_{mp}^o) + \frac{A_1^S}{2} T_o^2 \left(\frac{1}{T_{mp}^o} - \frac{1}{T_{mp}}\right) - \frac{A_2^S}{6}(T_{mp}^2 - T_{mp}^{o2})$$

$$+ \frac{A_2^S}{3} T_o^3 \left(\frac{1}{T_{mp}^o} - \frac{1}{T_{mp}}\right) - \frac{A_3^S}{12}(T_{mp}^3 - T_{mp}^{o3}) + \frac{A_3^S T_o^4}{4}\left(\frac{1}{T_{mp}^o} - \frac{1}{T_{mp}}\right) \qquad \text{(I-20)}$$

CHAPTER II

EXPERIMENTAL APPARATUS

General

The experimental apparatus used to determine the phase equilibrium data in this work has been described in detail by Kirk[42] and in less detail by Kirk and Ziegler.[43] The single-pass, flow-type device is shown schematically in Figure 1. The description of the system will be discussed in terms of the argon-hydrogen system, following very closely the description of Kirk and Ziegler.[43] In addition to being used here to determine the gas phase and liquid phase compositions of the two binary systems as a function of temperature and pressure, the apparatus was also used to determine the locus of the three-phase line up to about 120 atmospheres pressure. The apparatus was primarily designed for the measurement of phase equilibria in binary systems in which the temperature is well below the critical temperature of one component and near or above the critical temperature of the other component. As Kirk[42] points out, the apparatus could be modified by the addition of a recirculating pump to permit the determination of phase equilibria in systems in which the critical temperatures are closer together and also for multicomponent systems.

High pressure hydrogen or an argon-hydrogen mixture is admitted to the high pressure panel where the pressure is regulated and measured. The gas flow is then directed into the phase equilibrium cell assembly.

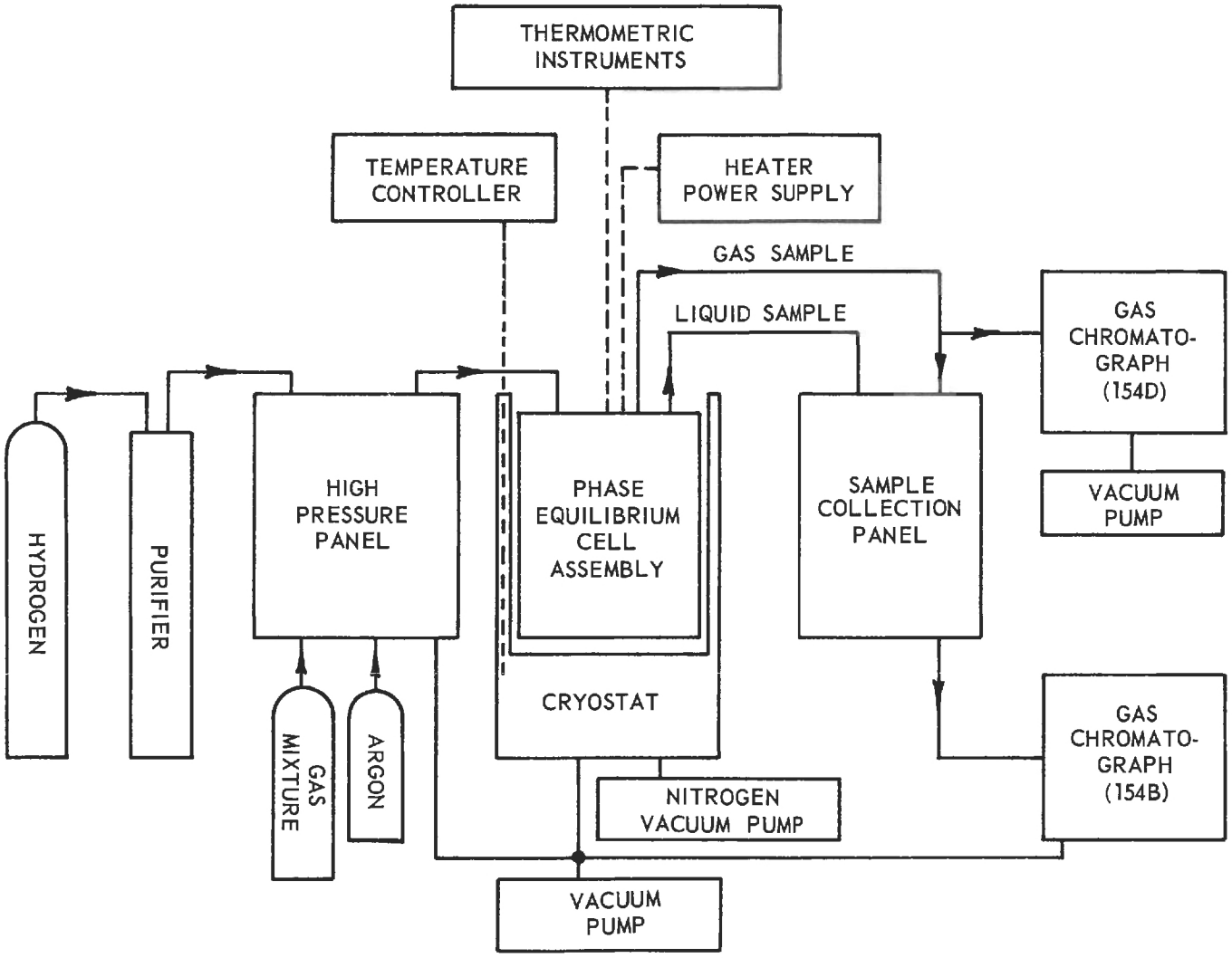

Figure 1. Schematic Diagram of Phase Equilibrium Apparatus.

The phase equilibrium cell assembly is suspended in a copper block cryostat, which is maintained at the desired temperature. The temperature is measured using one of several thermometric instruments. The gas, after passing through the phase equilibrium cell assembly, may pass in either of two directions; through the sample collection panel where portions may be collected for subsequent analysis in the gas chromatograph labeled 154(B) in Figure 1, or else directly to gas chromatograph 154(D) for analysis. Flow rates are controlled by a needle valve and measured with a wet-test meter. In the liquid-gas region, samples of the liquid may be withdrawn and collected on the sample collection panel for analysis.

The heater power supply furnishes direct current to a number of heaters which may be used in normal operations.

Cryostat

The type of cryostat used here is generally referred to as a copper block cryostat. A massive hollow cylinder of copper and brass, referred to here as the copper block, is suspended inside an evacuated container which is filled with a powder insulation. Suspended from the copper block is a reservoir for the cryogen, in this case nitrogen. The phase equilibrium cell is contained inside the hollow of the copper block, being thermally secured to its base with solder. By means of a differential pressure regulator, the pressure in the cryogen reservoir, suspended beneath the copper block, is maintained slightly higher than the pressure on the exit side of a throttling valve on a line leading from the copper block. The cryogen reservoir is connected to the annular space, partially filled with copper wool, between the phase

equilibrium cell and the copper block by a small capillary tube extending to the bottom of the reservoir. At temperatures above the boiling point of nitrogen, the refrigerant is injected through the capillary into the annular space where the liquid is immediately vaporized. The rate of refrigeration is controlled by throttling the vaporized gas through a valve in the exit line via a flowmeter. The rate of liquid injection is thus controlled by controlling the flow rate of the exit gas. At temperatures below the boiling point of nitrogen the throttling valve is opened and the injected liquid does not vaporize immediately but rises to a level in the annular space between the liquid reservoir and the annular space. The rate of refrigeration is controlled by throttling the gas from the boiling liquid to a vacuum pump.

Temperature is controlled by balancing the slight excess of refrigeration with an electric heater wrapped on the base of the copper block and controlled by an automatic temperature controller.

The automatic temperature controller is a photoelectric, proportional device in which the output of a six- or twelve-junction thermopile is balanced against a reference potentiometer.

In normal operations, this cryostat maintains temperatures constant within $\pm 0.03^{\circ}$ K at any point from near room temperature to near the nitrogen triple point; no load stability is better. It can be operated for about 20 hours without refilling.

Phase Equilibrium Cell Assembly

The phase equilibrium cell assembly is shown in Figure 2. It consists primarily of a nine pound copper body closed at both ends with

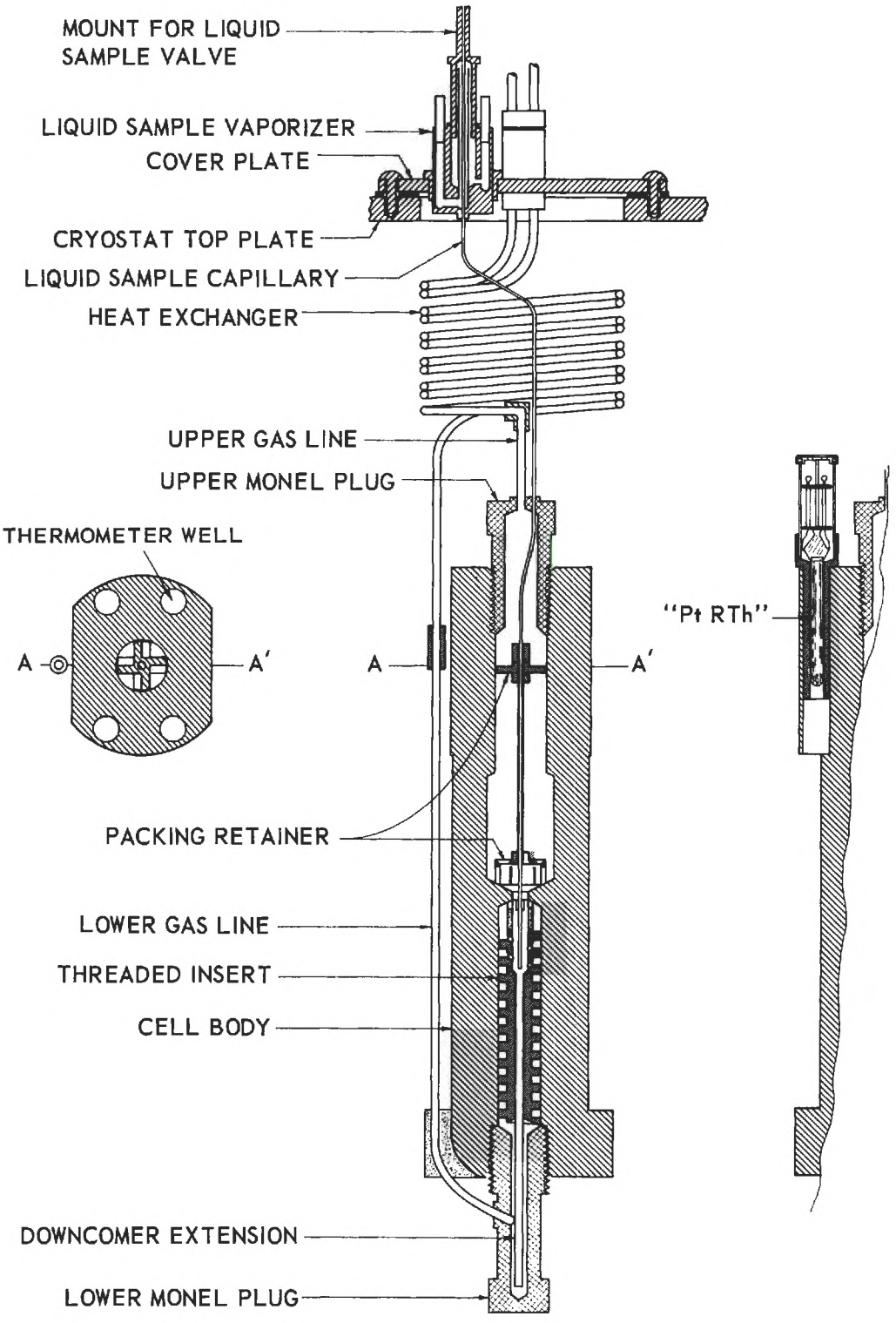

Figure 2. Structure of the Phase Equilibrium Cell Assembly.

threaded monel plugs sealed with solder. The lower section contains a spiral copper insert with a central downcomer. The upper section is fitted with graded copper packing (not shown) held in place by a packing retainer. The upper and lower gas lines are connected to a spiral-wound, counter-current, heat exchanger. The liquid sample line extends directly through the upper monel plug to a water heated vaporizer and room temperature sampling valve.

Temperature and Pressure Measurements

The primary thermometric instrument is a capsule-type, platinum resistance thermometer manufactured by Leeds and Northrup Company. The thermometer has a nominal resistance of 25 ohms at the ice point and has been calibrated by the National Bureau of Standards. This thermometer, labeled "PtRTh," is located in the phase equilibrium cell assembly as shown in Figure 2. Measurements of the resistance were made on a Leeds and Northrup Company G-2, Meuller Bridge, which has also been calibrated by the National Bureau of Standards. All temperatures are reported in degrees Kelvin with an assigned ice point of 273.15° K. Below 90.18° K the temperatures are on the NBS 1955 scale and above 90.18° K are on the International Practical Kelvin Scale.

In addition to the primary thermometer there are two, six-junction thermopiles, one located in a well adjacent to "PtRTh," and the other on the lower shoulder of the phase equilibrium cell assembly. These are used primarily as sensors for the automatic temperature controllers. There are a number of difference couples located in various places as described by Kirk.[42]

Pressures were measured with two Ashcroft, test quality, eight inch dial, mirror scale, bourdon type gauges. One of the gauges was graduated from 0 to 600 psig and the other 0 to 3000 psig. The gauges were calibrated by Kirk[42] against a dead weight tester and found to be accurate to within 1/2 per cent of the measured pressure over the range of pressures encountered in the present work.

Experimental Procedure

Gas-Liquid Region

Approximately 10 cc of liquid argon was first condensed into the bottom of the phase equilibrium cell assembly. This was a sufficient quantity to bring the liquid level slightly above the constriction in the cell and to have about 4 cc above the end of the liquid sample line. A slow flow of hydrogen was then bubbled through the liquid via the lower inlet and the spiral path. The flow rate of the gas was adjusted to approximately 100 cc (at cell T and P) per hour. The flow rate did not seem critical except that the slower the flow the longer one had to wait for the outlet gas to reach equilibrium. The criteria established by Kirk,[42] which seemed to be more than adequate for all conditions encountered here, was to flow enough gas to flush the cell twice after the temperature and pressure were adjusted to their final values. After equilibrium had been reached, a liquid sample was withdrawn through the liquid sampling line, vaporized, and collected for analysis on the sample collection board. The remainder of the liquid above the end of the liquid sample line was vented. The complete discharge of the liquid could be monitored by observing the sudden change in the emf

of a six-junction thermopile located across the ends of a small electric heater wound on the liquid sample line.

The liquid level in the phase equilibrium cell at this point was known to be just below the end of the liquid sample line. Approximately 3 to 5 cc of liquid argon as measured in a high pressure gas burette was then condensed into the phase equilibrium cell and the pressure adjusted for the next determination.

Gas-Solid Region

In the gas-solid region, a mixture of argon-hydrogen, which was slightly higher in argon content than the equilibrium mixture, was introduced into the phase equilibrium cell through the upper gas line. The excess argon condensed on the copper packing and the equilibrium gas mixture flowed down through the spiral insert and out through the lower gas line to the sample collection board. Samples of the gas were also withdrawn through the liquid sample line and collected for analysis.

To prevent plugging it was necessary to heat the upper monel plug during the run. This resulted in as much as an 0.08° K temperature difference along the phase equilibrium cell as determined by a six-junction thermopile between the upper and lower shoulder of the cell. The reported temperature was corrected for this temperature difference. Those samples withdrawn through the liquid sample line were corrected by 1/2 the temperature difference.

Three-Phase Line

For the determination of the locus of the three-phase line, the phase equilibrium cell was first completely filled with pure liquid

argon as indicated by observing a rapid rise in pressure. This was accomplished at a temperature slightly higher than the normal melting curve for pure argon. A very slow flow of hydrogen or helium was then bubbled through the liquid at constant pressure. The refrigeration rate was adjusted to a constant value and the electric heater, normally controlled by the automatic temperature controller, was adjusted manually until a cooling rate of approximately 0.006° K per minute was established. Since the solubility of helium and hydrogen diminishes with temperature at constant pressure in this region, saturation is easily established and maintained. Upon reaching the three-phase line a very sharp break is noted in the cooling rate, usually followed by a slight rise in temperature and then an essentially constant temperature for several minutes. Afterwards the temperature drops slowly for a considerable length of time. The maximum temperature which occurred after the break in the cooling curve was usually taken to be the temperature of the three-phase line at that particular pressure. On at least two of the runs the freezing occurred first in the inlet line at the bottom of the cell. When this happened the pressure dropped in the cell and resulted in a slightly different shape of the cooling curve. On these runs the temperature and pressure were assigned at the time of plugging.

Melting Curve of Pure Argon

The melting curve of pure argon was determined in a manner very similar to that described above for the three-phase line. The phase equilibrium cell was first filled with pure liquid argon. The pressure was maintained by pure argon gas with both the upper and lower gas

inlet lines open. The cooling rate was adjusted to an approximate value of 0.006° K per minute. The pure liquid argon usually supercooled by about 0.1° to 0.2° K before freezing. Upon freezing, the temperature rose sharply to the melting point and remained constant for 5 to 10 minutes, and then fell slowly for a considerable length of time.

Analysis of Gas Mixtures

General

Two series 154 Perkin-Elmer Vapor Fractometers, a model 154B and a model 154D, were used to analyze the mixtures of argon-helium and argon-hydrogen. The gas chromatographs had been slightly modified by Kirk[42] to obtain better precision. Only the composition of the minor component of the binary systems was determined. The mole fraction of the major component was assumed to be the remainder. All of the samples from the gas phase, at the equilibrium conditions studied, contained argon as the minor component. These were analyzed using helium as the carrier gas. The samples withdrawn from the liquid phase contained either hydrogen or helium as the minor component. These samples were analyzed using argon as the carrier gas. Thus, in only the gas phase of the argon-hydrogen system did the major component produce a peak on the chromatogram. Both Vapor Fractometers were operated using columns packed with Linde 5A molecular sieve.

The physical arrangement of the sampling system and method of operation was such that the model 154B Perkin-Elmer Vapor Fractometer was used to analyze the gas phase in the solid-gas region, and the

liquid phase in the liquid-phase region. Thus, the model 154D Vapor Fractometer was only used to analyze the gas phase in the liquid-gas region.

The samples to be analyzed by the 154B Vapor Fractometer were first collected over mercury in glass holders which held up to about 130 cc. Portions of these samples could then be introduced into the gas sampling valve of the 154B Vapor Fractometer. To accomplish this the gas sampling valve was first evacuated, the gas mixture introduced to a pressure slightly above atmospheric pressure and then vented to the atmosphere.

The model 154D was only used to analyze the effluent gas from the phase equilibrium cell. A continuous stream of gas was provided which could be passed directly through the gas sampling valve. A stopcock arrangement simply trapped a portion of this gas at slightly above atmospheric pressure. The sample was then vented to atmospheric pressure before being analyzed.

Calibration of the Chromatographs

The chromatographs were calibrated using gas mixtures prepared in a gas mixing apparatus described by Kirk.[42] This apparatus was capable of preparing gas mixtures over the concentration range encountered here with an accuracy of about ± 1/2 per cent of the mole fraction of the minor component. To maintain this calibration, a number of "standard" mixtures of the appropriate compositions were prepared in small compressed gas cylinders. During the calibration and all subsequent analyses, these "standard" mixtures were "analyzed" at frequent intervals to correct for small drifts in the calibration

curve. These "standard" mixtures were prepared with only an approximate knowledge of their composition, but during the course of calibration became quite accurately known. A more complete discussion of the calibration procedure is given in Appendix B.

CHAPTER III

EXPERIMENTAL RESULTS

Phase Composition Measurements

General

The phase equilibrium composition measurements were made, as nearly as possible, along isotherms at selected even pressures. Normally six different pressures could be determined along an isotherm in one day's operation. This number of points was found sufficient to define clearly an isotherm. At a particular pressure a number of samples were sometimes taken from the gas phase and analyzed. These were quite often taken before equilibrium was reached in order to observe the rapidity of equilibrium. These are not reported here. A total of 357 different samples and 527 analyses are reported in Tables 16 through 19 of Appendix C. The number of analyses made on each sample varied. If the sample was collected on the sample collection panel, usually at least two analyses were made. In the case of the liquid samples usually only one sample was obtained at each point, and therefore two or three analyses were made. In addition to the equilibrium compositions, the enhancement factor and Henry's law constant defined by Equations (I-1) and I-9) are also reported in Tables 16 through 19 in Appendix C. The vapor pressures used in the calculations were taken from the appropriate vapor pressure equations, Equations (V-1), (V-2), or (V-3). At each point a selected value is

given of the temperature, pressure, composition and either an enhancement factor or a Henry's law constant. These selected values were quite often an average value of the various samples and analyses, though sometimes the judgment of the investigator was considered more reliable than an average. These selected values were not smoothed values, and, in fact, were used to obtain a least squares fit to the data. In all plots of the experimental data these selected values were used simply to avoid an excessive number of points on each graph.

Argon-Helium

The gas phase composition in equilibrium with solid argon was measured along isotherms at 68.07°, 74.05° and 80.06° K at pressures up to 120 atmospheres. In addition, two points were determined at 60 and 80 atmospheres on the 77.90° K isotherm. The gas and liquid phase compositions were determined at 86.02°, 91.98°, 97.51°, and 108.02° K at pressures up to 120 atmospheres. No liquid sample was obtained at 120 atmospheres on the 86.02° K isotherm since at this pressure the condensed phase is solid. The gas phase compositions are presented in Table 16 in Appendix C. The liquid phase compositions are reported in Table 17 in Appendix C.

To check the effect of withdrawal rates on the liquid sample, the withdrawal rates of run F1 and F2 were varied as widely as possible to cover the entire range of withdrawal rates encountered in any of the measurements on either the argon-helium or argon-hydrogen systems. The rate of withdrawal of determination F1 was about 33 cc (S.T.P.)/sec and that of determination F2 was about 3 cc (S.T.P.)/sec. Neither of these points deviated significantly from the least squares surface fit; the deviations

of F1 and F2 expressed in terms of mole fraction of helium being + 0.3 and -0.85 per cent respectively. The reproducibility of the liquid and gas samples is indicated by F4 and F7, both points being determined at about 60 atmospheres pressure on the 97.51° K isotherm. The solubility of helium in argon deviates by -0.75 per cent and +0.27 per cent for F4 and F7, respectively, from the least squares fit. The mole fraction of argon in the gas phase deviates from the least squares fit by -0.41 and -0.92 per cent for F4 and F7, respectively. The points on this particular isotherm were determined beginning at 120 atmospheres with F1, and the pressure decreased in steps of 20 atmospheres to F6 at 20 atmospheres. The pressure was then set at 60 atmospheres and F7 determined. No significant effect was noted in this or any other isotherm on the order of determinations with respect to increasing or decreasing pressure.

Argon-Hydrogen

The composition of the gas phase in equilibrium with solid argon was determined at 68.04°, 73.05°, and 79.01° K at pressures from 20 to 110 atmospheres. The composition of the gas and liquid phases was determined in the argon-hydrogen system at 86.95°, 94.21°, 99.95° and 105.01° K at pressures from 20 to 120 atmospheres. At 120 atmospheres no liquid sample was obtained on the 86.95° K isotherm because of insufficient liquid in the cell. The gas phase compositions are reported in Table 18 and the liquid phase compositions in Table 19 of Appendix C.

Least Squares Fit of Experimental Enhancement Factors and Henry's Law Constants

General

For a number of reasons it is often desirable to represent the experimental data in an analytical form. For an experimental quantity which is a function of only one independent variable this is usually accomplished either by a least squares fit of a polynomial in powers of the dependent variable or some other appropriate function. For the case of a surface fit, i.e., two independent variables, the choice of functions seems to be quite important. A method of fitting by a least squares surface fit in a power series of the two independent variables is described in Appendix H. The general equation may be written as

$$z = \sum_{j=0}^{M} C_j \psi_j(x,y) \qquad \text{(III-1)}$$

The set $\{\psi_j(x,y)\}$ represents a set of functions which have been made orthogonal with respect to a particular data set consisting of N points.

$$\sum_{i=1}^{N} \psi_j(x_i,y_i)\psi_k(x_i,y_i) = 0 \qquad j \neq k \qquad \text{(III-2)}$$

The weighting factors, C_j, are determined by the criterion of fit, namely that the sum of the squares of the residuals be minimized.

Least Squares Fit of Enhancement Factors

The gas phase compositions of the two binary systems were adequately represented using the least squares surface fit described in Appendix H with the values of the dependent variable z, and the independent variables x and y given by Equations (III-3) through (III-5).

The variables chosen were normalized by the maximum value occurring in the data set

$$x = (P-p_{01})/(P-p_{01})_{max} \qquad \text{(III-3)}$$

$$y = (1/T)/(1/T)_{max} \qquad \text{(III-4)}$$

$$z = \left(\frac{\text{Log } \Phi}{P-p_{01}}\right) / \left(\frac{\text{Log } \Phi}{P-p_{01}}\right)_{max} \qquad \text{(III-5)}$$

The values of the orthogonal coefficients, the weighting factors and the normalizing values are given in Table 1 for the argon-helium system and Table 2 for the argon-hydrogen system. The best fit for the two systems was found to be for p = 3, q = 3 for argon-helium and p = 4, q = 3 for argon-hydrogen, where p and q refer to the maximum power of x and y (see Appendix H). The average deviation of $(\text{Log } \Phi)/(P-p_{01})$ from the experimental values was 5.3×10^{-5} for argon-helium and 2.9×10^{-5} for argon-hydrogen. The corresponding values of the standard error of estimate were 6.5×10^{-5} for the 47 argon-helium points and 3.7×10^{-5} for the 43 argon-hydrogen points.

Least Squares Fit of Henry's Law Constant

The liquid phase compositions of the two binary systems were represented using a similar approach as described for the enhancement factor and in Appendix H. Values of the variables are:

$$x = (P-p_{01})/(P-p_{01})_{max} \qquad \text{(III-6)}$$

$$y = (1/T)/(1/T)_{max} \qquad \text{(III-7)}$$

$$z = [\text{Log } (\overline{K})-2]/[\text{Log } (\overline{K})-2]_{max} \qquad \text{(III-8)}$$

Table 1. Coefficients, Weighting Factors and Normalizing Constants for Least Squares Fit of the Enhancement Factor of Argon in Helium.

		Coefficients, α_{ij}				
i	j	1	2	3	4	5
0		0.62045127	0.81365544	0.46394791	0.50405238	0.67409965
1			-0.00988879	1.1964232	0.81468159	-0.01717783
2				0.04402429	0.61382117	1.6436560
3					-0.00641979	-0.02183244
4						-0.04805636

	j	6	7	8	9
0		0.38236014	0.37709004	0.41688902	0.56831476
1		1.2142656	0.97702080	0.67392190	-0.02294142
2		-0.08111272	0.48380258	1.0054272	2.0507637
3		1.7389383	0.80948843	-0.02525852	-0.05144999
4		0.02255874	1.11871133	1.6366201	-0.11378367
5		-0.07107582	0.11787410	0.64950233	2.4490852
6			0.04544836	-0.029169182	0.00333213
7				-0.052040109	-0.01985489
8					0.00613056

(continued)

Table 1. Coefficients, Weighting Factors and Normalizing Constants for Least Squares Fit of the Enhancement Factor of Argon in Helium. (Concluded)

Weighting Factors, C_j				
j	0	1	2	3	4
	0.68073551	-0.29441770	0.80019809	0.24266136	0.22585073
	5	6	7	8	9
	2.6294435	-0.30757094	-1.4714614	-2.9673696	6.8741501

Normalizing Constants

$(P\text{-}p_{01})_{max} = 120.22184$; $(1/T)_{max} = 0.01469724$; $\left(\frac{\text{Log } \Phi}{P\text{-}p_{01}}\right)_{max} = 0.0036727528$

Table 2. Coefficients, Weighting Factors and Normalizing Constants for Least Squares Fit of the Enhancement Factor of Argon in Hydrogen.

		Coefficients, α_{ij}				
i	j	1	2	3	4	5
0		0.55053223	0.80040918	0.37921967	0.43907420	0.65558051
1			-0.02071044	1.1138205	0.78503630	-0.03636556
2				-0.01896782	0.53370141	1.6402459
3					-0.03688655	-0.00153183
4						-0.01279302
	j	6	7	8	9	10
0		0.29357183	0.30149218	0.35814953	0.54921786	0.24250537
1		1.0624023	0.87724239	0.62892744	-0.04812323	0.98555585
2		-0.03583157	0.34389005	0.87450361	2.0418356	-0.05345938
3		1.6766628	0.73775368	-0.06485699	-0.00341017	2.0534535
4		-0.08774551	1.0907287	1.6314677	-0.03224068	-0.19665029
5		-0.04527742	-0.01412151	0.54801796	2.4665569	-0.10124658
6			-0.01782679	-0.00397279	0.00692084	2.2641266
7				-0.01055614	0.00574270	-0.12610170
8					-0.03830147	-0.09725689
9						0.15776628

(continued)

Table 2. Coefficients, Weighting Factors and Normalizing Constants for Least Squares Fit of the Enhancement Factor of Argon in Hydrogen. (Continued)

	11	12	13
0	0.23276888	0.24505544	0.29869832
1	0.83545985	0.70556018	0.51434673
2	0.24406328	0.57544909	1.0874681
3	1.2663752	0.54821230	-0.08550799
4	0.94896446	1.7820507	2.0200298
5	-0.05684551	0.35502278	1.3542540
6	0.73843462	-0.04105274	-0.00341937
7	1.6449451	1.6206337	-0.02569681
8	-0.05394104	1.1117608	2.4961154
9	-0.15249333	-0.37943030	0.31667870
10	-0.10407210	0.01873334	0.02517153
11		-0.03506685	0.05282915
12			-0.54838015

Weighting Factors, C_j

j	0	1	2	3	4
	0.60188011	-0.14404164	1.5096718	0.0056826468	-0.46734395
j	5	6	7	8	9
	1.8582580	-0.038772462	-0.90469503	-1.5116336	1.3249409
j	10	11	12	13	
	-0.0062212836	0.67852461	-0.56060908	-2.1131558	

(continued)

Table 2. Coefficients, Weighting Factors and Normalizing Constants for Least Squares Fit of the Enhancement Factor of Argon in Hydrogen. (Concluded)

Normalizing Constants
$(P\text{-}p_{01})_{max} = 119.33469$; $(1/T)_{max} = 0.014705882$; $\left(\frac{\text{Log } \Phi}{P\text{-}p_{01}}\right)_{max} = 0.015319541$

The values of the orthogonal coefficients, the weighting factors and the normalizing values are given in Table 3 for the argon-helium system and Table 4 for the argon-hydrogen system. The best fit was found to be p = 2, q = 2 for both systems. The average deviation of Log $\overline{K}$ from the experimental values was 0.0016 for the 23 helium-argon points and 0.0011 for the 23 hydrogen-argon points. The corresponding values of the standard error of estimates were 0.0021 and 0.0017.

Henry's Law Constants at Infinite Dilution

The values of the Henry's law constants at infinite dilution defined by Equation (F-25) are given in Table 5 for helium and hydrogen in liquid argon. These values were obtained from the least squares coefficients given in Tables 3 and 4. Also given in Table 5 are the values of the Henry's law constants at infinite dilution defined by Equation (F-27). These values were obtained graphically from the selected liquid and gas phase equilibrium compositions given in Tables 16 through 19.

Comparison of Experimental Results with Least Squares Fit and Data of Other Investigators

Argon-Helium

The logarithm of the experimental enhancement factors of argon in helium are compared in Figure 3 with the results of the least squares fit at even pressures. The experimental values at even pressures were interpolated graphically from each of the measured isotherms reported in Table 16, Appendix C. The only other experimental values of the enhancement factor of argon in helium are those obtained from

Table 3. Coefficients, Weighting Factors and Normalizing Constants for Least Squares Fit of Henry's Law Constant for Helium in Argon.

Coefficients, α_{ij}

i ↓ j →	1	2	3	4	5
0	0.56115578	0.91160386	0.38939987	0.50595465	0.83578360
1		-0.07512543	1.1233292	0.87582371	-0.13541417
2			0.11073534	0.59610957	1.8037185
3				-0.09370514	-0.00399412
4					-0.14065213

Weighting Factors, C_j

j	0	1	2	3	4
	0.90105686	-0.04765371	1.0587829	0.001966542	0.04201267
	5				
	-0.45548984				

Normalizing Constants

$(P-p_{01})_{max}$ = 118.19645; $(1/T)_{max}$ = 0.01162791; $(Log(\overline{K})-2)_{max}$ = 2.1686921

Table 4. Coefficients, Weighting Factors and Normalizing Constants for Least Squares Fit of Henry's Law Constant for Hydrogen in Argon.

Coefficients, α_{ij}

i ↓ j→	1	2	3	4	5
0	0.55051152	0.90101617	0.38129990	0.49491117	0.81572939
1		-0.01417104	1.1107651	0.88709412	-0.02679465
2			-0.12055668	0.52345945	1.8283488
3				-0.02322062	-0.00389126
4					-0.01966436

Weighting Factors, C_j

j	0	1	3
	0.89677691	-0.012072112	0.85987915
	3	4	5
	-0.033821027	0.49758846	-0.50488642

Normalizing Constants

$(P-p_{01})_{max}$ = 118.36843; $(1/T)_{max}$ = 0.011502185; $[Log(\overline{K})-2]_{max}$ = 0.98667879

Table 5. Henry's Law Constants for Helium and Hydrogen in Argon at Infinite Dilution*

T °K	$\bar{K}^{o}.10^{-2}$ atm	$\hat{K}^{o}.10^{-2}$ atm
	- - - -Argon-Helium- - - -	
108.03	43.6	41.8
97.51	70.7	69.1
91.98	93.7	92.0
86.02	130.0	129.5
	- - - -Argon-Hydrogen- - - -	
105.01	6.81	6.30
99.95	7.26	6.86
94.21	7.82	7.70
86.95	8.62	8.57

*$\bar{K}^{o}$ defined by Equations (F-24) and (F-25).

$\hat{K}^{o}$ defined by Equations (F-26) and(F-27).

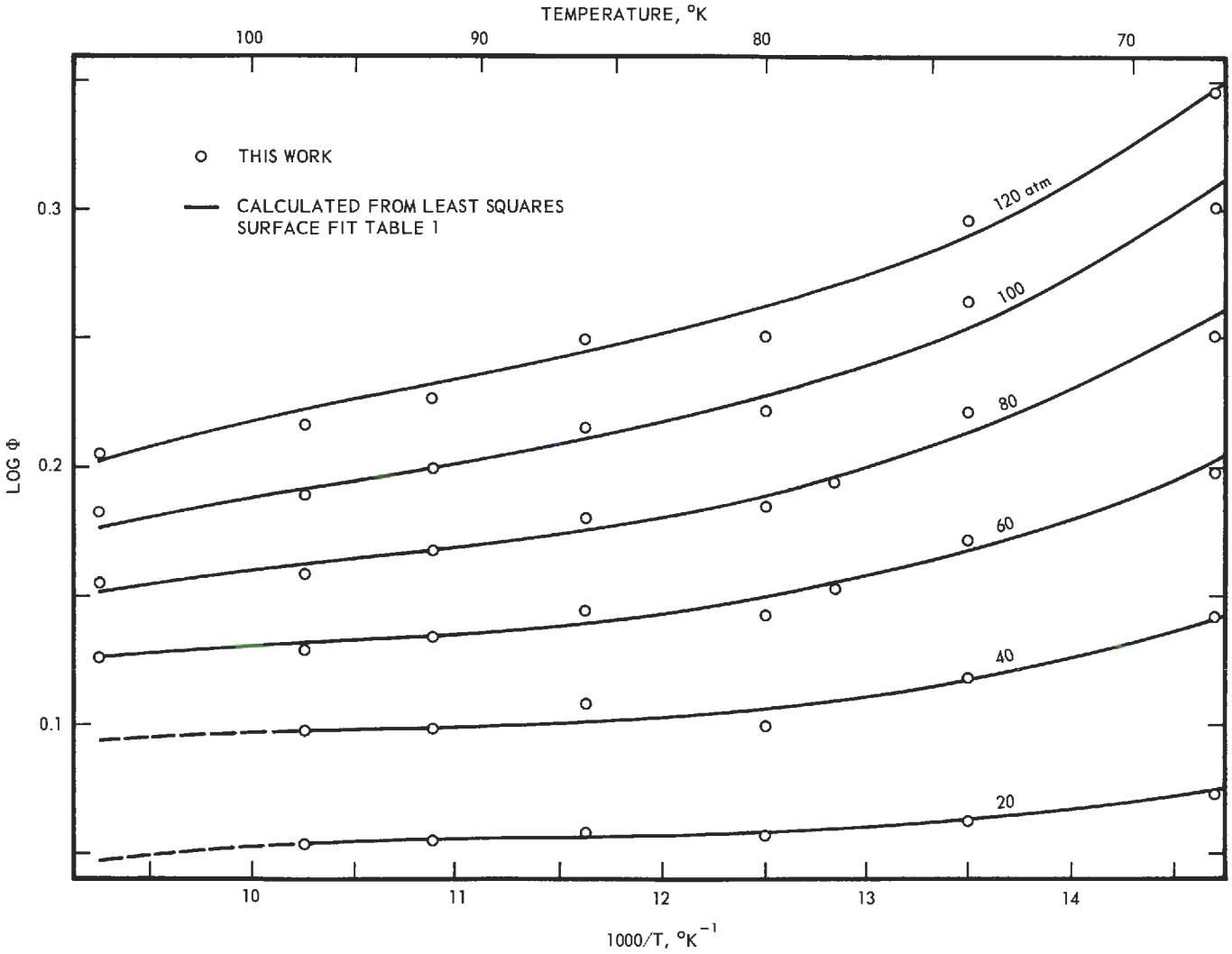

Figure 3. Experimental Enhancement Factors for Argon-Helium at Even Pressures.

the dew-point data of McCain[51] between 99.74° and 150.62° K. The values in the region of overlap deviate by as much as 40 per cent from the values obtained in this work. It has been shown[59] that these results of McCain are likely in error in the region of interest here. His results at higher temperatures appear to be more accurate.

The experimentally determined compositions of the liquid phase, expressed in terms of the logarithm of the Henry's law constant defined by Equation (I-9), are compared in Figure 4 with the least squares fit and the experimental bubble points of McCain[51] in the region of interest. Three of the four points of McCain deviate by less than five per cent, but the point at 99.92° K is not consistent with the majority of his data and deviates by about 20 per cent from the data of this work. The Henry's law constants for helium in argon determined by Karasz[36,37] between 84.05° and 87.53° K at pressures less than 1.2 atmospheres are not shown in Figure 4. The values of Henry's law constants of this work extrapolated to low pressure are approximately two to three times greater than the results of Karasz. No explanation can be offered for the great difference.

Argon-Hydrogen

The logarithm of the experimental enhancement factors of argon in hydrogen are shown in Figure 5 compared with the results of the least squares fit at even pressures. The results appear to be internally consistent. No experimental results for the gas phase composition of this system have been reported by other investigators.

The composition of the liquid phase expressed in terms of the logarithm of Henry's law constant defined by Equation (I-9) are shown

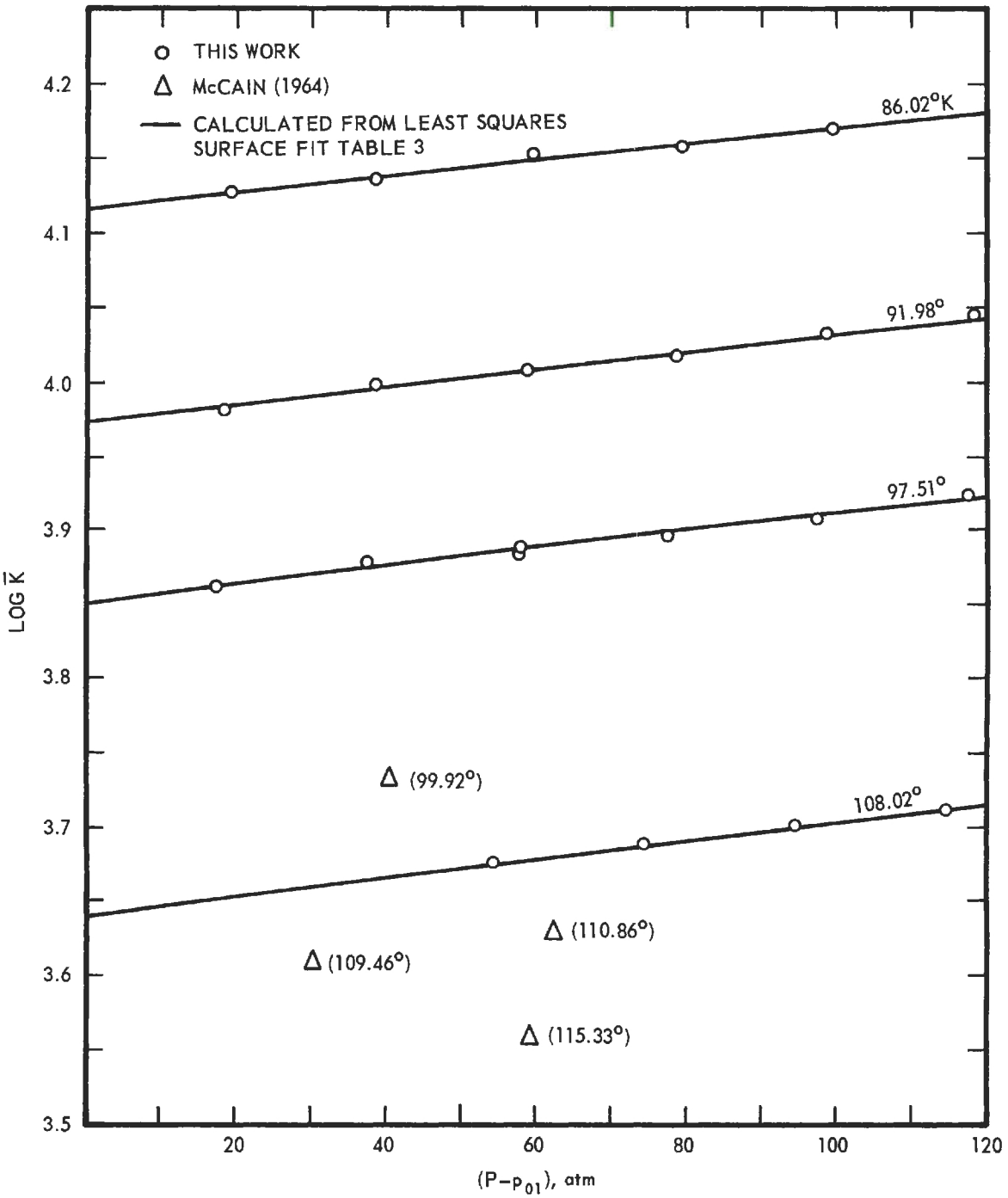

Figure 4. Henry's Law Constant for Helium in Liquid Argon.

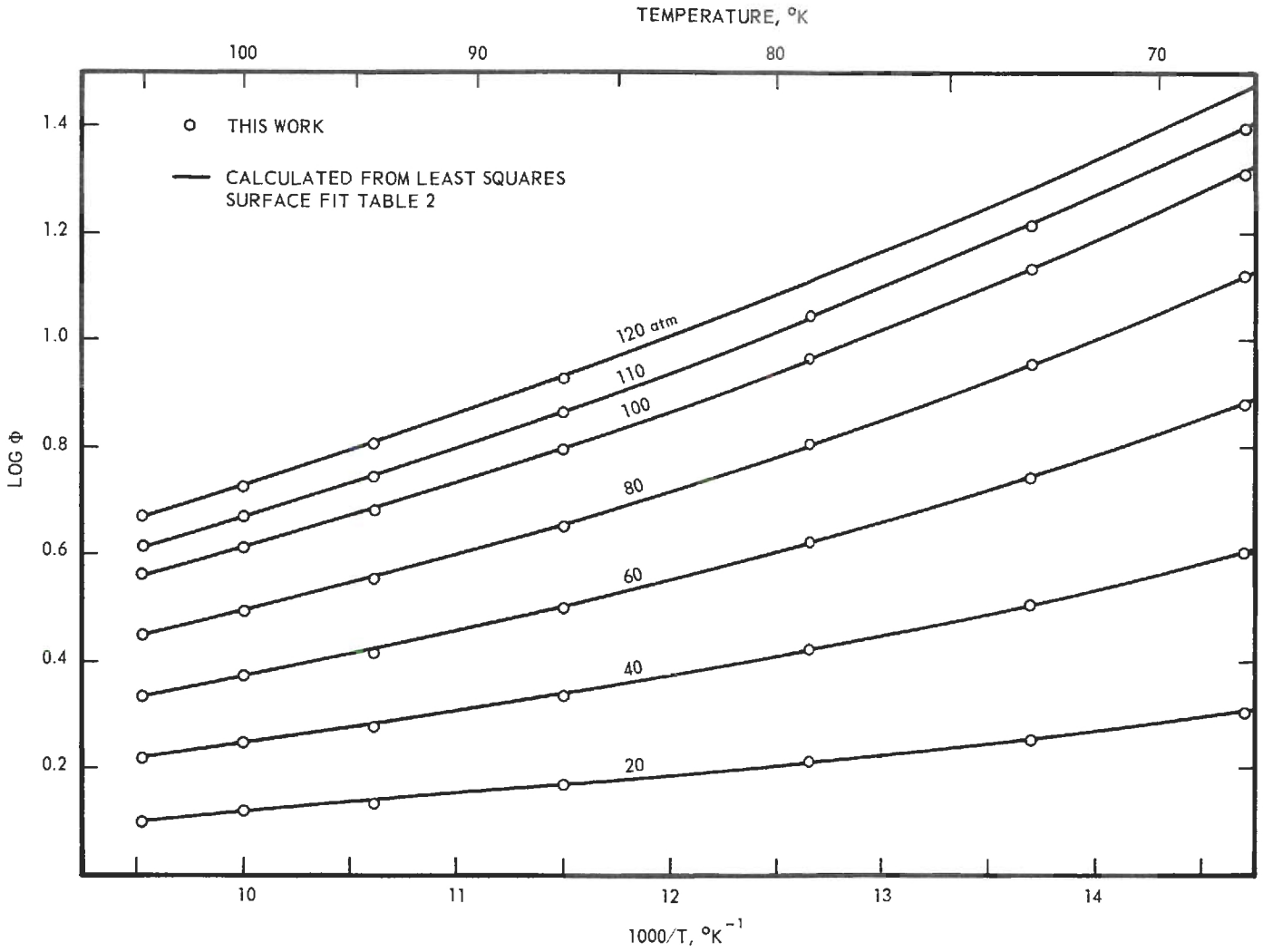

Figure 5. Experimental Enhancement Factors for Argon-Hydrogen at Even Pressures.

in Figure 6 compared with the results of Volk and Halsey.[78] The results of Volk and Halsey agree well at low pressures, but deviate by as much as 15 per cent at higher pressures.

Three-Phase Line of Argon-Helium and Argon-Hydrogen and the Melting Curve for Pure Argon

The results of the determination of the three-phase lines and the normal melting curve for pure argon are given in Table 6. These results consist of six determinations along the three-phase line of the argon-helium system and six along the three-phase line of the argon-hydrogen system up to about 120 atmospheres pressure. Only four determinations were made of the normal melting curve of pure argon up to 120 atmospheres pressure.

The four points determined on the melting curve of pure argon were primarily to check on the method used here. The melting curve of argon has been studied by Bridgman,[10] Simon et al.[73] and Clusius and Weigand.[15] Only Clusius and Weigand have studied it at pressures less than 250 atmospheres. Clusius and Weigand represented their data with the following equation:

$$T = 83.76 + 2.552 \times 10^{-2}P - 3.57 \times 10^{-6}P^2 \ . \qquad \text{(III-9)}$$

This equation gives a triple point of 83.78° compared with the selected value of 83.81° K. Correcting the temperatures from Equation (III-9) by the ratio (83.81/83.78), the experimental determinations are compared with the results of Clusius and Weigand in Figure 7.

The experimental three-phase line results were least squared to obtain the following equations:

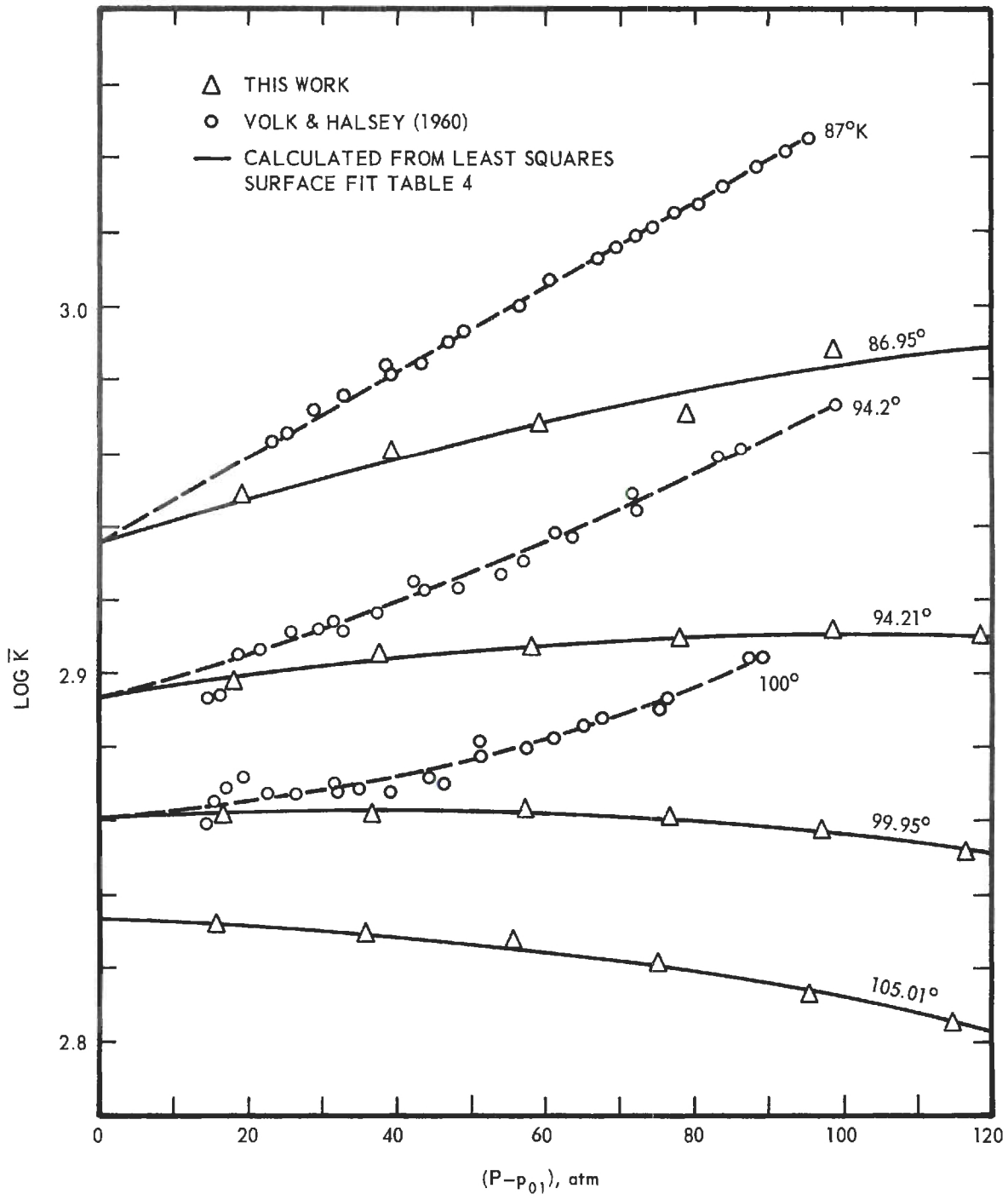

Figure 6. Henry's Law Constant for Hydrogen in Liquid Argon.

Table 6. Experimental Freezing Point Determinations

Run No.	P atm	T(OBS) °K	ΔT(CALC-OBS)[a] °K
		PURE ARGON	
1	40.3	84.80	0.013
2	120.3	86.75	0.059
3	99.5	86.28	0.015
4	69.5	85.52	0.027
		ARGON-HELIUM	
1	120.0	86.33	-0.006
2	80.3	85.54	-0.014
3	114.3	86.21	0.006
4	100.1	85.93	0.006
5	60.0	85.08	0.011
6	30.0	84.44	-0.003
		ARGON-HYDROGEN	
1	80.3	82.71	0.003
2	60.1	82.86	-0.016
3	40.9	83.02	0.025
4	19.7	83.40	-0.018
5	19.8	83.38	0.000
6	119.7	82.59	0.000

[a] Calculated temperatures are from Equations (III-9), (III-10) and (III-11). The temperatures calculated from Equation (III-9) have been corrected by the ratio (83.81/83.78) to correspond with the triple point of argon selected in this work.

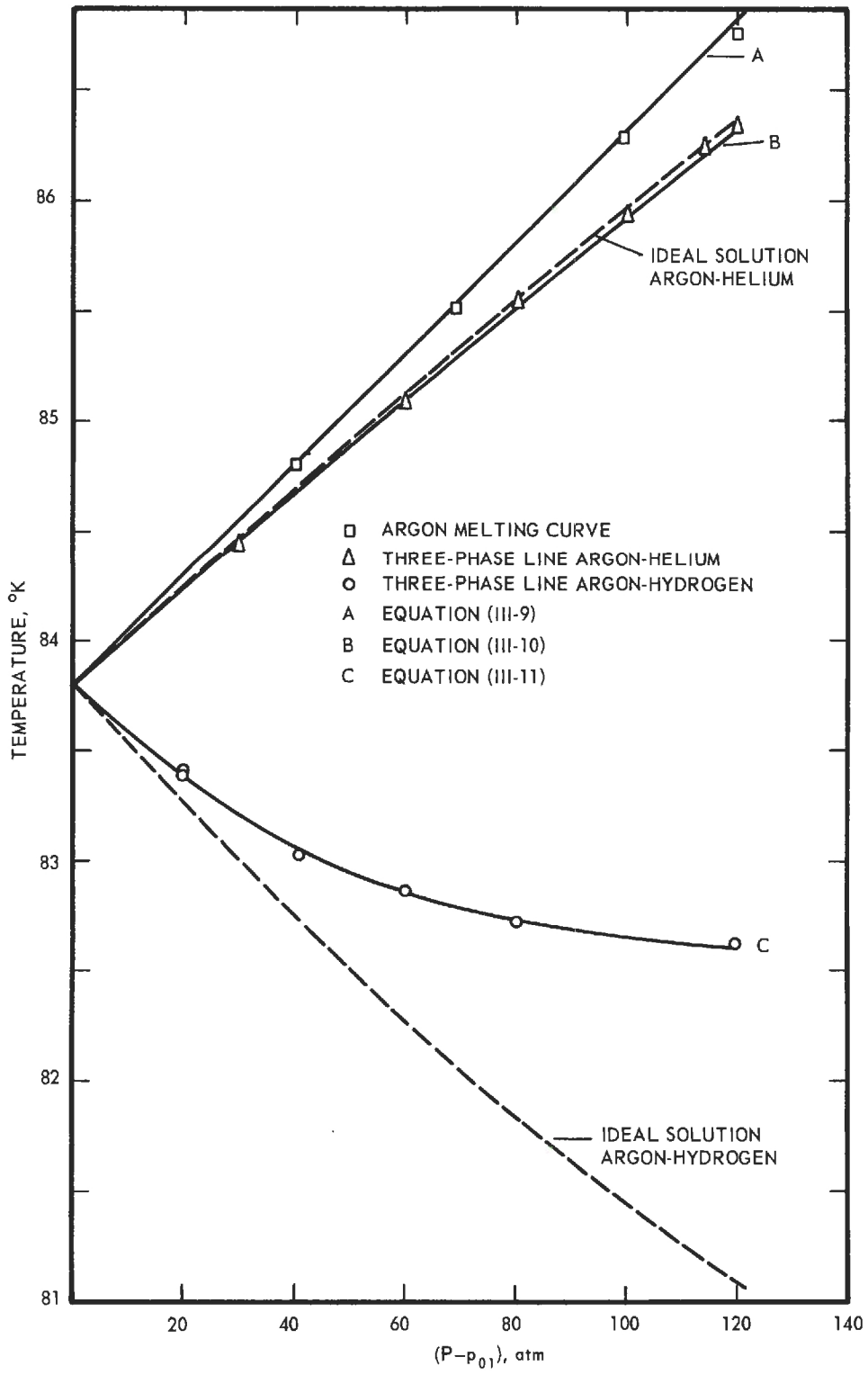

Figure 7. Melting Curve of Pure Argon and the Three-Phase Lines for Argon-Helium and Argon-Hydrogen as a Function of Pressure.

For A-He,

$$T = 83.796 + 2.0837 \times 10^{-2}P + 2.267 \times 10^{-5}P^2 - 1.726 \times 10^{-7}P^3 \qquad \text{(III-10)}$$

For A-H_2,

$$T = 83.830 - 2.6454 \times 10^{-2}P + 2.0055 \times 10^{-4}P^2 - 5.518 \times 10^{-7}P^3 \qquad \text{(III-11)}$$

The experimental points are compared to the fitted curves in Figure 7. The ideal freezing point curves shown in Figure 7 are discussed in Chapter VI. These were calculated based on the assumptions of an ideal liquid solution and a pure condensed solid.

Vapor Pressure of Argon

At the conclusion of all phase equilibrium measurements, the vapor pressure of pure argon was measured between 12.1 and 42.6 atmospheres pressure. These are given in Table 20 in Appendix D compared with the results of Michels et al.[55] These measurements were made as a consistency check on the pressure measurements, temperature measurements and the purity of the argon. The deviations of the observed and calculated vapor pressures are in general less than the 1/2 per cent accuracy claimed over the range of pressures in the phase equilibrium measurements.

Accuracy of Phase Equilibrium Measurements

Gas and Liquid Phase Compositions

The equilibrium gas phase compositions are believed to be accurate to within ± 3 per cent and ± 2 per cent of the mole fraction of argon in the argon-helium and argon-hydrogen systems, respectively. The equilibrium liquid phase compositions are believed to be accurate to

within ± 2 per cent of the mole fraction of either helium or hydrogen in liquid argon. These assignments of accuracy are based on the ability to determine the temperature to within ± 0.03° K and the pressure to within ± 1/2 per cent of the measured value along with considerations of nearness to equilibrium and problems associated with composition analysis discussed elsewhere.

Three-Phase Lines and Melting Curve of Argon

The determination of the three-phase lines and the melting curve of pure argon were not accomplished at equilibrium conditions, but from cooling curves, thus making the assessment of their accuracies somewhat more difficult. Based on the agreement of the melting curve with Equation (III-9) given by Clusius and Weigand[15] and the overall precision of the determinations of both three-phase lines and the normal melting curve of argon, the reported values of temperature and pressure are believed to be accurate to within ± 0.05° K and ± 1/2 per cent of the reported pressure.

CHAPTER IV

METHODS OF PREDICTING ENHANCEMENT FACTORS AND OTHER RELATED CALCULATIONS

General

In Chapter I a number of general thermodynamic relations were given. These relations are used in conjunction with various equations of state to predict the enhancement factor and to make a number of other calculations of interest. One such calculation is that of the second virial interaction coefficient, B_{12}, from the experimental values of the phase compositions at equilibrium and other experimental quantities. Kirk[42] and Kirk et al.[44] have studied a number of methods of predicting the enhancement factor. A number of the relations used here are taken from Kirk[42] using essentially the same nomenclature to permit ease in comparison of results and conclusions regarding the methods of prediction.

Originally this work was not intended to include methods of correlation, but only methods of prediction of gas phase compositions from the properties of the pure components. However, a simple correlation for the argon-helium gas phase compositions developed by Mullins and Ziegler[59] is presented. In addition, a correlation for the liquid and gas phase compositions of the argon-hydrogen system is suggested by several calculations using the BWR equation of state to represent both gas and liquid phases.

Prediction of Enhancement Factor

Equation (I-7) is the thermodynamic relation used to predict the enhancement factor. The solution of Equation (I-7) requires, in general, a knowledge of the compressibility of the pure condensed argon, the second and third virial coefficients of pure argon, an equation of state for the gas mixture, and a knowledge of the composition and activity coefficient of the argon in the condensed phase. Quite often in the type of system considered here, the solubility of component 2 in the condensed phase is quite small and can be neglected. Kirk,[42] in his study of the prediction of the enhancement factor for methane in hydrogen, neglected the term $\ln \gamma_1' x_1$ in Equation (I-7) because of the low solubility of hydrogen in liquid methane and the uncertainty of the value of γ_1'. In the solid-gas region the neglect of the term is likely completely insignificant in the methane-hydrogen system as well as in the systems studied here. Because the solubility of helium and hydrogen in argon was measured here, and also because measurements of the three-phase line indicate that the value of γ_1' is very nearly unity, the term $\ln \gamma_1' x_1$ was evaluated. This permits a better comparison of the equations of state used to predict the properties of the gas mixture.

Equations of State Considered

The equations of state considered here may be broadly grouped into three general categories: empirical equations of state, the virial equation of state, and "hybrid" equations of state. The "hybrid" equations of state are formed from a combination of the first two types.

Kirk[42] considered two empirical equations of state, the Benedict-Webb-Rubin[6] and the Beattie-Bridgeman[3] equations. The BWR equation is

an extension of the Beattie-Bridgeman equation and contains eight adjustable parameters, three more than the Beattie-Bridgeman equation. The Beattie-Bridgeman equation was not examined in the present work.

The virial equation of state was examined here using methods for computing the second and third virial coefficients of the gas similar to those of Kirk.[42] One generalized correlation of the second and third virial coefficient was examined. This was a three parameter, reduced correlation developed by Pitzer and Curl[61] and extended by Prausnitz and Gunn.[64] Two theoretical methods of computing the second virial coefficient were examined. One of these methods, based on the two-parameter, Lennard-Jones (6-12) intermolecular potential function, was also used to compute the third virial coefficient. The other statistical mechanical second virial coefficient calculation was based on the Kihara core model[40] with a (6-12) intermolecular potential function as given by Prausnitz and Myers.[66] The Kihara core model contains five parameters, but three are related to the shape and size of the core and are not independent.

General Mixture Rules

Kirk[42] has discussed at length the various equations of state and the mixture rules used to predict the properties of mixtures from the parameters for the pure components. The three mixture rules generally used to combine the constants of the pure components are given by Equations (IV-1) through (IV-3). These are normally referred to as the linear, the geometric, and the Lorentz averages.

$$N_{12} = (N_1 + N_2)/2 \qquad \text{(IV-1)}$$

$$N_{12} = (N_1 N_2)^{1/2} \qquad \text{(IV-2)}$$

$$N_{12} = [(N_1^{1/3} + N_2^{1/3})/2]^3 \qquad \text{(IV-3)}$$

For $N_1 \neq N_2$, the linear average is greater than the Lorentz, which is greater than the geometric. The linear average is usually associated with length quantities, the geometric with energy parameters, and the Lorentz with volume quantities.

Virial Equation of State

From statistical mechanics the equation of state for a gas may be expressed as a power series in gas density or reciprocal volume.[34]

$$\frac{PV}{RT} = 1 + \frac{B}{V} + \frac{C}{V^2} + \frac{D}{V^3} + \ldots \qquad \text{(IV-4)}$$

For the particular gas or gas mixture, the coefficients B, C, and D are functions of temperature only. For a gas mixture the second and third virial coefficients are given by

$$B_m = y_1^2 B_{11} + 2y_1 y_2 B_{12} + y_2^2 B_{22} \qquad \text{(IV-5)}$$

$$C_m = y_1^3 C_{111} + 3y_1^2 y_2 C_{112} + 3y_1 y_2^2 C_{122} + y_2^3 C_{222} \qquad \text{(IV-6)}$$

The values of B and C may be obtained from experimental measurements or calculated assuming a particular expression for the potential energy function between two molecules. Integration of Equation (I-7) using these relations for the virial equation of state yields the following expression for the enhancement factor.

$$\ln \Phi = \frac{1}{RT}\left[a(P-p_{01}) + \frac{b}{2}(P-p_{01})^2 + \frac{c}{3}(P-p_{01})^3\right]$$

$$+ \frac{2B_{11}}{V_{01}} + \frac{3C_{111}}{2V_{01}^2} - \ln Z_{01} - 2(y_1B_{11} + y_2B_{12})/V_m$$

$$- 3(y_1^2C_{111} + 2y_1y_2C_{112} + y_2^2C_{122})/2V_m^2$$

$$+ \ln Z_m + \ln \gamma_1' x_1 \qquad \text{(IV-7)}$$

The methods used for calculating the second and third virial coefficients and the various interaction coefficients are described in the following sections.

Lennard-Jones (6-12)

Lennard-Jones Classical (LJCL). The virial coefficients of a gas can be calculated, in principle, from statistical mechanics if the intermolecular potential between molecules is known. The Lennard-Jones (6-12) intermolecular potential function is one model which has been widely used to describe the potential energy between non-polar molecules. This function is a two-parameter, spherically symmetric function with an attractive force inversely proportional to the seventh power of the distance between the molecules and a repulsive force inversely proportional to the thirteenth power of the distance between the molecules, which are assumed to be mass points. The potential energy is given by Equation (IV-8).

$$U(r) = 4e\left[\left(\frac{\sigma}{r}\right)^{12} - \left(\frac{\sigma}{r}\right)^{6}\right] \qquad \text{(IV-8)}$$

The two parameters e and σ have the dimensions of energy and length. The quantity σ is the value of r at $U(r) = 0$ and e is the minimum potential energy which occurs at $r = 2^{1/6}\,\sigma$.

From this potential function, Hirschfelder et al.[34] present methods of obtaining the reduced second virial coefficient, B^*_{CL}, as a function of the reduced temperature, T^*.

$$B_{ij} = (b_o)_{ij} B^*_{CL}(T^*) \qquad \text{(IV-9)}$$

$$T^* = T/(e/k) \qquad \text{(IV-10)}$$

The reducing parameter, b_o, which has the units of volume, is related to the parameter σ by Equation (IV-11).

$$b_o = \frac{2\pi N_A \sigma^3}{3} \qquad \text{(IV-11)}$$

Hirschfelder et al.[34] also present methods of obtaining the reduced third virial coefficient as a function of T^*. The reduced third virial is defined by

$$C_{ijk} = b^2_{o_{ijk}} C^*_{CL}\ (T^*_{ijk}) \qquad \text{(IV-12)}$$

The mixing rules used for the two parameters in the Lennard-Jones (6-12) intermolecular potential function were

$$(e/k)_{ij} = (e/k)_i^{1/2}\ (e/k)_j^{1/2} \qquad \text{(IV-13)}$$

$$(e/k)_{ijk} = (e/k)_i^{1/3}\ (e/k)_j^{1/3}\ (e/k)_k^{1/3} \qquad \text{(IV-14)}$$

$$b_{o_{ij}} = \frac{1}{8}\left[b_{o_i}^{1/3} + b_{o_j}^{1/3}\right]^3 \qquad \text{(IV-15)}$$

$$b_{o_{ijk}} = 1/27\left[b_{o_i}^{1/3} + b_{o_j}^{1/3} + b_{o_k}^{1/3}\right]^3 \qquad \text{(IV-16)}$$

Lennard-Jones Quantum (LJ3Q). At low temperatures the second virial coefficient of the light gases, in this case helium and hydrogen,

should be corrected for quantum effects. Hirschfelder et al.[34] give the following series containing the first three translational quantum correction terms and the ideal gas quantum correction term, B_o^*.

$$B_{ij}/(b_o)_{ij} = B_{CL}^* + \Lambda_{ij}^{*2} B_I^* + \Lambda_{ij}^{*4} B_{II}^* + \Lambda_{ij}^{*6} B_{III}^* + \ldots - \Lambda_{ij}^{*3} B_o^* \qquad \text{(IV-17)}$$

The three translational quantum correction terms, B_I^*, B_{II}^* and B_{III}^*, and the ideal gas quantum correction term B_o^*, are functions of the reduced temperature, T^*. The quantum mechanical parameter Λ^* is given by Equation (IV-18).

$$\Lambda_{ij}^{*2} = \frac{h^2}{k\sigma_{ij}^2 m_{ij}(e/k)_{ij}} \qquad \text{(IV-18)}$$

In Equation (IV-18) the mixing rules for σ_{ij} and m_{ij} are given by Equations (IV-19) and (IV-20) and $(e/k)_{ij}$ by Equation (IV-13).

$$\sigma_{ij} = (\sigma_i + \sigma_j)/2 \qquad \text{(IV-19)}$$

$$m_{ij} = 2m_i m_j/(m_i + m_j) \qquad \text{(IV-20)}$$

DeBoer and Michels[21] have obtained series approximations for B_I^* and B_{II}^* and their results are published in Hirschfelder et al.[34] Unfortunately there are several small errors in the series coefficients. These are discussed by Kirk,[42] who recomputed the first 42 coefficients of each of the series approximations for the first three translational quantum correction terms, B_I^*, B_{II}^* and B_{III}^*, from relations given by Kihara.[41] These recomputed coefficients agree with the 14 values given by Kihara[41]

for each of the series coefficients. The values given by Kirk[42] are used in this work. The sign of the quantum correction term for the ideal gas, B_o^*, in Equation (IV-17) is given here for the Bose-Einstein gas. The value of B_o^* is given by Equation (IV-21).

$$B_o^* = \frac{3}{32\pi^{5/2}(T^*)^{3/2}} \qquad \text{(IV-21)}$$

Kihara Core Model (KIH)

Kihara[40] has derived general expressions for the second virial coefficient of gases assuming an impenetrable core rather than a point mass for the molecules as used in the Lennard-Jones model. The core may be any convex shaped model. The shape is normally determined by the geometry of the molecule. The potential energy for a pair of molecules is expressed as a function of the shortest distance, ρ, between the molecular cores. For a (6-12) potential function the potential energy, U, is given by the following relation.

$$U = U_o \left[\left(\frac{\rho_o}{\rho}\right)^{12} - 2\left(\frac{\rho_o}{\rho}\right)^{6}\right] \qquad \text{(IV-22)}$$

The parameter ρ_o is the shortest distance between molecular cores at the minimum potential energy, U_o. Kihara[41] gives the following expression for gas mixtures.

$$\frac{(B_k)_{ij}}{N_A} = \frac{2\pi}{3}(\rho_o)_{ij}^3 F_3 + \frac{(M_o)_i + (M_o)_j}{2}(\rho_o)_{ij}^2 F_2 + \left[\frac{(S_o)_i + (S_o)_j}{2} + \frac{M_{oi}M_{oj}}{4\pi}\right](\rho_o)_{ij} F_1 + \frac{(V_o)_i + (V_o)_j}{2} + \frac{(M_o)_i(S_o)_j + (M_o)_j(S_o)_i}{8\pi} \qquad \text{(IV-23)}$$

The three functions F_1, F_2, and F_3 are functions of Z ($Z = U_o/kT$), and may be obtained from tabular results[16] or calculated from the relation given by Kihara.[40]

$$F_s = - \frac{s}{12} \sum_{j=0}^{\infty} \left[\frac{2^j}{j!} \Gamma \left(\frac{6j-s}{12} \right) \right] Z^{(6j + s)/12} \qquad \text{(IV-24)}$$

Equation (IV-24) may be rewritten as

$$F_s = \sum_{j=0}^{\infty} b_s(j) \, Z^{(6j + s)/12} \qquad \text{(IV-25)}$$

The first 40 coefficients have been calculated for s = 1, 2, 3 and are given by Kirk.[42] These coefficients were used here to calculate the values of F_1, F_2 and F_3 rather than the tabular values of Connolly and Kandalic.[16]

The three parameters M_o, S_o, and V_o are related to the core size and shape and have the dimensions of length, area, and volume.

Prausnitz and Myers,[66] in determining the constants for the Kihara core model with a (6-12) intermolecular potential function, have included quantum corrections for helium, hydrogen and mixtures containing these light gases. The correction for the first two translational quantum terms used by Prausnitz and Myers[66] were based on the Lennard-Jones (6-12) model and is therefore strictly correct only for the case of a spherical core with vanishing radius. The equation used in the present work for helium, hydrogen and their interaction second virial coefficients with argon is expressed as

$$B_{ij} = (B_K)_{ij} + (b_o)_{ij} \left[\Lambda_{ij}^{*\,2} B_I^* + \Lambda_{ij}^{*\,4} B_{II}^* + \ldots - \Lambda_{ij}^{*\,3} B_o^* \right] \qquad \text{(IV-26)}$$

The value of σ for the Lennard-Jones (6-12) intermolecular potential function is related to the Kihara core model parameter, ρ_o, by Equation (IV-27), which is exact for the spherical core.

$$\sigma_{ij} = 2^{-1/6} \rho_{oij} + \frac{M_{oi} + M_{oj}}{4\pi} \qquad \text{(IV-27)}$$

The mixture rule for ρ_{oij} is the same as for σ_{ij}, namely Equation (IV-19), and that for $(U_o/k)_{ij}$ is the same as for $(e/k)_{ij}$, Equation (IV-13).

Pitzer-Prausnitz-Gunn (PPG)

Pitzer and coworkers[18,19,60,61,62,63] have developed a generalized three-parameter correlation for predicting the thermodynamic properties of fluids. Their correlation is based on the concept of a "simple" fluid for which the reduced vapor pressure is defined to be 0.1 at a reduced temperature of 0.7 Fluids which follow this relation very closely are A, Kr, Xe and CH_4. They chose as their three parameters the critical pressure, temperature and the acentric factor, ω, which is defined as

$$\omega = - \log P_R - 1.000 \qquad \text{(IV-28)}$$

where P_R is the reduced vapor pressure at a reduced temperature of 0.7. Pitzer et al.[63] give tables for the compressibility factor Z, as a function of ω and the compressibility of a simple fluid. Pitzer and Curl[61] give the following expressions for the second virial coefficient of a fluid.

$$\frac{B P_c}{RT_c} = B^o_{RP} + \omega B'_{RP} \qquad \text{(IV-29)}$$

B^{o}_{RP} is the second virial coefficient of a "simple" fluid given by

$$B^{o}_{RP} = 0.1445 - \frac{0.330}{T_R} - \frac{0.1385}{T_R^2} - \frac{0.0121}{T_R^3} \qquad \text{(IV-30)}$$

and

$$B'_{RP} = 0.073 + \frac{0.46}{T_R} - \frac{0.50}{T_R^2} - \frac{0.097}{T_R^3} - \frac{0.0073}{T_R^8} \qquad \text{(IV-31)}$$

Prausnitz and Gunn[64] have modified and extended the acentric factor to permit the estimation of the virial coefficients of mixtures. To permit more rational mixture rules based on a volumetric average, they reduce the virial coefficient with V_c rather than P_c/RT_c.

$$\frac{B_{ij}}{(V_c)_{ij}} = B^{o}_{RV}\,(T/T_{c_{ij}}) + \omega_{ij} B'_{RV}\,(T/T_{c_{ij}}) \qquad \text{(IV-32)}$$

where the two relations for B^{o}_{RV} and B'_{RV} are given by Equations (IV-33) and (IV-34).

$$B^{o}_{RV} = \frac{B^{o}_{RP}}{0.291} \qquad \text{(IV-33)}$$

$$B'_{RV} = \frac{0.274\, B^{o}_{RP} + B'_{RP}}{0.291 - 0.08\omega} \qquad \text{(IV-34)}$$

These two relations are derived from the relation given for Z_c based on the tables for Z given by Pitzer et al.[63]

$$Z_c = 0.291 - 0.08\omega \qquad \text{(IV-35)}$$

Prausnitz and Gunn[64] proposed the following mixture rules.

$$(T_c)_{12} = [(T_c)_1(T_c)_2]^{\frac{1}{2}} - \Delta(T_c)_{12} \qquad \text{(IV-36)}$$

$$(V_c)_{12} = \tfrac{1}{2}\,[(V_c)_1 + (V_c)_2] - \Delta(V_c)_{12} \qquad \text{(IV-37)}$$

$$\omega_{12} = \tfrac{1}{2}\,(\omega_1 + \omega_2) \qquad \text{(IV-38)}$$

Prausnitz and Gunn[64] note that from a theoretical standpoint the preferred mixture rule for $(V_c)_{12}$ is

$$(V_c)_{12} = \left[\frac{(V_c)_1^{1/3} + (V_c)_2^{1/3}}{2}\right]^3 \qquad \text{(IV-39)}$$

In their work Prausnitz and Gunn used the simple linear averages given by Equations (IV-37) and (IV-38) for $(V_c)_{12}$ and ω_{12} and then evaluated $(T_c)_{12}$ to fit experimental data for a number of systems. A graph is given for the evaluation of $\Delta(T_c)_{12}$ as a function of the ratio of the critical volumes. For systems where the ratio of the critical volumes exceeded three, they give an additional chart for the correction $\Delta(V_c)_{12}$ in Equation (IV-37). They point out that $\Delta(T_c)_{12}$ is positive for all systems studied, which is said to be in agreement with London's theory of dispersion forces, i.e., that the geometric average of the dispersion energy parameter for molecules of different sizes is an upper bound. In the present work $\Delta(T_c)_{12}$ was taken to be zero. The few values of $\Delta(V_c)_{12}$ calculated by Prausnitz and Gunn were all positive, indicating that the Lorentz average given by Equation (IV-39) would probably be better than the simple linear average. In the systems studied here the Lorentz average, Equation (IV-39), was used.

Gunn[32] presents tabular values for the reduced third virial coefficient, $C^{o}_{RV}(T_R)$ as a function of the reduced temperature, T_R.

$$C_{ijk} = (V_c)^2_{ijk} \left[C^{\circ}_{RV}(T_R)_{ijk} + 0.2\omega_{ijk} \right] \qquad \text{(IV-40)}$$

Kirk[42] has fitted the tabular data by a least squares procedure to obtain the two polynomials given by Equations (IV-41) and (IV-42).

For $T_R \leq 1.08$,

$$C^{\circ}_{RV} = -12.3645 + 39.5249/T_R - 46.9218/T_R^2 + 26.1531/T_R^3 - 5.91949/T_R^4 \qquad \text{(IV-41)}$$

For $T_R > 1.08$,

$$C^{\circ}_{RV} = -0.252166 + 1.87811/T_R - 3.19188/T_R^2 + 2.85512/T_R^3 - 0.818336/T_R^4 \qquad \text{(IV-42)}$$

The following mixture rules were used here for Equation (IV-40).

$$(T_c)_{ijk} = \left[(T_c)_i (T_c)_j (T_c)_k \right]^{1/3} \qquad \text{(IV-43)}$$

$$(V_c)_{ijk} = \left[\frac{V_{c_i}^{1/3} + V_{c_j}^{1/3} + V_{c_k}^{1/3}}{3} \right]^3 \qquad \text{(IV-44)}$$

$$\omega_{ijk} = \frac{1}{3} (\omega_i + \omega_j + \omega_k) \qquad \text{(IV-45)}$$

Benedict-Webb-Rubin Equation of State (BWR)

The Benedict-Webb-Rubin equation of state[6] is an eight-parameter, empirical equation of state which is an extension of the Beattie-Bridgeman equation of state.[3] The constants for argon and hydrogen were determined in this work as described in Appendix A. There appear to be no published constants for helium and none were determined here. For a mixture of either gases or liquids the BWR equation may be written[42]

$$P = RT\rho_m + RTB_m \rho_m^2 + RTC'_m \rho_m^3 + a_m\alpha_m \rho_m^6 + \frac{c_m (1 + \gamma_m\rho_m^2) \exp(-\gamma_m\rho_m^2)\rho_m^3}{T^2} \quad \text{(IV-46)}$$

where

$$B_m = (B_o)_m - \frac{(A_o)_m}{RT} - \frac{(C_o)_m}{RT^3} \quad \text{(IV-47)}$$

$$C'_m = b_m - \frac{a_m}{RT} \quad \text{(IV-48)}$$

The mixture rules as originally proposed[7] are

$$N_m = z_1^2 N_{11} + 2z_1 z_2 N_{12} + z_2^2 N_{22} \quad \text{(IV-49)}$$

for $N = A_o$, B_o, C_o and γ. Values of N_{12} are given by

$$N_{12} = (N_1 N_2)^{\frac{1}{2}} \quad \text{(IV-50)}$$

for A_o, C_o and γ.

For B_o both the Lorentz average and the linear average have been investigated.

$$(B_o)_{12} = \left[(B_o)_1 + (B_o)_2\right]/2 \quad \text{(linear)} \quad \text{(IV-51)}$$

$$(B_o)_{12} = \left[(B_o)_1^{1/3} + (B_o)_2^{1/3}\right]^3/8 \quad \text{(Lorentz)} \quad \text{(IV-52)}$$

According to Benedict et al.,[7] the Lorentz average gives the best results for fitting PVT properties, but for predicting phase equilibria in the light hydrocarbons, the linear average gives the best agreement with experimental data.

The mixture relation for the remaining four parameters, a, b, c and α, is

$$N_m = z_1^3 N_{111} + 3z_1^2 z_2 N_{112} + 3z_1 z_2^2 N_{122} + z_2^3 N_{222} \qquad \text{(IV-53)}$$

where

$$N_{ijk} = (N_i N_j N_k)^{1/3} \qquad \text{(IV-54)}$$

Equation (IV-54) is an extension of Equation (IV-2).

The fugacity of a binary fluid mixture is given by[7]

$$\begin{aligned}
\ln \frac{\bar{f}_i}{z_i} = {} & \ln(RT\rho_m) + 2(z_i B_{ii} + z_j B_{ij})\rho_m + \frac{3}{2}\left[\bar{b}_m^{2/3} b_i^{1/3} - \frac{a_m^{2/3} a_i^{1/3}}{RT}\right]\rho_m^2 \\
& + \frac{3}{5RT}\left(a_m \alpha_m^{2/3} \alpha_i^{1/3} + \alpha_m a_m^{2/3} a_i^{1/3}\right)\rho_m^5 \\
& + \frac{c_m^{2/3}}{RT^3 \gamma_m}\left\{3c_i^{1/3} - 2c_m^{1/3}\left(\frac{\gamma_i}{\gamma_m}\right)^{1/2} - \left[3c_i^{1/3}\left(1 + \frac{\gamma_m \rho_m^2}{2}\right)\right.\right. \\
& \left.\left. - c_m^{1/3}\left(\frac{\gamma_i}{\gamma_m}\right)^{1/2}\left(2 + 2\gamma_m \rho_m^2 + \gamma_m^2 \rho_m^4\right)\right] \exp(-\gamma_m \rho_m^2)\right\}
\end{aligned} \qquad \text{(IV-55)}$$

The enhancement factor equation, resulting from an integration of Equation (I-7) with the gas phase represented by Equation (IV-46) is

$$\begin{aligned}
\ln \Phi = {} & \frac{1}{RT}\left[a(P - p_{01}) + \frac{b}{2}(P - p_{01})^2 + \frac{c}{3}(P - p_{01})^3\right] + 2\frac{B_{11}}{V_{01}} + \frac{3}{2}\frac{C'_{111}}{V_{01}^2} - \ln Z_{01} \\
& + \ln Z_m - 2(y_1 B_{11} + y_2 B_{12})\rho_m - \frac{3}{2}\left(y_1^2 C'_{111} + 2y_1 y_2 C'_{112}\right. \\
& \left. + y_2^2 C'_{122}\right)\rho_m^2 - 3\left(a_m \alpha_{1mm} + \alpha_m a_{1mm}\right)\frac{\rho_m^5}{5RT} - \frac{3c_{1mm}}{RT^3 \gamma_m} + \frac{2c_m \gamma_{1m}}{RT^3 \gamma_m^2} \\
& + \left[\frac{3c_{1mm}}{RT^3 \gamma_m} - \frac{2c_m \gamma_{1m}}{RT^3 \gamma_m^2} + \frac{3c_{1mm}\rho_m^2}{2RT^3} - \frac{2c_m \gamma_{1m} \rho_m^2}{RT^3 \gamma_m} - \frac{c_m \gamma_{1m} \rho_m^4}{RT^3}\right] \\
& \times \left[\exp(-\gamma_m \rho_m^2)\right]
\end{aligned} \qquad \text{(IV-56)}$$

In Equation (IV-56) only the second and third virial coefficients are used to represent the properties of pure argon at p_{01}. Equation (IV-56) can also be derived from the fugacity relation given by Equation (IV-55). The mixture rules for B_{ij} and C'_{ijk} in Equation (IV-56) and B_{ij} in (IV-55) are given by Equations (IV-57) and (IV-58).

$$B_{ij} = (B_o)_{ij} - \frac{(A_o)_{ij}}{RT} - \frac{(C_o)_{ij}}{RT^3} \qquad \text{(IV-57)}$$

$$C'_{ijk} = b_{ijk} - \frac{a_{ijk}}{RT} \qquad \text{(IV-58)}$$

The mixing relations for the parameters are given by Equations (IV-49) through (IV-54). For the constants containing m as a subscript, the same relations apply but with two applications of the mixing relation. For example,

$$\gamma_{1m} = (\gamma_1\gamma_m)^{1/2} = \left[\gamma_1 \left(y_1^2\gamma_1 + 2y_1y_2\gamma_{12} + y_2^2\gamma_2\right)\right]^{1/2} \qquad \text{(IV-59)}$$

$$a_{1mm} = (a_1a_m^2)^{1/3} = \left[a_1(y_1^3a_1 + 3y_1^2y_2a_{112} + 3y_1y_2^2a_{122} + y_2^3a_2)^2\right]^{1/3} \qquad \text{(IV-60)}$$

Another slightly different mixture rule for the combined parameter $(a\alpha)$, proposed by Hydrocarbon Research, Inc.,[49] was evaluated by Kirk[42] for the methane-hydrogen system.

$$(a\alpha)_m = \left[y_1(a\alpha)_1^{1/6} + y_2(a\alpha)_2^{1/6}\right]^6 \qquad \text{(IV-61)}$$

Use of this mixture rule results in the substitution of

$$-6(a_1\alpha_1)^{1/6}\left[y_1(a_1\alpha_1)^{1/6} + y_2(a_2\alpha_2)^{1/6}\right]^5 \rho_m^5/5RT$$

for the term

$$-3(a_m\alpha_{1mm} + \alpha_m a_{1mm})\rho_m^5/5RT$$

in Equation (IV-56).

Calculation of the Second Virial Interaction Coefficient from Experimental Phase Equilibrium Data

Equation (IV-7) may be rearranged to solve for the second virial interaction coefficient, B_{12}.

$$B_{12} = \frac{V_m}{2y_2}\left\{\frac{2B_{11}}{V_{01}} + \frac{3C_{111}}{2V_{01}^2} - \ln Z_{01} + \frac{1}{RT}\left[a(P-p_{01}) + \frac{b}{2}(P-p_{01})^2 + \frac{c}{3}(P-p_{01})^3\right]\right.$$

$$- \frac{2y_1B_{11}}{V_m} - 3(y_1^2C_{111} + 2y_1y_2C_{112} + y_2^2C_{122})/2V_m^2$$

$$\left. + \ln Z_m + \ln \gamma_1'x_1 - \ln \Phi\right\} \qquad \text{(IV-62)}$$

Any of the methods discussed in the previous sections may be used to represent the second and third virial coefficient and the third virial interaction coefficients. Equation (IV-62) is then solved at each experimental point on an isotherm. The value of B_{12} obtained from each experimental point is plotted against $(P-p_{01})$. The value extrapolated to $(P-p_{01}) = 0$ is then assumed to be the correct value of B_{12}. Since only the extrapolated value is used, the calculated values of B_{12} need not be solved iteratively. The value of B_{12} used to calculate the volume of the gas mixture V_m, may be calculated from the mixture rules assumed in the previous sections. One might suppose that the solubility of the gas in the liquid argon can be neglected, since the term $\ln \gamma_1'x_1$ is 0 at $(P-p_{01}) = 0$. If B_{12}' is the value calculated assuming $\ln \gamma_1'x_1 = 0$,

then it can be shown that

$$B_{12} \cong B'_{12} - \frac{RTZ_{01}}{2\hat{K}^{o}} \qquad \text{(IV-63)}$$

where $\hat{K}^{o}$ is defined by Equation (IV-64).

$$\hat{K}^{o} = \lim_{x_2 \to 0} \frac{Py_2}{x_2} \qquad \text{(IV-64)}$$

At 100° K for the two systems considered here, the error in B_{12} would be approximately 0.6 cc/gm mole for argon-helium and 5.3 cc/gm mole for argon-hydrogen.

Prediction of Phase Equilibria with BWR Equation

General

The BWR equation of state[6] was, from its inception, intended to be used to predict phase equilibria in the light hydrocarbon systems. Good agreement was found between computed and experimental vapor-liquid equilibrium data by Benedict et al.[7,9] for a number of the hydrocarbon systems ranging from methane up to heptane. The equation has also been used by Stotler and Benedict[75] to correlate phase equilibria in the nitrogen-methane system. They found that it was necessary to adjust one of the mixture constants, $(A_o)_{12}$, to obtain a good correlation. Price et al.[67] calculated K values for the methane-ethane-propane system, and found that the agreement between the predicted and experimental K values for methane was good, but that at temperatures below the boiling point of ethane and propane the K factors for those two components deviated considerably from experimental results with decreasing temperature. Schillar and Canjar[72] obtained good results for the pre-

diction of K factors for the nitrogen-carbon monoxide system. Motard and Organick[58] have used the equation to correlate phase equilibrium data in the hydrogen-methane-propane system with good results for the K factors of hydrogen and methane, but were unable to predict the K factors for propane. At 144° K the K factors were in disagreement by as much as two orders of magnitude. Prausnitz and Keeler[65] have suggested that the experimental K factors for propane are probably in error. Motard and Organick[58] adjusted C_o and γ of hydrogen to obtain their correlation. These adjusted values of γ were then used with good success to predict K factors in hydrogen-methane-ethane and hydrogen-methane-ethylene systems.

Phase Equilibria in the Argon-Hydrogen System

The applicability of the BWR equation of state, Equation (IV-46), to the prediction of phase equilibria in the argon-hydrogen system was investigated in the present work. At equilibrium, the following relations must be satisfied for a binary system.

$$P(\rho_m^G, y_1) = P(\rho_m^L, x_1) \qquad \text{(IV-65)}$$

$$\bar{f}_1^G(\rho_m^G, y_1) = \bar{f}_1^L(\rho_m^L, x_1) \qquad \text{(IV-66)}$$

$$\bar{f}_2^G(\rho_m^G, y_1) = \bar{f}_2^L(\rho_m^L, x_1) \qquad \text{(IV-67)}$$

These relations can be calculated from Equation (IV-46) and (IV-55). The mixture relations were the same as used for the enhancement factor equation except that the linear average, Equation (IV-51), was used for $(B_o)_{12}$. The mixture relation for $(a\alpha)$ proposed by Hydrocarbon Research, Inc.[49] was also investigated. The computational procedure for solving

Equations (IV-65) through (IV-67) is discussed in Appendix E.

CHAPTER V

COMPUTATIONS

Selection of Data for Computations

General

The selection of the necessary data for use in the calculations described in the preceding and subsequent sections are summarized here. A number of the parameters for argon were taken from the vapor pressure calculations of Ziegler et al.[84] Values of the equation of state parameters for hydrogen were the same as those used by Kirk[42] with the exception of the Benedict-Webb-Rubin constants, which have been determined in the present work from the PVT data of Goodwin et al.[31] and Michels et al.[54] The determination of the BWR constants for argon and hydrogen is discussed in detail in Appendix A.

Vapor Pressure

The vapor pressure of argon below 88° K has been calculated by Ziegler et al.[84] and compared to the available experimental data. For use in the present work, the calculated values of the vapor pressure have been adjusted by the ratio of the normal boiling point of oxygen on the NBS 1955 Scale (90.18° K) and the normal boiling point selected by Ziegler et al.[84] (90.168° K). These adjusted values have been fitted to two equations over the indicated temperature range.

$T \leq 83.81^{\circ}$ K

$$\text{Log}_{10}p_{01}(\text{atm}) = 5.9057813 - \frac{740.68409}{T} + \frac{35110.773}{T^2} - \frac{1661065.3}{T^3} + \frac{28979491.0}{T^4} \qquad \text{(V-1)}$$

$83.81^{\circ} \leqq T \leq 88.0^{\circ}$ K

$$\text{Log}_{10}p_{01}(\text{atm}) = 3.7109859 - \frac{298.12324}{T} \quad \frac{2257.2649}{T^2} \qquad \text{(V-2)}$$

Above 88° K the vapor pressure of argon was represented by Equation (V-3) given by Michels et al.[55]

$$\text{Log}_{10}p_{01}(\text{atm}) = -\frac{550.8211}{T} - 8.7849395\ \text{Log}_{10}(T) + 0.0174713(T) + 21.83790 \qquad \text{(V-3)}$$

Molal Volume of Condensed Argon

Solid Argon. The density of solid argon has been determined by a number of investigators. A summary of the experimental results is given in Table 7. The results of Dobbs et al.[24] are the smoothed results of determinations between 20° and 80° K. Between 20° and 60° K the values were determined from X-ray measurements. Above 60° K the density was determined by the condensation of gas into a known volume. Their results are stated to be accurate to 0.001 gm/cc. The change in volume at the triple point has been determined by Clusius and Weigand,[15] and Simon et al.[73] from the melting curve and the Clapeyron equation. Bridgeman[10] has measured the change in volume along the melting curve. Other X-ray determinations at single points were made by de Smedt and Keesom[23] at 20° K and by Simon and von Simson[74] at 40° K. A recent determination of the density at 4.2° K was made by Henshaw[33] using

Table 7. Density and Molal Volume of Solid Argon

Temperature (°K)	Density (gm/cc)	Molal Volume (cc/gm mole)	Year	Investigator
4.2	1.83	21.83	1958	Henshaw[33]
20	1.68	23.78	1925	de Smedt and Keesom[23]
20	1.764 ± 0.001	22.64	1956	Dobbs et al.[24]
40	1.737 ± 0.001	23.00	1956	Dobbs et al.[24]
40	1.65 ± 0.02	24.21	1924	Simon and von Simson[74]
60	1.691 ± 0.001	23.62	1956	Dobbs et al.[24]
80	1.636 ± 0.001	24.42	1956	Dobbs et al.[24]
83.80		24.64[a]	1940	Clusius and Weigand[15]
83.80		25.21[a]	1930	Simon, Ruhemann and Edwards[73]
83.80		24.99[a]	1934	Bridgman[10]

[a] Molal volume computed using the ΔV reported by the investigator and a value of the molal volume of the liquid of 28.17 cc/gm mole obtained by extrapolation of the data of van Itterbeek and Verbeke.[76]

neutron diffraction. In determining the best values for the molal volume a smooth curve was drawn using only the values of Dobbs et al.,[24] Clusius and Weigand,[15] and Henshaw.[33] The selected values are given in Table 8 at temperatures corresponding to the experimental phase equilibrium isotherms studied here.

Liquid Argon. The density of liquid argon as a function of temperature and pressure was determined by van Itterbeek and Verbeke[76] from 86.6° to 90.5° K and by van Itterbeek et al.[77] from 90° to 148° K. These values are in good agreement with the saturation data of Mathias et al.,[50] which cover the range from 90° to 148° K. The earlier density values of Baly and Donnan[2] measured over the range 84.5° to 89° K are somewhat higher than those of van Itterbeek and Verbeke.[76]

The data of van Itterbeek[76,77] up to 130° K and at pressures up to 150 atmospheres were fit to a double power series in $(P-p_{01})$ and T using the least squares technique described in Appendix H. The resulting equation in this case may be written as,

$$z = \sum_{j=0}^{5} C_j \psi_j(x,y) \qquad (V-4)$$

where,

$$x = T/T_{max} \qquad (V-5)$$

$$y = (P-p_{01})/(P-p_{01})_{max} \qquad (V-6)$$

$$z = v_1^L/(v_1^L)_{max} \qquad (V-7)$$

Equation (V-4) represents the data of van Itterbeek with an accuracy sufficient for the purposes for which it is to be used, and in a form suitable for computational work. The molal volume of the liquid argon

Table 8. Selected Values of the Molal Volume of Solid Argon

Temperature °K	Molal Volume cc/gm mole	Temperature °K	Molal Volume cc/gm mole
68.04	23.93	77.90	24.33
68.07	23.93	79.01	24.38
73.05	24.13	80.06	24.43
74.05	24.17		

was fitted with an average per cent deviation of 0.1926 and a standard error of estimate of 0.095 cc/gm mole. Values of the orthogonal coefficients, the weighting factors, and the normalizing constants are given in Table 9.

Heat Capacity of Condensed Argon

The heat capacity of saturated argon has been measured by a number of investigators. Ziegler et al.[84] in calculating the vapor pressure for argon, represented the heat capacity of saturated solid argon by a series of polynomials fit to the data of Flubacher et al.[29] Equation (V-8), which was used by Ziegler et al.[84] to represent the heat capacity of solid argon from 50° to the triple point, 83.81°, was used in this work to represent the heat capacity in the region of the triple point.

$$c_s^S = -2.8014270 + 0.38832982T - 0.60113758T^2 \times 10^{-2} + 0.35483745T^3 \times 10^{-4} \qquad \text{(V-8)}$$

The liquid heat capacity was assumed to be constant and equal to 10.586 cal/gm mole °K. This value was also based on the data of Flubacher et al.[29]

Heat of Fusion of Argon

The value of the heat of fusion at the triple point of 282.6 cal/gm mole selected in the vapor pressure calculation[84] was also used here. This value was based on an average of the heat of fusion measured by Clusius,[14] and Flubacher et al.[29].

Table 9. Coefficients, Weighting Factors and Normalizing Constants for Least Squares Fit of the Molal Volume of Liquid Argon as a Function of Temperature and Pressure.

Coefficients, α_{ij}

i	j	1	2	3	4	5
0		0.74161135	0.48357268	0.56104979	0.35776613	0.31013003
1			-0.07745182	1.6364241	0.40152561	0.07050932
2				-0.00185100	0.76244139	1.0022584
3					-0.12739752	-0.33516535
4						-0.096096257

Weighting Factors, C_j

j	0	1	2
	0.78601251	0.55552200	-0.041263703
	3	4	5
	0.63080202	-0.23959787	0.016574555

Normalizing Constants

T_{max} = 130.85 $\quad (P-p_{01})_{max}$ = 150.998 $\quad (v_1^L)_{max}$ = 0.037735

Effect of Pressure on Enthalpy of Condensed Argon

The effect of pressure on the enthalpy of solid and liquid argon in the vicinity of the triple point temperature was estimated from the relation

$$\left(\frac{\partial H}{\partial P}\right)_T = V - \left(\frac{\partial V}{\partial T}\right)_P^T \qquad \text{(V-9)}$$

For the liquid phase a mean value of 16.5 cc/gm mole was estimated from the tables of Van Itterbeek et al.[77] For the solid phase a value of 20.8 cc/gm mole was estimated from the data for the molal volume of the solid phase at the triple point with no correction for the effect of pressure. These values are estimates needed to make small corrections for the enthalpy of the solid and liquid phases to predict the activity coefficient from Equation (I-20) and are not considered as selected "best" values.

Benedict-Webb-Rubin Constants

Argon Constants. The Benedict-Webb-Rubin constants for argon appear not to have been previously published. The constants given in Table 10 have been determined using a procedure described in Appendix A. The P-V-T data of Michels et al.[54] were fit by a method of least squares with the compressibility factor, Z, as the dependent variable, and restricting the fit to the experimental critical point of Michels et al.[55] A more detailed description of the agreement and the method of fitting is given in Appendix A.

Hydrogen Constants. There have been several sets of BWR constants published for hydrogen.[26,49,58] The parameters used by Kirk[42] for calculating the enhancement factor in the CH_4-H_2 system were those

Table 10. Selected Parameters for Computation of Gas Properties

Parameter		Argon	Helium	Hydrogen*
Benedict-Webb-Rubin Equation of State, Units are liter-atm-°K-gm mole	A_o	1.2874358	-	2.0432380(-1)
	B_o	3.7352552(-2)	-	2.1746707(-2)
	C_o	Eq. (A-31)	-	5.4767237(+1)
	a	1.7373414(-2)	-	-8.4030059(-4)
	b	1.9170501(-3)	-	5.8987532(-4)
	c	6.6467852(+2)	-	1.9138500
	α	5.9791362(-5)	-	-8.2694217(-5)
	γ	0.0036	-	0.0030
Lennard-Jones (6-12) Potential Function (Classical)	e/k, °K	119.30	6.96	31.41
	b_o, cc/gm mole	50.91	22.9	32.98
Lennard-Jones (6-12) Potential Function (Quantum)	e/k, °K	-	10.22	36.26
	b_o, cc/gm mole	-	21.0	35.50
Kihara Core Model	U_o/k, °K	146.10	9.927	46.00
	ρ_o, Å	3.328	2.921	2.808
	M_o, Å	2.199	0.0	2.330
	S_o, Å^2	0.3848	0.0	0.0
	V_o, Å^3	0.02245	0.0	0.0

(continued)

Table 10. Selected Parameters for Computation of Gas Properties (Concluded)

	Parameter	Argon	Helium	Hydrogen*
Pitzer-Prausnitz-Gunn Generalized Correlation	T_c °K	150.86	8.96	40.47
	V_c cc/gm mole	74.56	29.70	46.09
	ω	-0.005	0.0	0.0

*In all computations the sign of a and α was changed to +, and b′ calculated from Equation (V-10).

given by Hydrocarbon Research Inc.[49] None of the sets were based on the more recent, extensive, low temperature P-V-T data of Goodwin et al.[31] For this reason the constants given in Table 10 were redetermined using data of Goodwin down to 40° K and data of Michels et al.[53] up to 198° K. Densities were restricted to those below about 31 liters/gm mole or slightly less than twice the critical density. The constants were not restricted to fit the critical point, nor were they adjusted to fit vapor pressure data.

Two of the constants, a and α, were found to be negative. In order that this difficulty be circumvented, the suggestion of Eubanks[26] as given by Motard and Organick[58] was followed. The signs of a and α were changed and the value of b was modified to

$$b' = b + \frac{2|a|}{RT} \qquad \text{(V-10)}$$

For a more complete discussion of the constants, the reader is referred to Appendix A.

Parameters for the Lennard-Jones (6-12) Potential Function

Argon. The values of e/k (119.3° K) and b_o (50.91 cc/gm mole) for argon determined by Levelt[48] have been selected for use in this work. These values were previously used in the calculation of the vapor pressure of argon by Ziegler et al.[84] after a review of the available second virial coefficient data for argon. Quantum effects on the second virial coefficient of argon are small and were not considered in this investigation.

Helium. Two sets of parameters were desired for the Lennard-

Jones (6-12) potential function for helium. One of these sets, referred to as LJCL, was determined in the present work (see below) by fitting the second virial coefficient data of White et al.[81] with no quantum corrections. This set of constants was then used to predict the values of the third virial coefficient of helium and the third interaction coefficients of argon-helium. The second set of parameters, referred to as LJ2Q, were values of e/k (10.22° K) and b_o (21.0 cc/gm mole) determined by de Boer and Michels[21] from the second virial coefficient data above 40° K of several investigators, taking into account the first two translational quantum correction terms in Equation (IV-17). There were several small errors in the values of the series coefficients used to calculate B^*_{II} by de Boer and Michels.[20] These errors have been discussed in some detail by Kirk,[42] who gives the corrected values of the series coefficients and also gives additional coefficients through the third translational term B^*_{III}. The values of the parameters given by de Boer and Michels[21] were deemed to be sufficiently accurate not to warrant reevaluation of the parameters.

The LJCL parameters were determined by fitting the experimental second virial coefficient data of White et al.[81] at two temperatures. From a graphical interpolation of the data of White et al.[81] the temperature corresponding to B = 0 was found to be 23.8° K. Since at this point T^* = 3.418 (interpolated from Table I-B of Hirschfelder et al.[34]), the value of e/k was found to be 6.96° K. The value of b_o may then be determined from any other value of the second virial coefficient. In this case a value of B at 100° K (11.6 cc/gm mole) resulted in a value of 22.9 cc/gm mole for b_o.

Hydrogen. As in the case of helium, it is desirable to have two sets of parameters for the Lennard-Jones (6-12) potential function; one set which uses no quantum corrections, but adequately fits the low temperature second virial data, and the other set of parameters which fits the data with quantum corrections. Kirk[42] has made an analysis of the second virial coefficient data of hydrogen and determined two such sets of constants. The "classical" parameters were obtained by fitting the second virial coefficient data of White and Johnston[80] over the range 65° to 125° K. The values of these parameters were $e/k = 31.41^{\circ}$ K and $b_o = 32.98$ cc/gm mole. For the "quantum" parameters Kirk determined the values of $e/k = 36.26^{\circ}$ K, $b_o = 35.50$ cc/gm mole using a graphical method and the same virial coefficient data as was used to determine the classical parameters.

Kihara Core Model Parameters

The parameters of the Kihara Core Model for argon, helium, and hydrogen have been determined recently by Prausnitz and Myers.[66] These values were selected for use here and are given in Table 10. For helium and argon the core was assumed to be spherical, but hydrogen was assumed to be a spherocylinder of zero radius. All of the parameters were determined from second virial coefficient data. For helium and hydrogen the first two translational quantum corrections in Equation (IV-26) were made.

Pitzer-Prausnitz-Gunn Parameters

Argon. The selected values of T_c(150.86° K) and P_c (48.34 atm) used to calculate the acentric factor for argon from Equation (IV-28)

were taken from Michels et al.[54] The value of the acentric factor, ω, was found to be -0.005, compared with a value of -0.002 given by Pitzer et al.[63] Using the relation between Z_c and ω given by Prausnitz and Gunn,[64]

$$Z_c = 0.291 - 0.08\omega \qquad \text{(V-10)}$$

a value of 0.2914 was calculated for the critical compressibility of argon. From this value of Z_c the critical volume was found to be 74.62 cc/gm mole in excellent agreement with the value of 74.56 cc/gm mole experimentally determined by Michels et al.[54] The experimental value of V_c of Michels et al.[54] was selected for use in this work.

Helium. The parameters of the PPG equation were obtained by assuming that the acentric factor is zero and calculating a set of "pseudo critical" constants from the second virial coefficient data of White et al.[81] From the Boyle point (T = 23.8° K) obtained graphically from the data of White et al.,[81] and the relation of Danon and Pitzer[19] expressing the Boyle point as a function of the critical temperature, the effective value of the critical temperature was found to be 8.96° K. From the second virial coefficient at 100° K (11.6 cc/gm mole), obtained graphically from the data of White et al.,[81] the effective value of the critical volume was found to be 29.7 cc/gm mole. This value was calculated from Equations (IV-30), (IV-32) and (IV-33).

Hydrogen. The parameters for the PPG relations for hydrogen were taken from Kirk.[42] These values were obtained by him in a manner similar to that used here for helium. Assuming $\omega = 0$ for hydrogen, he then computed values of a set of pseudocritical constants of 40.47° K and

46.09 cc/gm mole for T_c and V_c respectively.

Comparison of Calculated Second Virial Coefficients with Experimental Data

Helium. A review of the experimental second virial coefficients of helium prior to about 1941 was made by Keesom.[38] He arrived at a selected set of values which have been rather widely used since then. These selected values are shown in Figure 8. In addition, the more recent values of White et al.,[81] Michels and Wouters[56] and Canfield et al.[12] are also given. The various methods of calculating the second virial coefficient used in this work are shown for comparison. The constants of the Kihara core model, the PPG equation, and the LJ (6-12) "classical" equation were all based on the data of White et al., whereas the earlier parameters of the LJ (6-12) "quantum" equation given by de Boer and Michels[20] were based on earlier values of the second virial coefficient. Since there is still some uncertainty as to which values of the second virial coefficients are the better ones, no attempt was made to redetermine the constants given by de Boer.

Hydrogen. A comparison of the experimental data for the second virial coefficient of hydrogen determined by White and Johnston,[80] Michels et al.,[52] Knaap et al.[45] and Goodwin[30] with the various methods of calculation is given in Figure 9.

Argon. The second virial coefficient of argon determined experimentally by Whalley and Schneider,[79] Michels et al.,[54] Kerr,[39] Cath and Onnes,[13] and Fender and Halsey[28] are shown in Figure 10. These experimental values are compared with the various methods of calculation used in this work.

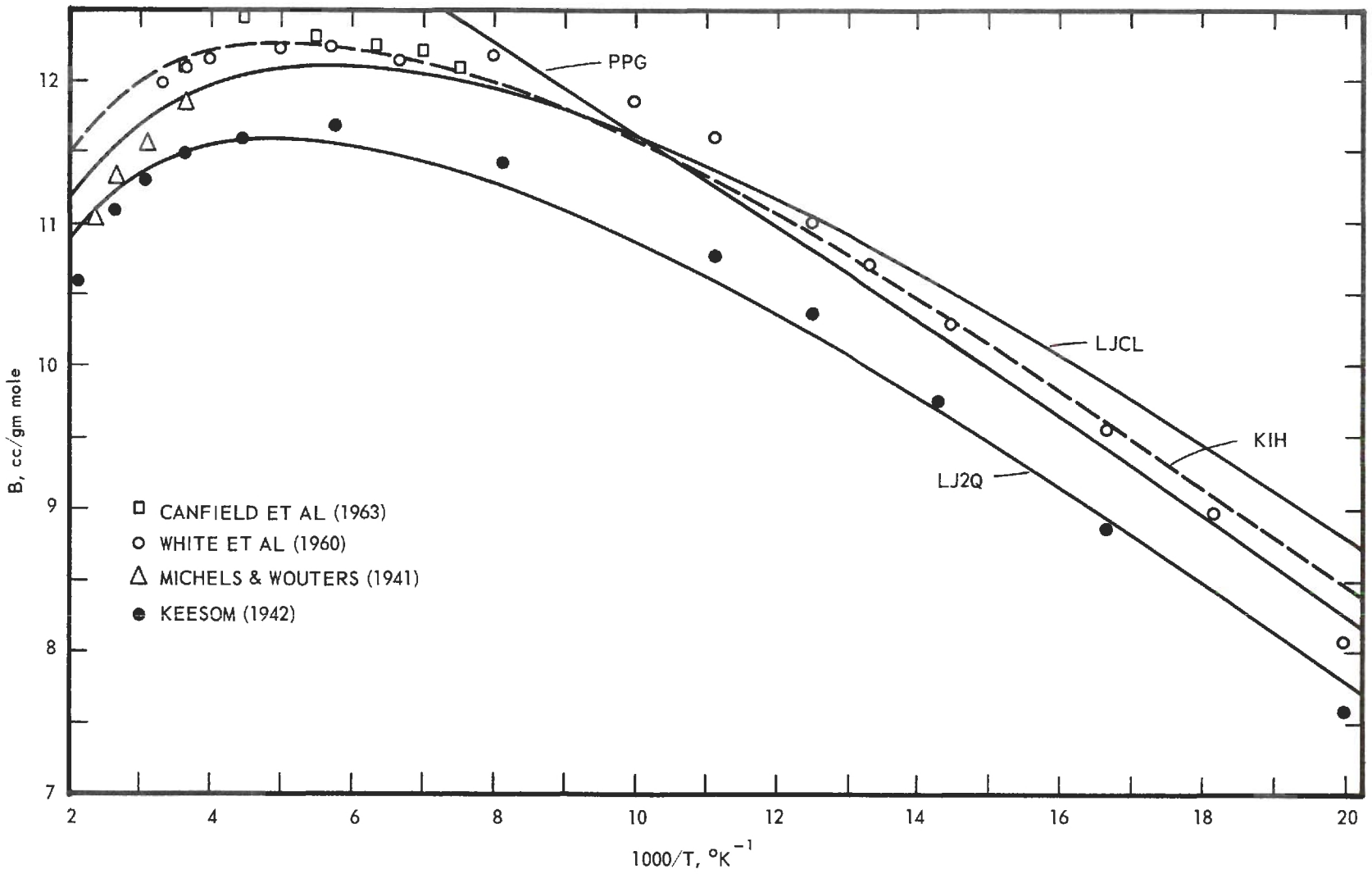

Figure 8. Comparison of Calculated and Experimental Second Virial Coefficients of Helium.

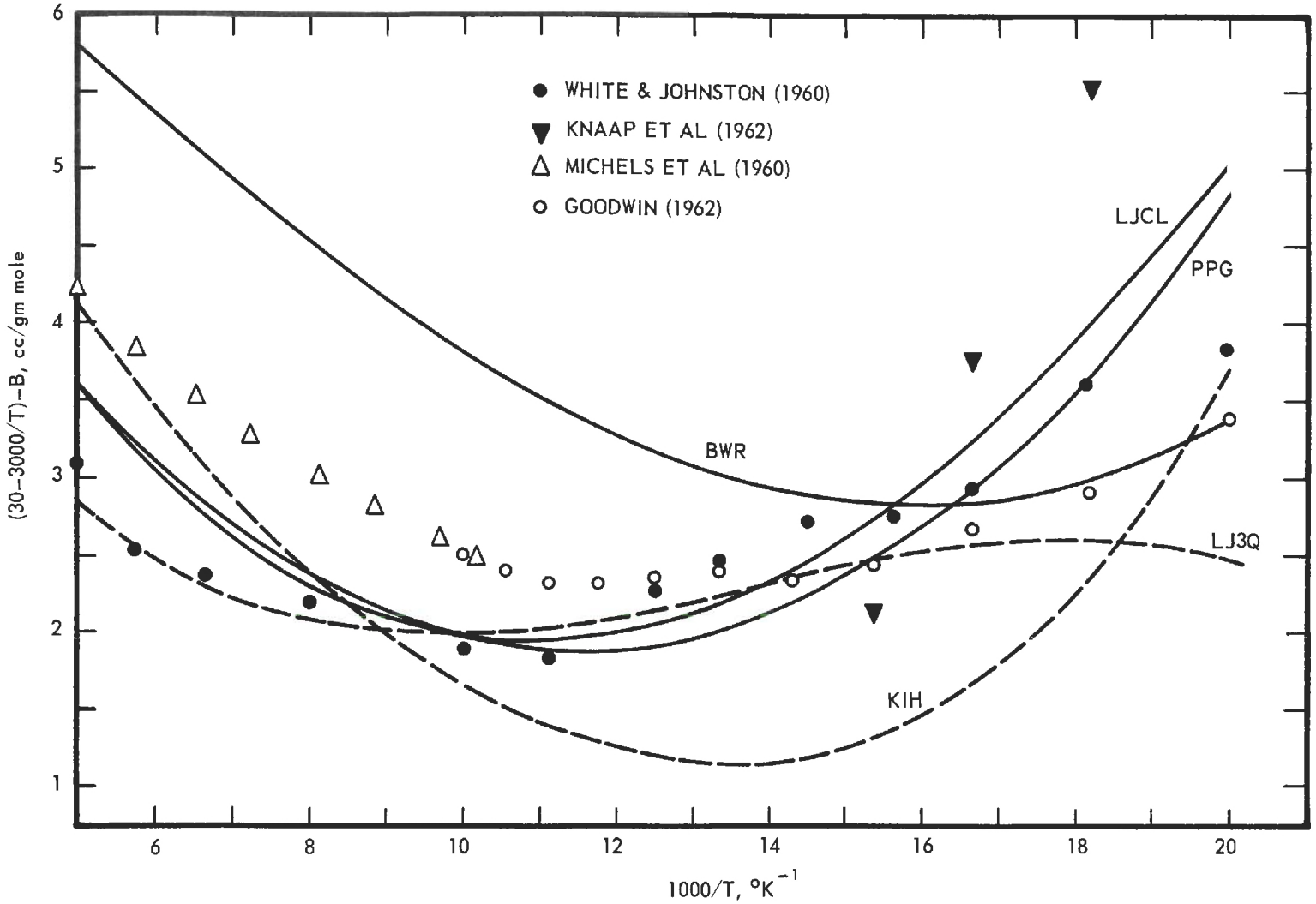

Figure 9. Comparison of Calculated and Experimental Second Virial Coefficients of Hydrogen.

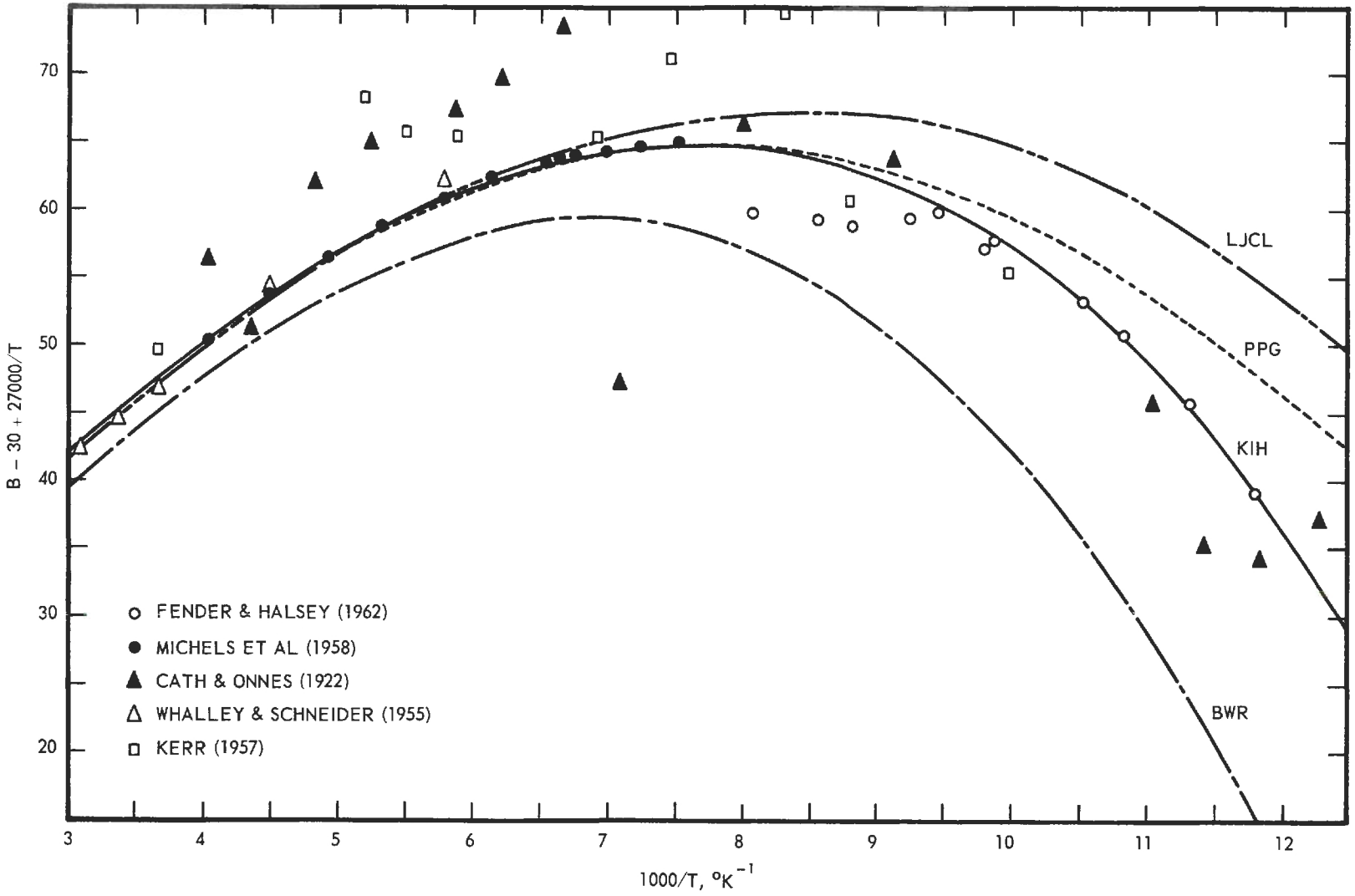

Figure 10. Comparison of Calculated and Experimental Second Virial Coefficients of Argon.

Computational Methods

The computations in this thesis were performed on a Burroughs 220 electronic digital computer. All of the programs were written in Burroughs Algebraic Compiler language, a dialect of ALGOL 58. All of the computations except the determination of the BWR constants described in Appendix A were performed in single precision (8 place) floating point arithmetic. The least squares fit of the BWR constants was accomplished using triple precision (28 place) in all operations where loss of significant figures could occur.

A complete description of all the different programs used in the computations would be impractical. The enhancement factor calculations were accomplished with a general program with different subprograms for the particular equation of state considered. The details of this program were given by Kirk.[42] It was slightly modified here. The general method of calculation was to begin at low pressures along an isotherm, compute an initial value of y_1 based on an enhancement factor of unity, compute a gas volume by iterative solution of the particular equation of state, and from these initial values of y_1 and V_m compute a corrected value of the enhancement factor. This iteration was continued until the change in y_1 was less than 0.01 per cent.

One computer program which perhaps is worth including in some detail is the one used to compute phase equilibria in the argon-hydrogen system directly from the BWR equation of state. The method, though used here for a binary system, could be generalized to include more components. The method of approach was worked out jointly with Dr. Kirk,

though he did the complete programming. This was accomplished after the completion of his thesis work and is therefore described in some detail in Appendix E.

CHAPTER VI

COMPARISON OF PREDICTED AND EXPERIMENTAL RESULTS

Enhancement Factors

General

Enhancement factors were calculated for each of the experimental isotherms for both the argon-helium and argon-hydrogen systems and compared with the experimental results. The calculated results are given at 10 atm intervals up to 120 atm in Tables 21 through 23 in Appendix I. In describing the various methods of prediction, the nomenclature used is consistent with that of Kirk.[42] Table 11 gives this nomenclature and the equation numbers from which the predictions are made. One difference is significant, however; all of these methods do include the term $\ln \gamma_1' x_1$, which was assumed to be zero by Kirk. Kirk referred to two types of prediction; those based on "homogeneous" methods and "hybrid" methods. The "homogeneous" methods refer to predictions for which the various interaction terms and the volume of the gas mixture, V_m, in the enhancement factor equation, Equation (I-7), are computed from a single equation of state. For the methane-hydrogen system, Kirk found that the best prediction methods were those which combined the qualities of the virial equation of state with those of the BWR equation of state. These were referred to as "hybrid" methods of prediction. The second virial interaction coefficient and in some cases the second virial coefficient of the pure components were

Table 11. Symbols for Methods of Predicting Enhancement Factors

Symbol	Eq. Numbers[a] for Calculating Φ	Eq. Numbers[a] for Calculating V_m	Eq. Numbers[a] for Mixture relations
	- - - -Homogeneous- - - -		
BWR	56, 47, 48, A-31	46-48	49, 50, 52-54
PPGL	7, 32, 40	4, 32, 40	36, 38, 39
LJCL	7, 9, 12	4, 9, 12	13-16
LJ3Q	7, 12, 17	4, 12, 17	13-16, 18-20
KIH	7, 12, 26	4, 12, 26	13, 14, 16, 19, 23, 27
KIHA*	7, 12, 26	4, 12, 26	14, 16, 19, 23, 27

	B_{11} and B_{22}		B_{12}		$(a\alpha)_m$
Symbol	Symbol	Eq. No.	Symbol	Eq. No.[a]	Eq. No.[a]
	- - - -Hybrid- - - -				
B1	PPGL	32, 40	PPGL	32	53, 54
B2	BWR	57	LJCL	9	53, 54
B3	LJCL	9	LJCL	9	53, 54
B4	LJCL				
	LJ3Q	9, 17	LJ3Q	17	53, 54
B5	KIH	23, 26	KIH	26	53, 54

(continued)

Table 11. Symbols for Methods of Predicting Enhancement Factors. (Concluded)

	B_{11} and B_{22}		B_{12}		$(a\alpha)_m$
Symbol	Symbol	Eq. No.[a]	Symbol	Eq. No.[a]	Eq. No.[a]
H1	BWR	57	PPGL	32	61
H2	PPGL	32, 40	PPGL	32	61
H3	KIH	23, 26	KIH	26	61
H4	BWR	57	KIH	26	61
H5	LJCL	9	LJCL	9	61
H6	LJCL				
	LJ3Q	9, 17	LJ3Q	17	61

[a] Equation numbers refer to Chapter IV, unless otherwise indicated.

* KIHA is a method of correlating the argon-helium system based on an adjusted average of the parameter $(U_o/k)_{12}$.

calculated from the theoretical methods, LJ3Q, LJCL, and KIH, or from the generalized method, PPGL, and the higher terms calculated from the BWR equation of state. The difference between the H and B series of "hybrid" calculations is in the mixture relation for $(a\alpha)_m$. However, it should be noted that there is not necessarily a correspondence between like numbers in the B and H series, e.g., B_1 and H_1 do not use the same method of calculating B_{11} and B_{22}. Since no BWR constants were available for helium, the "hybrid" methods are restricted to the argon-hydrogen system.

The "homogeneous" method, KIHA, is not strictly a method of prediction. This is a method of correlating the argon-helium enhancement factors developed by Mullins and Ziegler[59] based on an adjustment of the mixing rule for $(U_o/k)_{12}$ and is discussed later in this chapter. It is included in Table 11 for reference since it appears on the following figures.

Argon-Helium System

The selected values of the experimentally determined enhancement factors from Table 16 for the 68.07°, 80.06°, 86.02° and 108.02° K isotherms are shown in Figures 11 through 14 compared with the various prediction methods. The other isotherms gave similar results. None of the methods of prediction work well for this system. The fault with all of the methods is the inability of the mixture rules to accurately predict B_{12}, the second virial interaction coefficient. It is interesting that the more exact quantum methods, LJ2Q and KIH do not give as good results as the classical LJCL and the generalized PPGL. The close agreement between the PPGL and LJCL is not surprising. The reduced second virial

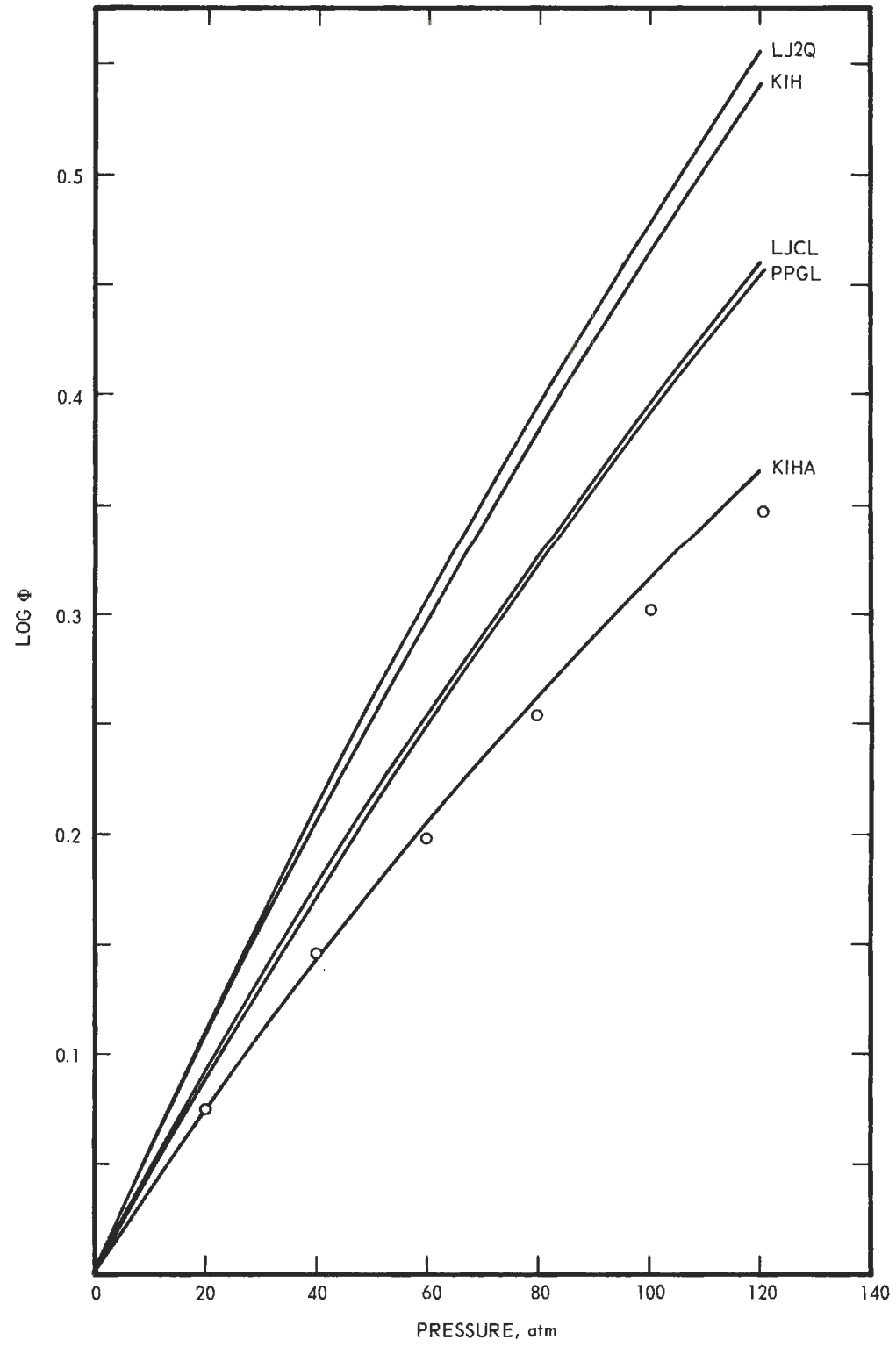

Figure 11. Comparison of Predicted and Experimental Enhancement Factors for Argon-Helium at 68.07° K.

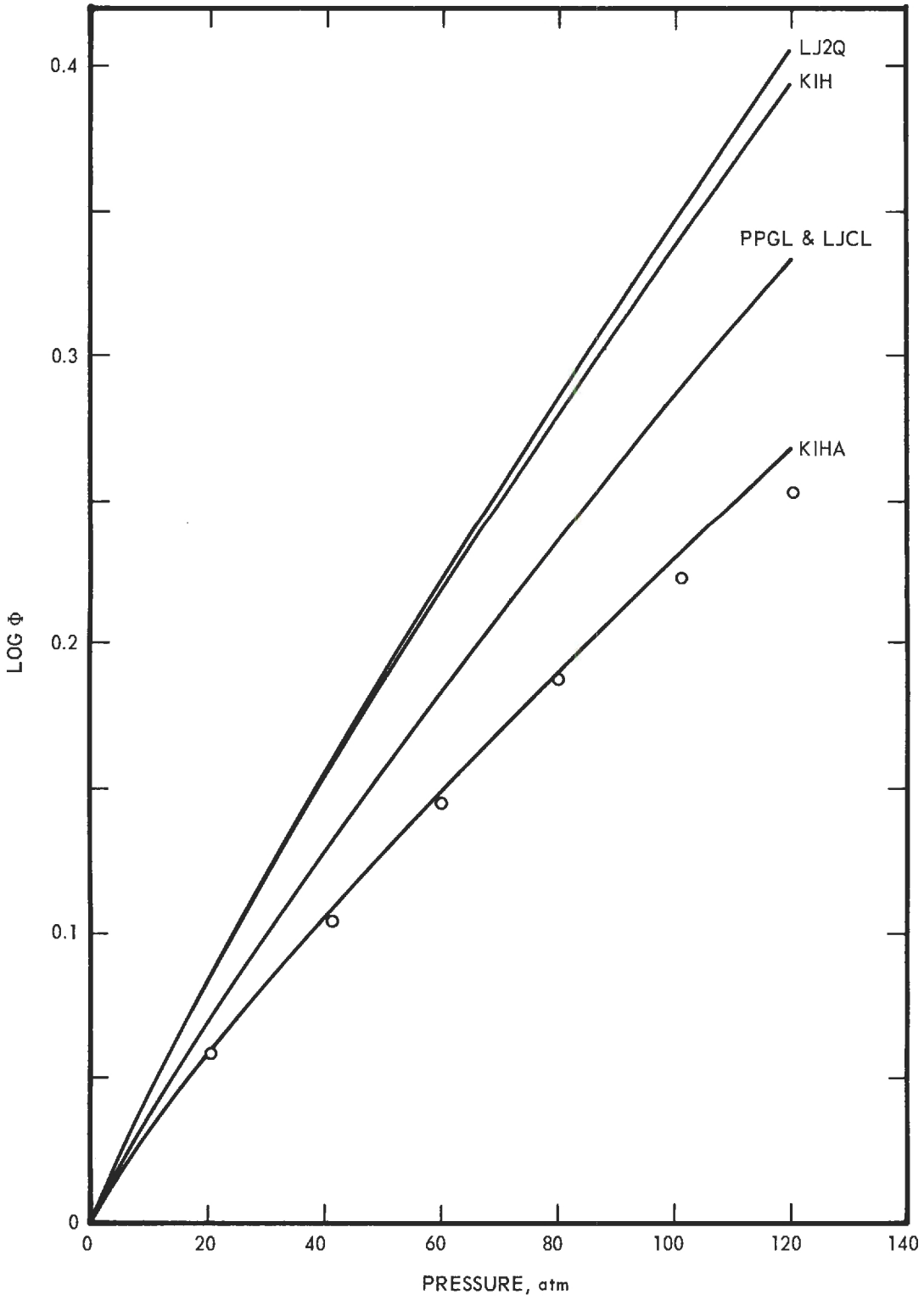

Figure 12. Comparison of Predicted and Experimental Enhancement Factors for Argon-Helium at 80.06° K.

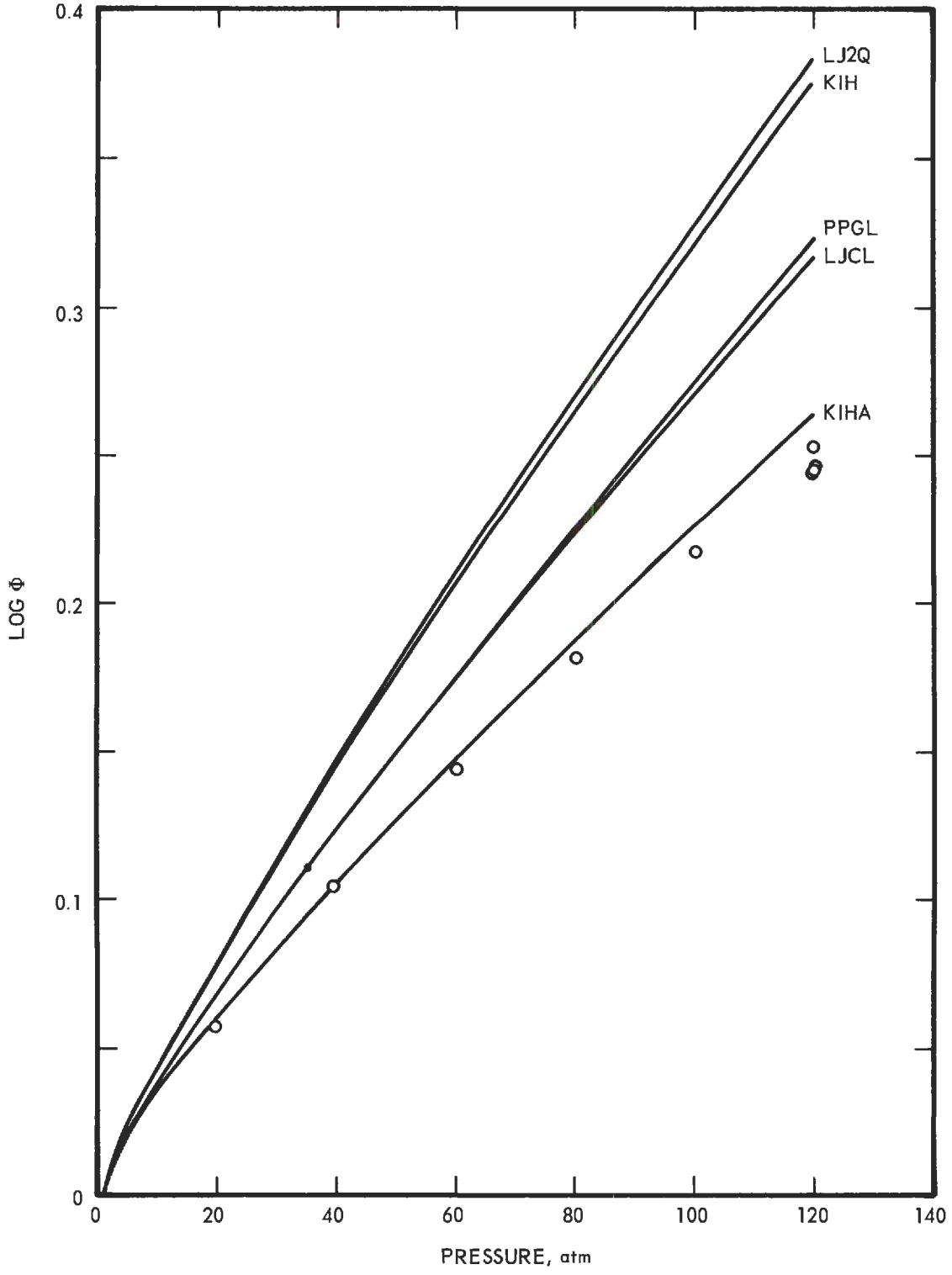

Figure 13. Comparison of Predicted and Experimental Enhancement Factors for Argon-Helium at 86.02° K.

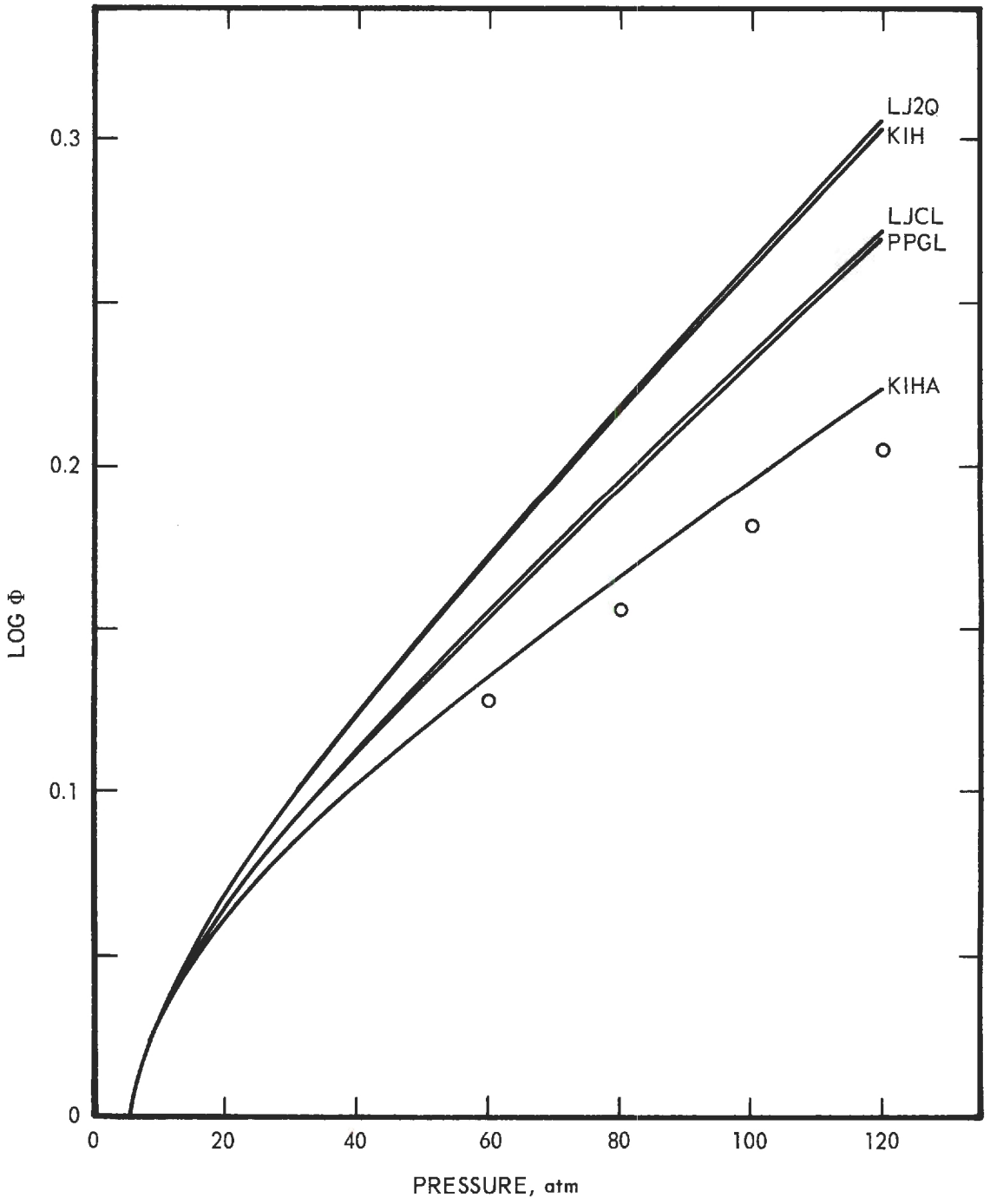

Figure 14. Comparison of Predicted and Experimental Enhancement Factors for Argon-Helium at 108.02° K.

relations of Pitzer and Curl[61] were originally chosen to agree with the LJCL at low temperatures.

Argon-Hydrogen System

The selected values of the experimentally determined enhancement factors from Table 18 for the 68.04°, 79.01°, 86.95°, and 105.01° K isotherms are shown in Figures 15-18 compared with the "homogeneous" and selected "hybrid" methods of prediction. All of the "homogeneous" methods which utilized the individually calculated virial coefficients, LJ3Q, LJCL, KIH, and PPGL are in excellent agreement with the experimental values up to about 40 atmospheres at 68.04° K and 60 atmospheres at 105.01° K. Above these pressures the "homogeneous" methods diverge, with the exception of PPGL and BWR. The reason that PPGL does not diverge appears to be because of a slightly low fit at the low pressures rather than because of a better overall fit. The BWR equation predicts, in general, values of the enhancement factor which are too low. This is true in spite of the fact that the pure second virial coefficients, B_{11} and B_{22}, predicted by BWR are much too negative (see Figures 9 and 10). This implies that had the BWR equation predicted correct values of B_{11} and B_{22}, the agreement would have been much worse. This conclusion is in accord with that reached by Kirk[42] for the hydrogen-methane system.

Of the various "hybrid" methods of prediction listed in Table 11, calculations were made on at least one isotherm for all but B2 and H4. These calculated values are given at 10 atm intervals up to 120 atm in Table 23, Appendix I. The value of the enhancement factor at 110 atmospheres for each experimental isotherm is compared with these various

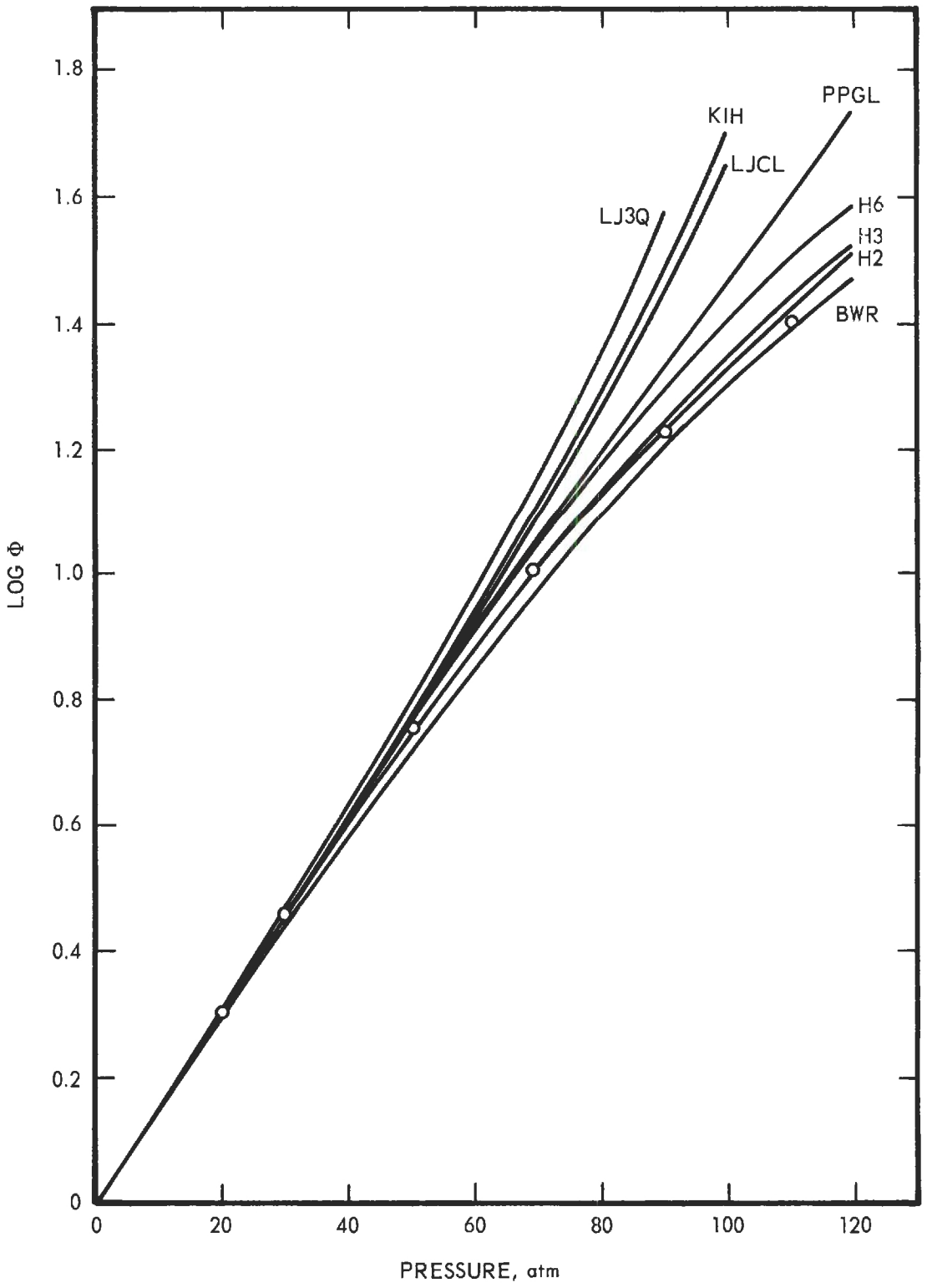

Figure 15. Comparison of Predicted and Experimental Enhancement Factors for Argon-Hydrogen at 68.04° K.

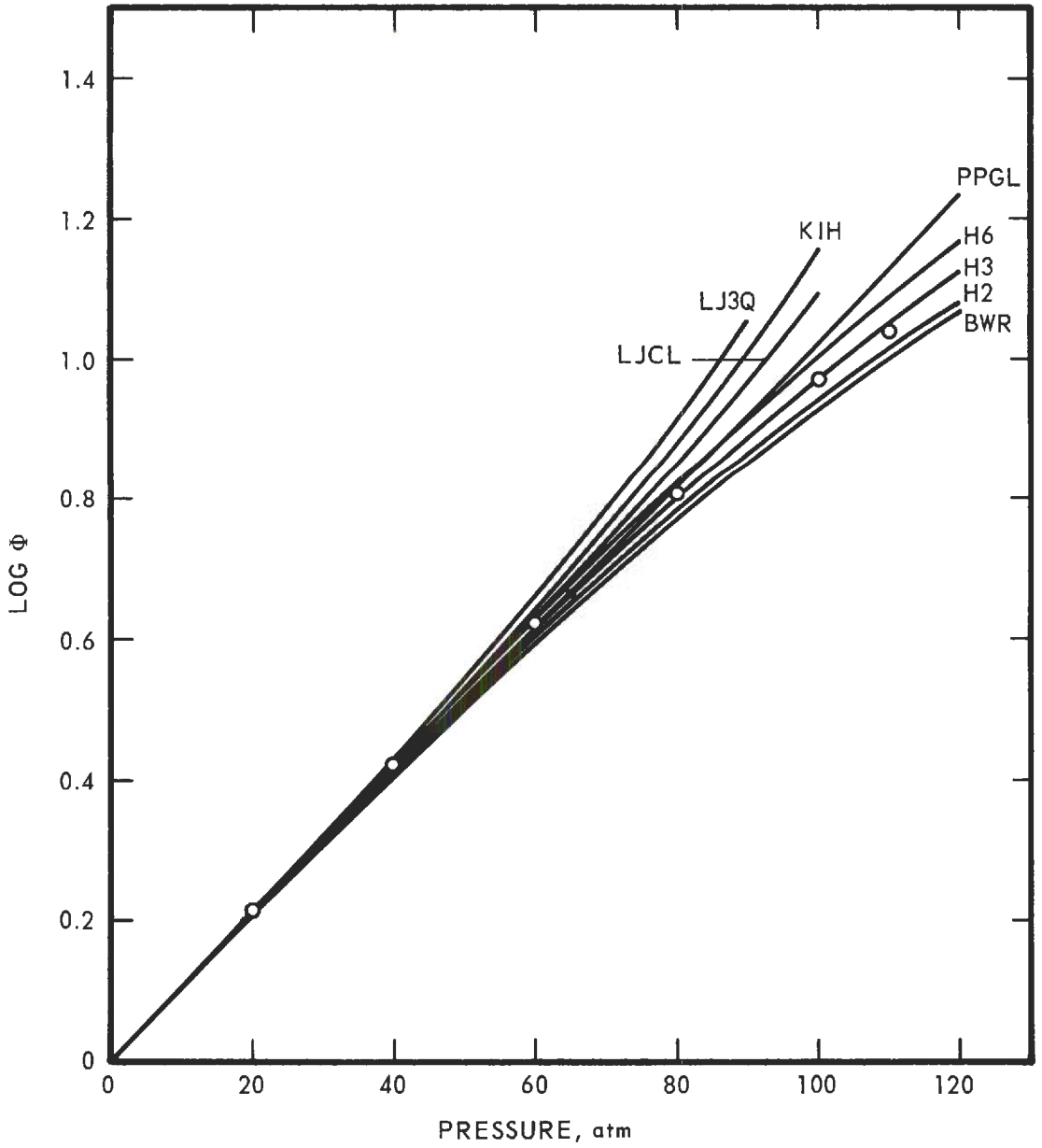

Figure 16. Comparison of Predicted and Experimental Enhancement Factors for Argon-Hydrogen at 79.01° K.

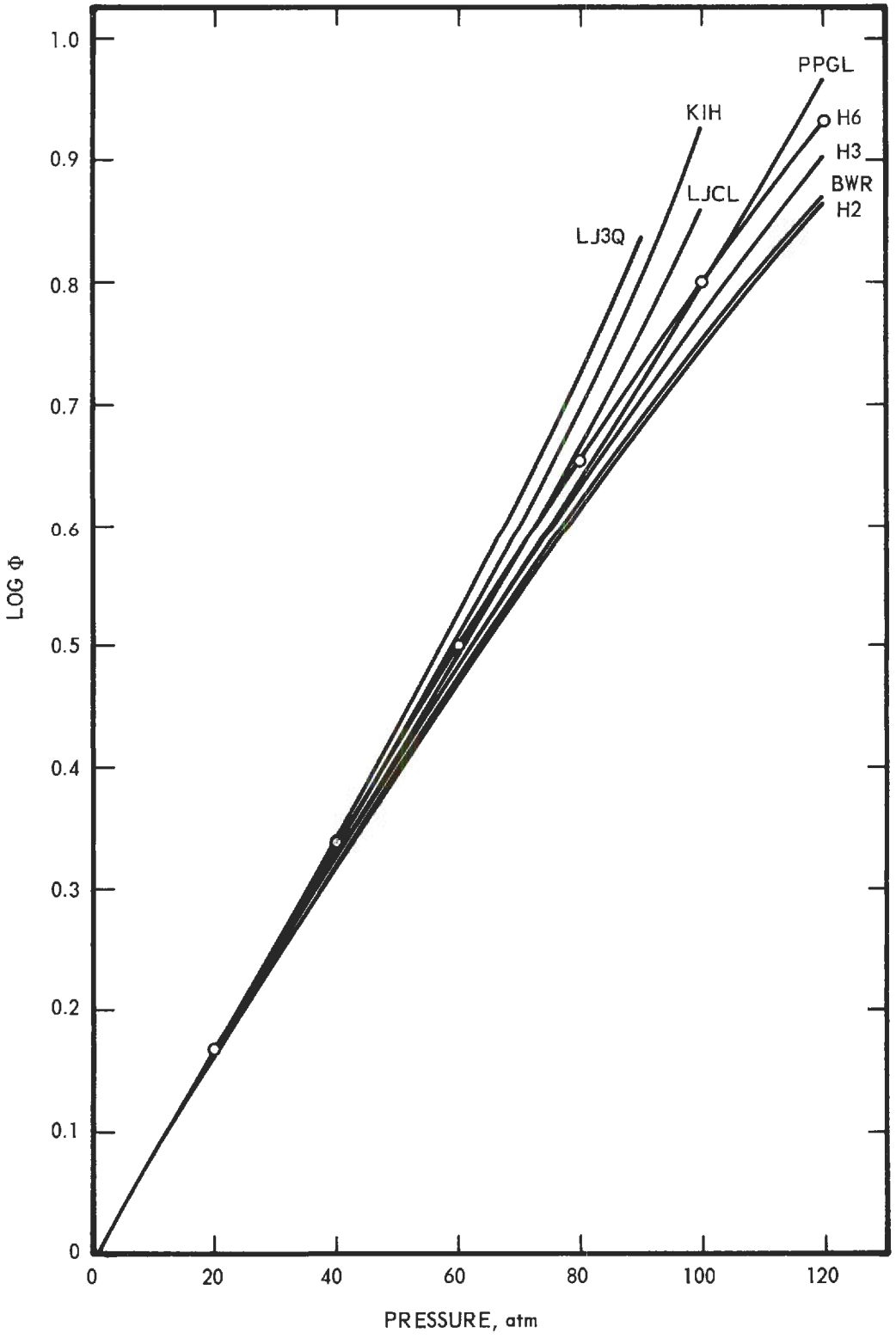

Figure 17. Comparison of Predicted and Experimental Enhancement Factors for Argon-Hydrogen at 86.95° K.

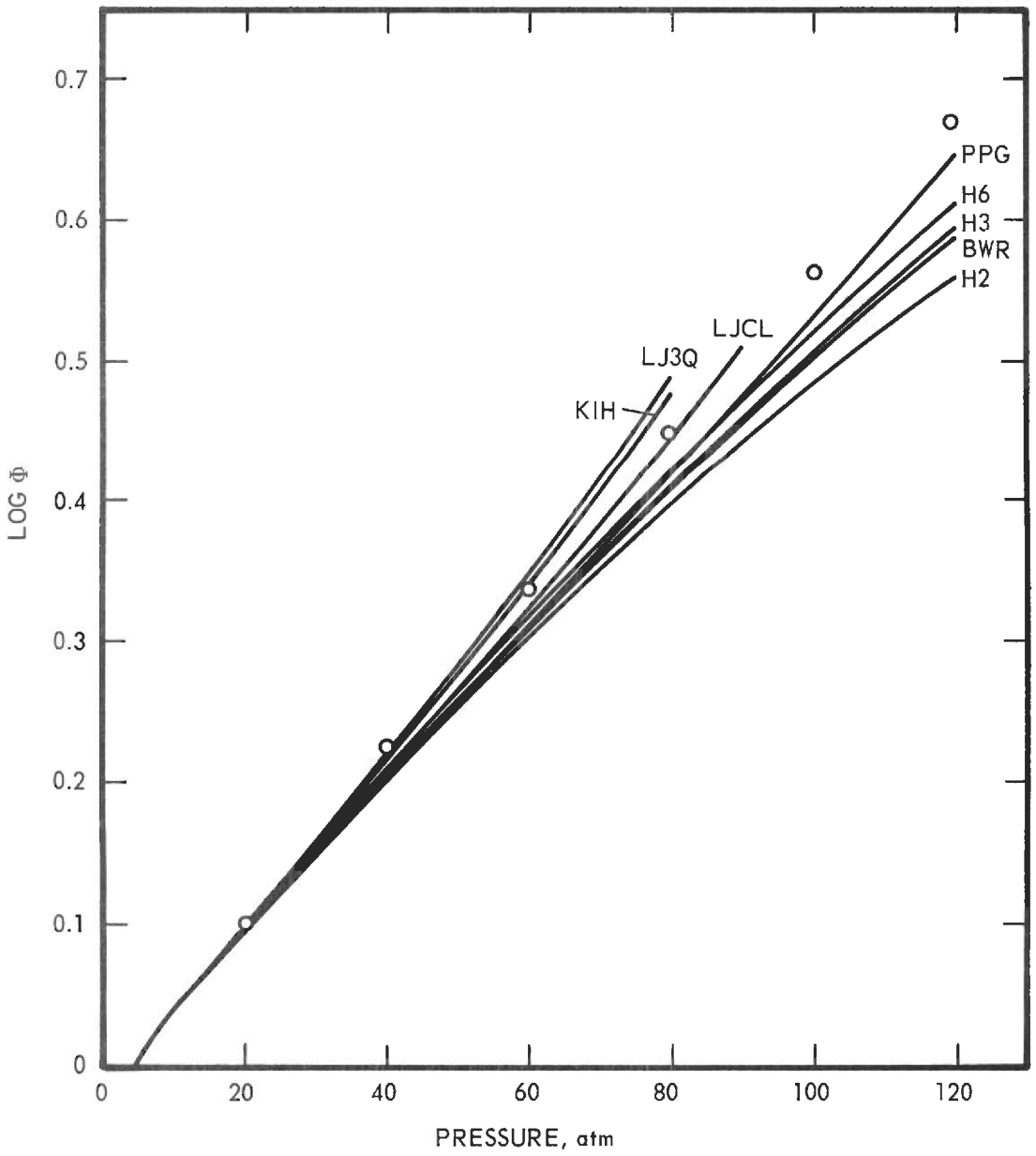

Figure 18. Comparison of Predicted and Experimental Enhancement Factors for Argon-Hydrogen at 105.01° K.

Table 12. Results of Hybrid Calculations for the Enhancement Factor of Argon in Hydrogen at 110 Atmospheres Pressure Compared with Experimental Values

	Log Φ						
Temperature, °K	68.04	73.05	79.01	86.95	94.21	99.95	105.01
Method							
B1	1.421	1.207	1.019	0.806	0.673	0.588	0.524
B2	-	-	-	-	-	-	-
B3	-	-	-	-	0.666	-	-
B4	1.484	1.272	1.084	0.866	0.727	0.637	0.568
B5	1.432	1.225	1.044	0.835	0.702	0.617	0.551
H1	1.450	-	1.053	0.841	-	-	0.557
H2	1.427	-	1.022	0.808	-	-	0.525
H3	1.438	1.229	1.047	0.837	0.704	0.618	0.553
H4	-	-	-	-	-	-	-
H5	-	-	-	-	0.668	-	-
H6	1.491	1.277	1.088	0.869	0.729	0.638	0.569
Experimental	1.399	1.213	1.038	0.864	0.745	0.671	0.616

"hybrid" methods of prediction in Table 12. The difference between calculations of the B series and the corresponding H series (e.g., B1 and H2) was extremely small, indicating that the different $(a\alpha)_m$ mixture rules are not significant in this system at pressure levels less than 110 atmospheres. The results for H2, H3, and H6 are shown in Figures 15 through 18 compared with the various "homogeneous" methods and the experimental results. The "hybrids," B2, H1, and H4 are not recommended because the BWR is used to predict the virial coefficients B_{11} and B_{22}. Although the agreement with the experimental values is no worse than some of the other hybrids, the agreement is considered somewhat fortuitous. H1 and H2 were found by Kirk[42] to represent best the hydrogen-methane system. H1 is not recommended here for the reason mentioned above. H2 is in excellent agreement over the solid-gas region, but the predicted values of the enhancement factor appear to be almost twenty per cent low at 105.01° K and 120 atmospheres. This is interesting, because had the solubility of hydrogen in argon been neglected or the product $\gamma_1' x_1$ been taken as one, the agreement would have been improved considerably. The other two "hybrids" H3 and H6, shown in Figures 15-18 were considered promising because LJ3Q and KIH appeared to give the best representation of the second virial interaction coefficients and the second virial interaction coefficient, B_{12}. H6 predicts enhancement factors which are approximately 21 per cent high at 68.04° K and 110 atmospheres, and about 14 per cent low at 105.01° K and 120 atmospheres. H3 predicts enhancement factors which are approximately 10 per cent high at 68.04° K and 110 atmospheres and 14 per cent low at 105.01° K and 120 atmospheres.

Three-Phase Line

Equation (I-20) relates the value of ln $\gamma_1' x_1$ to the freezing point depression. From Equations (III-10) and (III-11), which represent the three-phase line of argon-helium and argon-hydrogen, and Equation (III-9) which was selected to represent the melting curve of pure argon, the value of ln $\gamma_1' x_1$ was calculated at 10 atmosphere intervals up to 120 atmospheres. From the least squares surface fit of the Henry's law constants, given by Equations (III-6) through (III-8) and the coefficients given in Tables 3 and 4, the value of x_1 and γ_1' were calculated at each point. These values are given in Table 13. The activity coefficients for argon in the argon-helium system are very consistent and very nearly unity. As might be expected, the activity coefficients of argon in the argon-hydrogen system deviate more from unity and indicate a positive deviation from Raoult's law.

Equation (I-20) was also used to predict the three-phase line assuming that the liquid solution was ideal and the solid pure argon. Since x_1 is a function of both T and P, the equation must be solved iteratively. The results are shown in Figure 7.

Second Virial Interaction Coefficient

The second virial interaction coefficient of argon-helium and argon-hydrogen were calculated from Equation (IV-56) and the experimental enhancement factors in Tables 16 and 18. The results are shown in Figures 19 and 20 as a function of $(P-p_{01})$. The values of B_{11} and B_{22} and all other necessary quantities were calculated as in the enhancement factor calculations for KIH. The values of B_{12} obtained by graph-

Table 13. Activity Coefficient of Liquid Argon Along Locus of the Three-Phase Line

Pressure P, atm	Melting Point[a] of Pure Argon T, °K	Three-Phase[b] Line T, °K	Comp. of Liquid Mole Percent Argon	Activity Coefficient γ_1
		- - - -Argon-Helium- - - -		
20	84.299	84.220	99.870	0.9997
40	84.805	84.655	99.735	0.9996
60	85.309	85.091	99.601	0.9997
80	85.809	85.520	99.466	0.9998
100	86.307	85.934	99.333	0.9996
120	86.802	86.324	99.201	0.9991
		- - - -Argon-Hydrogen- - - -		
20	84.299	83.376	97.934	1.0023
40	84.805	83.057	95.957	1.0064
60	85.309	82.845	94.114	1.0121
80	85.809	82.714	92.373	1.0190
100	86.307	82.638	90.709	1.0269
120	86.802	82.590	89.101	1.0354

[a] Calculated from Equation (III-9)

[b] Calculated from Equations (III-10) and (III-11).

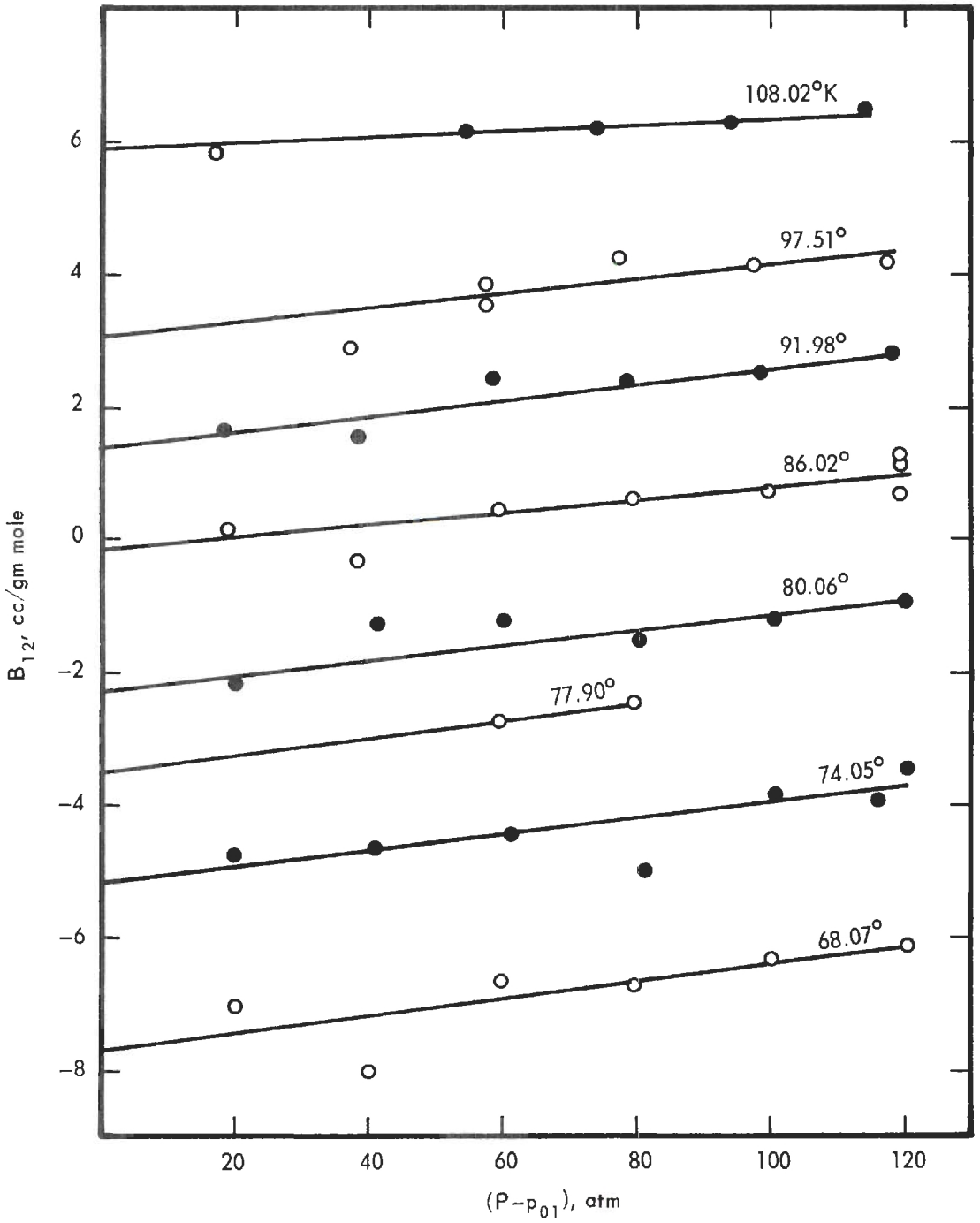

Figure 19. Second Virial Interaction Coefficient of Argon-Helium Calculated from Experimental Enhancement Factors.

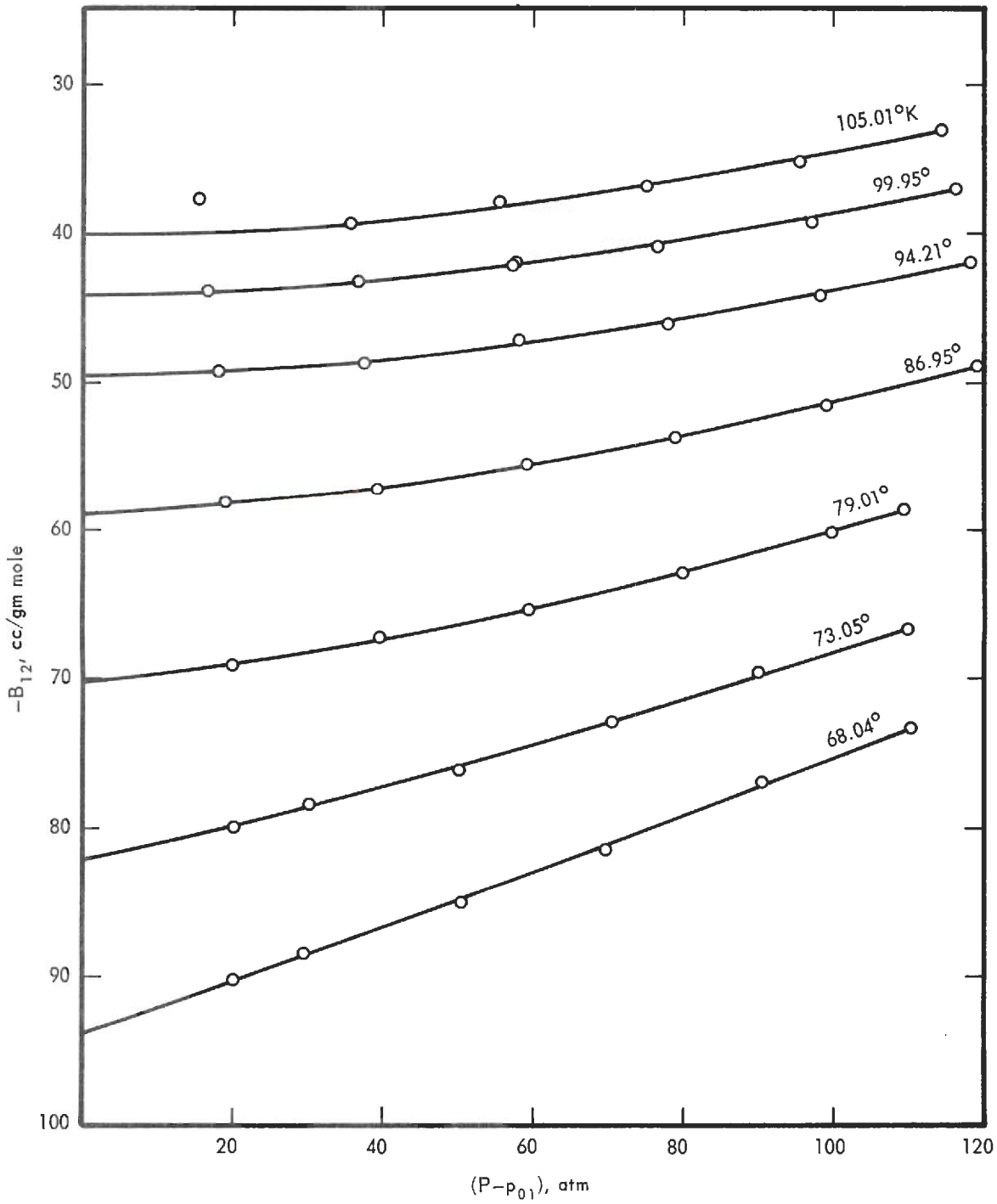

Figure 20. Second Virial Interaction Coefficient of Argon-Hydrogen Calculated from Experimental Enhancement Factors.

ical extrapolation of the curves in Figures 19 and 20 to $(P-p_{01}) = 0$ are given in Table 14. These extrapolated values are compared in Figures 21 and 22 with the various values of B_{12} given by the prediction methods used in the enhancement factor calculations and the experimental determinations of B_{12} by Knobler et al.[46] as adjusted by Prausnitz and Myers.[66]

The predicted second virial interaction coefficients of argon-helium do not agree well with the values obtained from the experimental enhancement factors. This was not unexpected in view of the poor prediction of the enhancement factor discussed earlier. The curve labeled KIHA is based on an adjusted mixing rule for $(U_o/k)_{12}$ in the Kihara core model and is discussed in the next section. The one other experimental value of B_{12} reported in this temperature range was obtained at 90° K from differential PVT measurements by Knobler et al.[46] The originally reported value of + 6.6 cc/gm mole has been corrected to + 0.4 cc/gm mole by Prausnitz and Myers[66] to agree with the values of B_{11} and B_{22} given by the Kihara core model and the parameters of Table 10. In determining a value of B_{12} from PVT measurements it is necessary to know the values of B_{11} and B_{22}. The corrected value of B_{12} of + 0.4 cc/gm mole is compared with the results of this work in Figure 21 and is seen to be in good agreement.

The predicted values of the second virial interaction coefficient of argon-hydrogen agree well with the values obtained from the experimental enhancement factors. Note that the BWR gives values somewhat high even though both virial coefficients B_{11} and B_{22} predicted by BWR

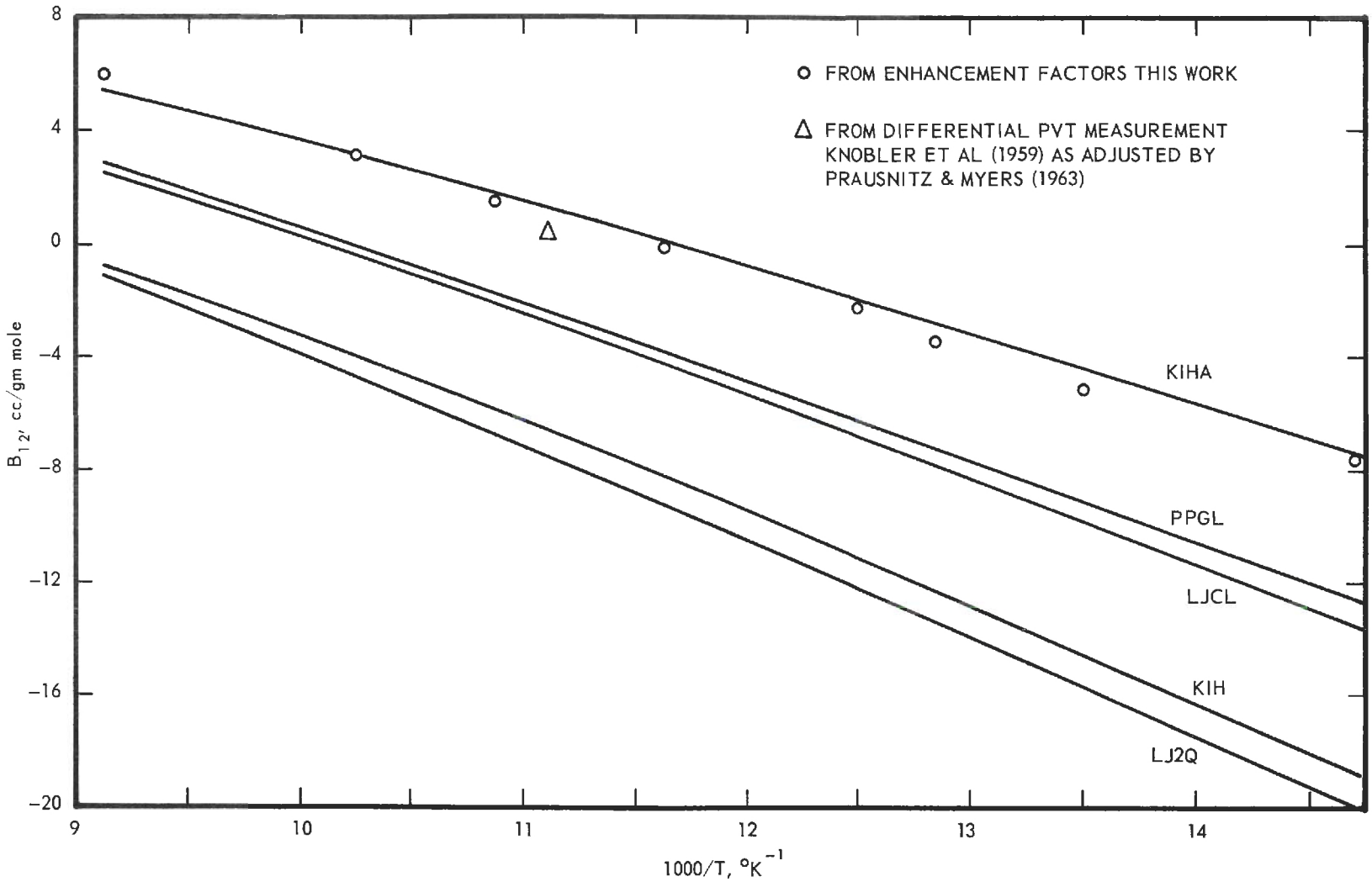

Figure 21. Comparison of Predicted and Experimental Second Virial Interaction Coefficients of Argon-Helium.

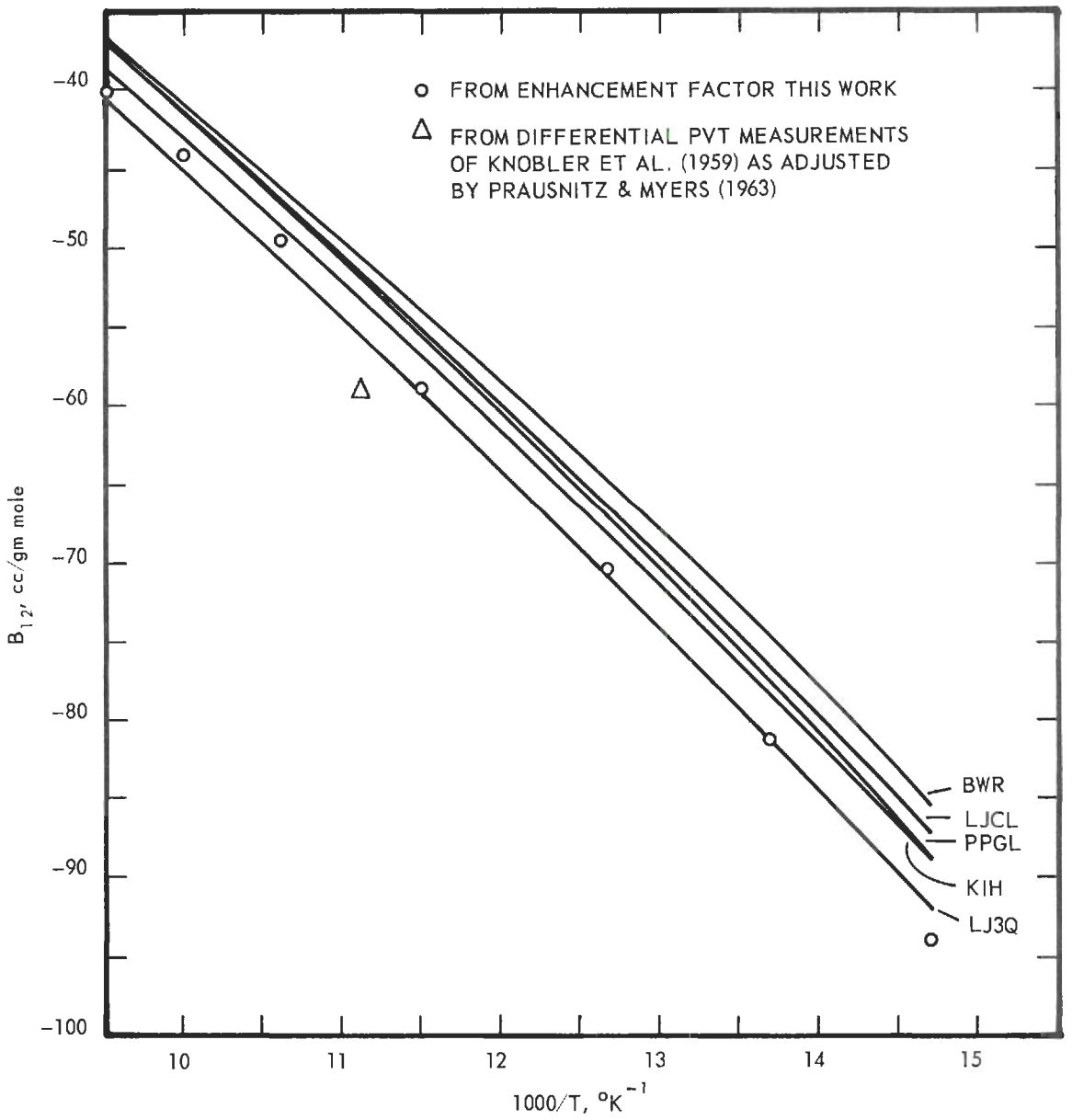

Figure 22. Comparison of Predicted and Experimental Second Virial Interaction Coefficients of Argon-Hydrogen.

Table 14. Second Virial Interaction Coefficients Calculated From Experimental Phase Equilibrium Data

Argon-Helium		Argon-Hydrogen	
Temperature °K	B_{12} cc/gm mole	Temperature °K	B_{12} cc/gm mole
68.07	-7.7	68.04	-93.8
74.05	-5.2	73.05	-81.2
77.90	-3.5	79.01	-70.3
80.06	-2.3	86.95	-58.9
86.02	-0.2	94.21	-49.5
91.98	+1.4	99.95	-44.1
97.51	+3.1	105.01	-40.1
108.02	+5.9		

were low (see Figures 9 and 10). Also shown in Figure 22 is one experimental value of B_{12} reported by Knobler et al.[46] from differential PVT measurements as corrected by Prausnitz and Myers.[66] The original value reported was -52.1 cc/gm mole compared with the corrected value shown in Figure 23 of -58.9 cc/gm mole.

It is interesting to note that the values of B_{12} obtained here for both argon-helium and argon-hydrogen lie between the values reported by Knobler et al.[46] and these same values corrected by Prausnitz and Myers[66] to another choice of the pure second virial coefficients, B_{11} and B_{22}. The values of B_{12} as obtained here are essentially independent of the pure second virial coefficients.

Correlation of Enhancement Factor for Argon-Helium

A simple method of correlating the enhancement factor for the argon-helium system is given by the curves labeled KIHA in Figures 11-14. This method described elsewhere[59] is the same as KIH with an adjusted value of the energy parameter $(U_o/k)_{12}$ for the Kihara core model. The value of 38.08° K given by the geometric average was arbitrarily adjusted to a value of 29.8° K to fit the values of B_{12} computed from the experimental enhancement factors. The agreement of B_{12} calculated using this adjusted value with the experimental values is seen in Figure 21. Prausnitz and coworkers[64,66] have pointed out that if the forces of interaction are primarily London dispersion forces the geometric average for the energy parameter gives too large a value and is actually an upper limit on the correct value. Thus the value of $(U_o/k)_{12}$ was adjusted in the expected direction.

The agreement of the experimental enhancement factors with KIHA is excellent up to about 70 atmospheres for all isotherms and is only about 5 per cent high at 120 atmospheres.

Phase Equilibria of Argon-Hydrogen Predicted By the BWR Equation of State

Solutions of Equations (IV-65), (IV-66) and (IV-67) were made at the temperatures corresponding to the experimental phase equilibrium measurements in the liquid-gas region and at pressures up to 120 atm using the parameters for the BWR equation given in Table 10. The method of calculation is described in Chapter IV and Appendix E. The predicted gas and liquid compositions are labeled as curves A in Figure 23 for the 94.21° K isotherm and Figure 24 for the 105.01° K isotherm. Motard and Organick[58] have found a good correlation for the H_2-CH_4-C_2H_6 system by arbitrarily adjusting γ_2. In their fit of PVT data for hydrogen, they had not found the fit sensitive to γ_2 and therefore could arbitrarily adjust γ_2 in fitting phase equilibrium data without changing the calculated PVT properties. The effect on the argon-hydrogen system of arbitrarily changing the value of γ_2 from 0.0030 to 0.0022 is shown by curve B in Figures 23 and 24. The agreement is good. The maximum error in the gas and liquid phase composition is less than 10 per cent. The effect of using the $(a\alpha)_m$ mixture rule (Equation (IV-61) as proposed by Hydrocarbon Research Inc.[49] is to predict better agreement for the liquid composition, but worse agreement for the gas phase composition. These results are not shown in Figures 23 and 24. No attempt has been made here to examine carefully the best method of predicting phase

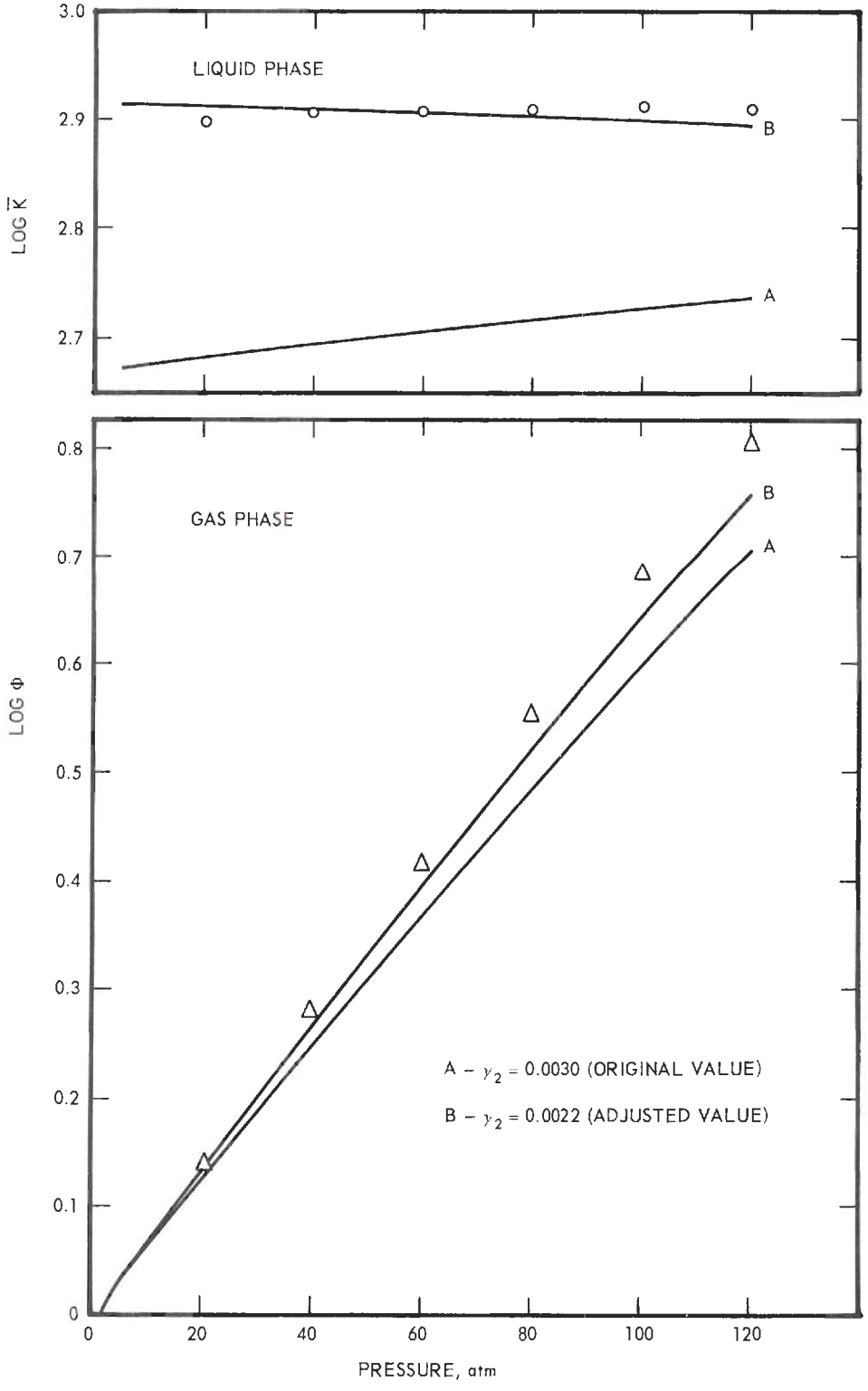

Figure 23. Comparison of Liquid and Gas Compositions in the Argon-Hydrogen System Predicted by BWR Equation with Experimental Results at 94.21° K.

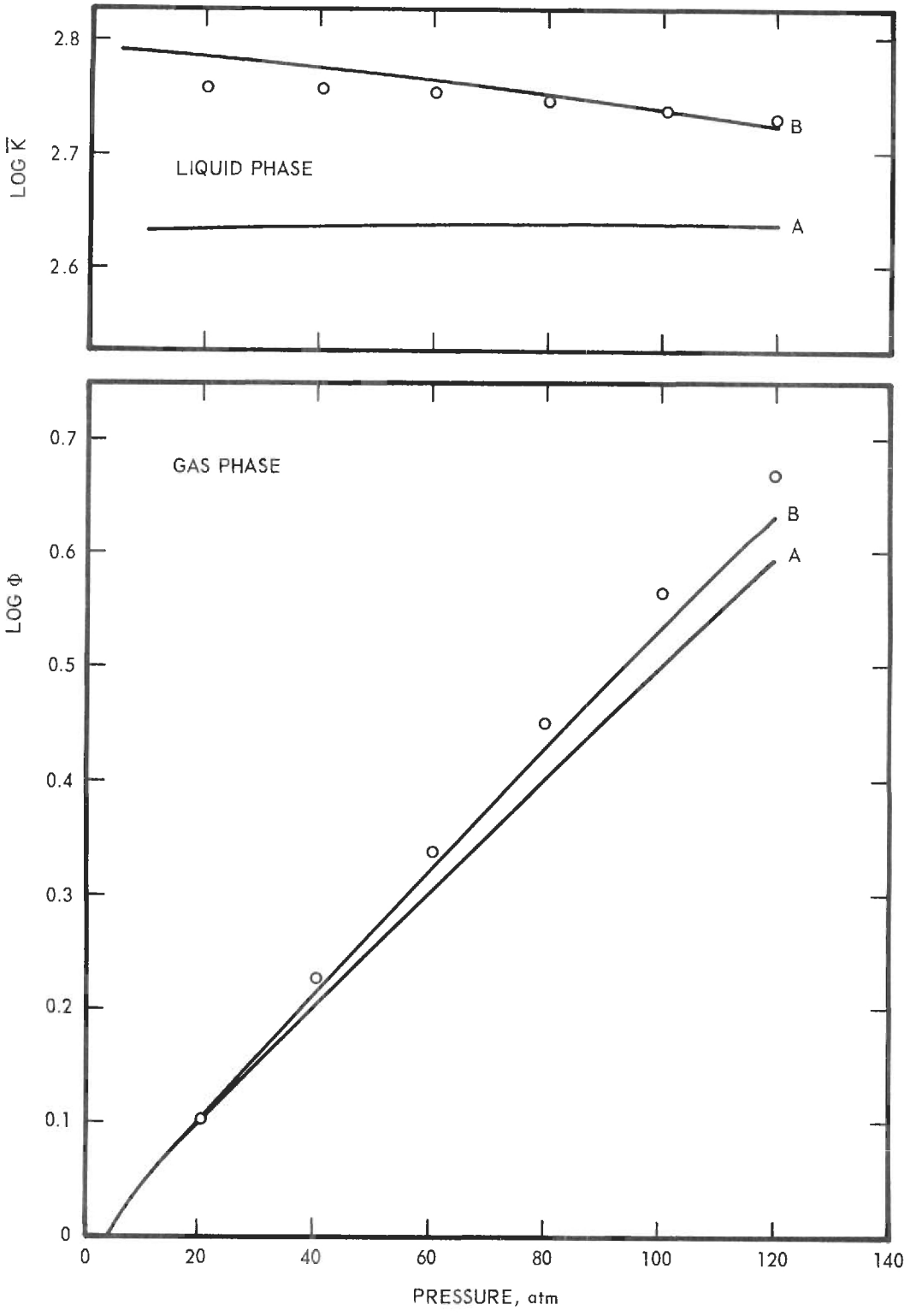

Figure 24. Comparison of Liquid and Gas Compositions in the Argon-Hydrogen System Predicted by BWR Equation with Experimental Results at 105.01° K.

equilibria in the argon-hydrogen system from the BWR equation, the purpose being to illustrate the feasibility of correlation, and to examine the results obtained from the set of constants obtained for hydrogen in this work from the low temperature PVT data of Goodwin et al.[31] and the data of Michels et al.[53]

The values of the activity coefficient of argon in the liquid phase predicted by the adjusted value of γ_2 are shown in Figure 25 as a function of temperature. These values are in excellent agreement with the values of the activity coefficient determined from the freezing point depression given in Table 13, also shown in Figure 25.

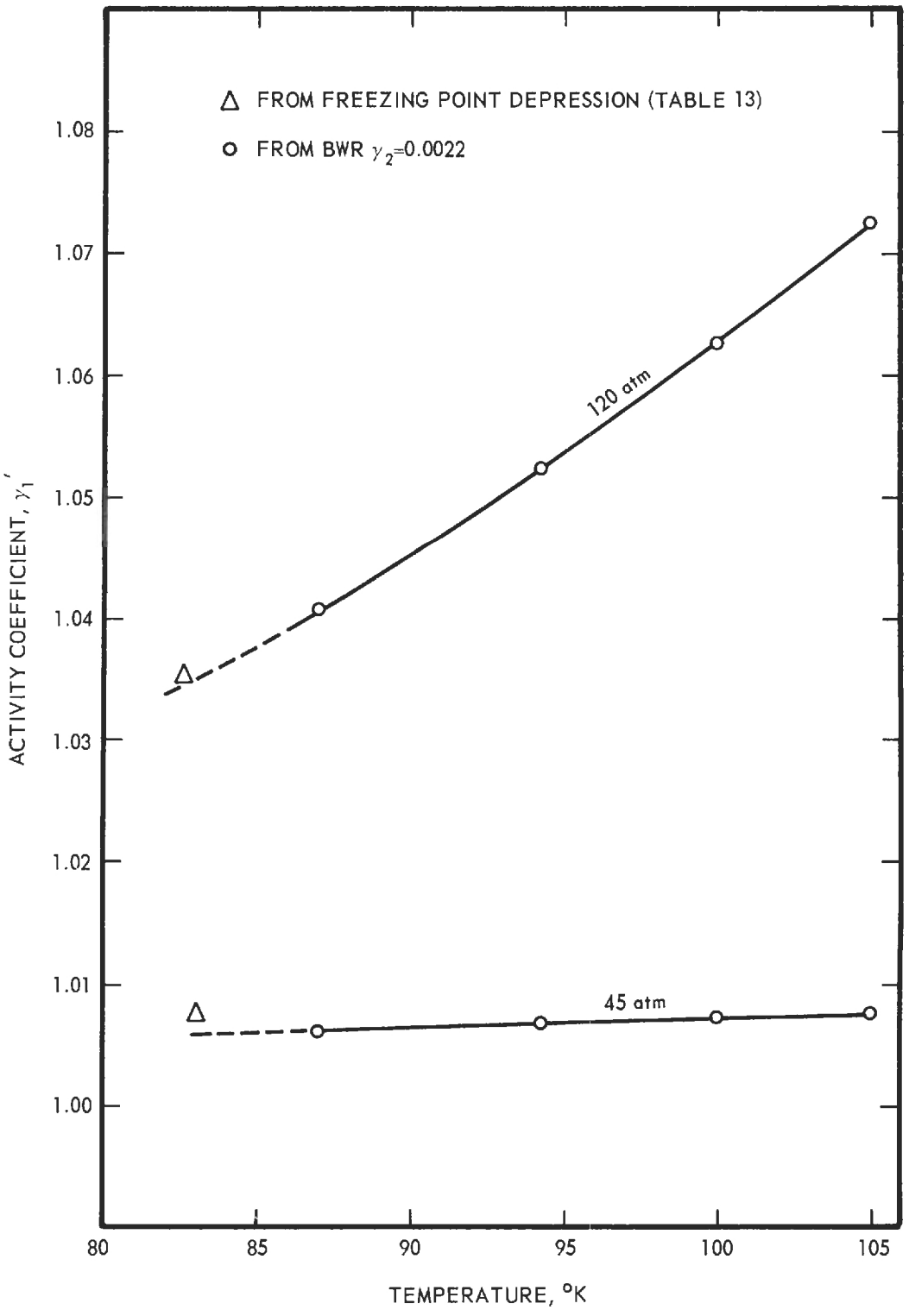

Figure 25. Comparison of Activity Coefficients of Argon in Saturated Liquid Solution of Argon-Hydrogen Calculated from Freezing Point Depression and BWR Equation.

CHAPTER VII

CONCLUSIONS AND RECOMMENDATIONS

Conclusions

Equilibrium gas compositions of the argon-helium system have been determined along isotherms in the gas-solid region at 68.07°, 74.05°, 77.90°, and 80.06° K and in the gas-liquid region at 86.02°, 91.98°, 97.51°, and 108.02° K at pressures up to 120 atm with an accuracy of ± 3 per cent of the mole fraction of argon. Equilibrium liquid compositions were determined with an accuracy of ± 2 per cent of the mole fraction of helium. The gas phase compositions do not agree with the dew-point data of McCain[51] which appear to be in error by as much as 40 per cent in the region of overlap (99.74°-108.02° K). The liquid phase compositions agree well with the data of McCain[51] below 120° K except for his lowest point at 99.92° K which appears to be in error by about 20 per cent. The Henry's law constants extrapolated to low pressure do not agree with the results of Karasz[36,37] between 84.05° and 87.53° K being about two to three times greater.*

Equilibrium gas phase compositions of the argon-hydrogen system

---

* After the completion of this work, preliminary data for the solubility of helium in argon were obtained in a private communication from W. B. Streett. The values of Henry's law constant at infinite dilution determined from his data appear to agree with the values obtained in the present work within ± 5 per cent over the temperature range 92.0° to 107.24° K. Dr. Streett also indicated that preliminary data for the gas phase composition agree quite well with the data of the present work. His measurements extend to 1000 psia.

have been determined along isotherms in the gas-solid region at 68.04° 73.05°, and 79.01° K at pressures up to 110 atm. In the liquid-gas region the liquid and gas compositions were determined at 86.95°, 94.21°, 99.95°, and 105.01° K at pressures up to 120 atm. All compositions are believed accurate to ± 2 per cent of the mole fraction of the minor component. The solubility of hydrogen in argon measured here agrees well with the data of Volk and Halsey[78] at low pressures but differs by as much as 15 per cent at 101 atm, the highest pressure measured by Volk and Halsey. Their results are believed to be in error at high pressures.

The gas phase and liquid phase compositions expressed in terms of the enhancement factor and Henry's law constant are accurately represented by an analytical representation obtained by a least squares surface fit. In this fitting procedure the independent variables chosen were $(1/T)$ and $(P-p_{01})$.

The methods used to predict the enhancement factor for the argon-helium system are not adequate because no method correctly predicts the value of the second virial interaction coefficient. The more theoretically correct methods involving quantum corrections, KIH and LJ2Q, give much poorer results than the LJCL and PPGL. A simple correlation (KIHA) developed by Mullins and Ziegler[59] by adjusting the value of the parameter $(U_o/k)_{12}$ in the Kihara core model (KIH) to 29.8° K agrees with the experimental results for the enhancement factor within three per cent up to 60 atm and within five per cent up to 120 atm.

The "homogeneous" methods used to predict the enhancement factor in the argon-hydrogen system gave good results up to about 50 atm

pressure, but with the exception of PPGL all failed to converge (i.e., prediction of negative volumes) at pressures as high as 120 atm. All methods produced results which agree within ten per cent up to 50 atm. The "hybrid" methods converged at all pressures up to 120 atm and gave, in general, results which were in good agreement with the experimental results. No significant difference results in the use of the $(a\alpha)_m$ mixture rule (Equation (IV-61)) proposed by Hydrocarbons Research, Inc.[49] The results predicted by the "hybrid" methods were essentially the same as the "homogeneous" methods up to 50 atm, and at 110 atm agreed within 25 per cent of the experimental results.

The second virial interaction coefficients calculated from the experimental phase equilibrium data for both the argon-helium and argon-hydrogen systems agree well with the results of Knobler et al.[46] at 90° K from differential PVT measurements as corrected by Prausnitz and Myers,[66] the difference being about 0.6 cc/gm mole for argon-helium and 5.0 cc/gm mole for argon-hydrogen. The accuracy of the values determined in this work are thought to be ± 3 cc/gm mole for the B_{12} of argon-helium and ± 2 cc/gm mole for argon-hydrogen.

The BWR equation was used with unexpected success to predict the phase equilibrium compositions of both the liquid and gas phases of the argon-hydrogen system. The predicted value of the gas phase composition agrees within ± 25 per cent of the experimental results at 110 atm between 86.95° and 105.01° K, and within ± 40 per cent of the experimental solubility of hydrogen in argon. By adjusting one parameter, γ_2, the predicted values were improved such that the results agreed within

± 15 per cent in the gas and ± 8 per cent in the liquid phase for the same conditions.

The three-phase line of the two systems and the melting curve for pure argon were determined to 120 atm pressure with an accuracy of ± 0.05° K or one half per cent of the reported pressure. The melting curve of pure argon agreed with the data of Clusius and Weigand[15] to within the above stated accuracy. The data indicate that the argon-helium solution is ideal along the three-phase line, and that the argon-hydrogen solution deviates positively from Raoult's law, the activity coefficient of argon being about 1.03 at 120 atm. These results for argon-hydrogen were found to agree well with the activity coefficients predicted by the BWR equation for the liquid phase. The results indicate that the choice of an ideal-solution in the prediction of the enhancement factor for argon-hydrogen is only slightly better than the assumption of a pure condensed phase.

Recommendations

Within the range of this work the least squares surface fit should be used for determining either the liquid phase or gas phase compositions in either of the two systems studied here.

For the prediction of the enhancement factor for the argon-helium system outside the range of this work, the KIHA method is recommended. This is, of course, nothing more than a sophisticated extrapolation method.

For the prediction of enhancement factors for the argon-hydrogen system outside the range of this work, one of the hybrid methods, either

H3 or H2, is recommended at pressures higher than 50 atm while any of the homogeneous methods may be used at low pressures. Within the accuracy of the prediction method, the solubility of hydrogen in argon may be ignored, though at temperatures above the range of this work the data of Volk and Halsey[78] extend to 140° K and 96 atm and could be used.

For future experimental work, it is recommended that the argon-helium and argon-hydrogen systems be investigated at higher temperatures by modification of the present apparatus. This should establish the validity of the data of McCain[51] at higher temperatures for the argon-helium system, and provide new data for the argon-hydrogen system.

The BWR equation should be tested for use in predicting systems such as those common in the air separation industries. The recent work of Wilson et al.[82] for the three-component system argon-nitrogen-oxygen should provide a good basis for comparison. To do this one would first have to obtain a set of constants for the BWR equation for oxygen.

More work should be done to obtain values of B_{12} from phase equilibrium data now available such as for the helium-nitrogen data of Rodewald et al.[70] and Buzyna et al.,[11] and the hydrogen-methane data of Hiza and Herring[35] and Kirk.[42] Only after adequate methods of predicting B_{12} are developed is it really meaningful to consider the smaller effects of the higher third virial interaction coefficients, C_{112} and C_{122}. To experimentally obtain values of the third virial interaction coefficients, possibly the solid-gas data such as given by Hiza and Herring[35] for the hydrogen-methane system at very low temperatures and

high pressures could be used in a manner similar to the method used here to obtain B_{12}. One such method would be to first obtain B_{12} by the method used here, and then fit the entire enhancement factor curve as a function of reciprocal volume by the method of least squares to obtain the higher interaction terms.

APPENDICES

APPENDIX A

EVALUATION OF BENEDICT-WEBB-RUBIN CONSTANTS

Determination of Constants with no Restrictions

The Benedict-Webb-Rubin equation of state may be written in the form

$$Z = 1 + \sum_{i=1}^{7} K_i \theta_i \qquad \text{(A-1)}$$

where

$\theta_1 = \rho$		$K_1 = B_o$	
$\theta_2 = \frac{\rho}{T}$		$K_2 = -\frac{A_o}{R}$	
$\theta_3 = \frac{\rho}{T^3}$		$K_3 = -\frac{C_o}{R}$	
$\theta_4 = \rho^2$		$K_4 = b$	
$\theta_5 = \frac{\rho^2}{T}$		$K_5 = -\frac{a}{R}$	
$\theta_6 = \frac{\rho^5}{T}$		$K_6 = \frac{a\alpha}{R}$	
$\theta_7 = \frac{\rho^2}{T^3}(1 + \gamma\rho^2)\exp(-\gamma\rho^2)$		$K_7 = \frac{c}{R}$	

Thus, for a particular value of γ, the equation may be made linear in the other seven constants.

For a particular set of experimental observations, $Z_n(\rho_n, T_n, P_n)$, it is desired to find a set of parameters for the BWR equation of state which will minimize the error in a particular chosen variable by the

method of least squares. The choice of what error to minimize is no clear choice. In this work the error in the compressibility factor was minimized. The compressibility factor was chosen simply for convenience and the fact that the value does not vary over wide ranges as does, for example, the pressure.

Having chosen the compressibility factor as the variable to fit by least squares, the sum of the squares of the residuals for a particular set of observations is given by Equation (A-2).

$$X = \sum_{n=1}^{N} \left[\left(Z_n - 1 \right) - \sum_{i=1}^{7} \left(K_i \theta_{i,n} \right) \right]^2 \qquad \text{(A-2)}$$

For a particular value of γ the sum of the squares of the residuals may be minimized by solving for the seven values of K_i which satisfy the "normal" equations. Taking the partial derivative of Equation (A-2) with respect to each K_i and setting the derivative equal to zero results in

$$\sum_{n=1}^{N} \theta_{k,n}(1-Z_n) + \sum_{i=1}^{7} K_i \sum_{n=1}^{N} \theta_{k,n}\, \theta_{i,n} = 0 \qquad \text{(A-3)}$$

where N is the total number of data points and k takes on values of 1, 2, 3, ..., 7.

The seven equations may be expressed in matrix notation as

$$\bar{\bar{A}}\, \bar{B} = \bar{C} \qquad \text{(A-4)}$$

or

$$\bar{B} = \bar{\bar{A}}^{-1}\, \bar{C} \qquad \text{(A-5)}$$

where

$$a_{ij} = \sum_{n=1}^{N} \theta_{i,n}\, \theta_{j,n} \tag{A-6}$$

$$b_i = K_i \tag{A-7}$$

$$c_i = \sum_{n=1}^{N} (Z_n - 1)\theta_{i,n} \tag{A-8}$$

It is to be noted that γ appears only in the last row and column of A and the last element in C. For this reason in solving for $\bar{A}^{-1}$ it is desirable to use a bordering method.[27] Letting $\bar{A}_6$ represent the first 6 rows and columns of $\bar{A}$

$$A = \begin{pmatrix} \bar{A}_6 & \bar{U}_7 \\ \bar{V}_7 & a_{77} \end{pmatrix} \tag{A-9}$$

where $\bar{U}_7$ is the column vector $(a_{1,7}, a_{2,7}, \ldots, a_{6,7})$
and $\bar{V}_7$ is the row vector $(a_{7,1}, \ldots, a_{7,6})$,

$$\bar{A}^{-1} = \begin{bmatrix} \dfrac{\bar{A}_6^{-1} + \bar{A}_6^{-1}\bar{U}_7\bar{V}_7\bar{A}_6^{-1}}{\alpha'} & -\dfrac{\bar{A}_6^{-1}\bar{U}_7}{\alpha'} \\ -\dfrac{\bar{V}_7\bar{A}_6^{-1}}{\alpha'} & \dfrac{1}{\alpha'} \end{bmatrix} \tag{A-10}$$

α' is defined by

$$\alpha' = a_{77} - \bar{V}_7\bar{A}_6^{-1}\bar{U}_7 \tag{A-11}$$

As in all other calculations in this work, the computations were carried out on a Burroughs 220 electronic digital computer. The procedure used was first to construct the matrix $\bar{A}$ from PVT data read in

on punched cards, and to store the PVT data on magnetic tape for further use. After the solution of the first set of parameters, the PVT data was then used to change only $\overline{U}_7$, $\overline{V}_7$, a_{77}, and c_7, and then a new set of parameters was determined for a second value of γ. The sum of the squares of the residuals was plotted versus gamma and subsequent values of gamma read into the computer as desired until the minimum value of the sum of the squares of the residuals was adequately defined. All operations involving the buildup and inversion of the matrices were carried out in triple precision arithmetic.

Determination of Constants Restricted at the Critical Point

The parameters of the BWR also may be determined such that the sum of the squares of the residuals is minimized subject to additional restrictions. In the present work three restrictions were imposed at the critical point in the determination of the constants for argon.

$$\left(\frac{\partial P}{\partial \rho}\right)_T = 0 \qquad \text{at } P_c,\ T_c \text{ and } \rho_c \tag{A-12}$$

$$\left(\frac{\partial^2 P}{\partial \rho^2}\right)_T = 0 \qquad \text{at } P_c,\ T_c \text{ and } \rho_c \tag{A-13}$$

$$\sum_{i=1}^{7} K_i \theta_i(\rho_c, T_c) = \frac{P_c}{RT_c\rho_c} - 1 \tag{A-14}$$

Not only does this insure that the parameters will fit the critical point but that the first and second derivatives of the pressure with respect to density evaluated at the critical point will also be zero.

Substitution of Equation (A-1) into Equations (A-11) and (A-12)

yields

$$1 + \sum_{i=1}^{7} K_i\theta_i + \rho \sum_{i=1}^{7} K_i\left(\frac{\partial\theta_i}{\partial\rho}\right)_T = 0 \quad \text{at } \rho_c \text{ and } T_c \tag{A-15}$$

$$2\sum_{i=1}^{7} K_i\left(\frac{\partial\theta_i}{\partial\rho}\right)_T + \rho \sum_{i=1}^{7} K_i\left(\frac{\partial^2\theta_i}{\partial\rho^2}\right)_T = 0 \text{ at } \rho_c \text{ and } T_c \tag{A-16}$$

Using the technique of undetermined multipliers, the function to be minimized is written as

$$F(K_i) = 2\beta\left[1 + \sum_{i=1}^{7} K_i\theta_i + \rho\sum_{i=1}^{7} K_i\left(\frac{\partial\theta_i}{\partial\rho}\right)_T\right]_c$$

$$+ 2\lambda\left[2\sum_{i=1}^{7} K_i\left(\frac{\partial\theta_i}{\partial\rho}\right)_T + \rho\sum_{i=1}^{7} K_i\left(\frac{\partial^2\theta_i}{\partial\rho^2}\right)_T\right]_c$$

$$+ 2\Lambda\left[\sum_{i=1}^{7} K_i\theta_i - (Z-1)\right]_c$$

$$+ \sum_{n=1}^{N}\left(1 - Z_m + \sum_{i=1}^{7} K_i\theta_{i,n}\right)^2 \tag{A-17}$$

In this expression n is the total number of data points and the subscript c indicates that the enclosed expression is to be evaluated at the critical point (ρ_c, T_c, P_c).

Minimizing Equation (A-17) with respect to each of the K_i yields

$$\beta\left[\theta_j + \rho\left(\frac{\partial\theta_j}{\partial\rho}\right)_T\right]_c + \lambda\left[2\left(\frac{\partial\theta_j}{\partial\rho}\right)_T + \rho\left(\frac{\partial^2\theta_j}{\partial\rho^2}\right)_T\right]_c$$

$$+ \Lambda\left[\theta_j\right]_c + \sum_{n=1}^{N}\theta_{j,n}(1-Z_n) + \sum_{i=1}^{7}K_i\sum_{n=1}^{N}\theta_{i,n}\theta_{j,n} = 0 \qquad \text{(A-18)}$$

where $j = 1, 2, \ldots, 7$.

Combination of the 7 equations from Equation (A-18) with the three restrictive Equations (A-12), (A-13), and (A-14) results in 10 linear equations. These can be written in matrix notation.

$$\overline{A}\,\overline{B} = \overline{C} \qquad \text{(A-19)}$$

or

$$\overline{B} = \overline{A}^{-1}\,\overline{C} \qquad \text{(A-20)}$$

$\overline{B}$ and $\overline{C}$ are column vectors defined as

$$\bar{B} = \begin{bmatrix} \beta \\ \lambda \\ \Lambda \\ K_1 \\ K_2 \\ K_3 \\ K_4 \\ K_5 \\ K_6 \\ K_7 \end{bmatrix} \qquad (A\text{-}21) \qquad \bar{C} = \begin{bmatrix} \sum \theta_{1,n}(Z_n-1) \\ \sum \theta_{2,n}(Z_n-1) \\ \sum \theta_{3,n}(Z_n-1) \\ \sum \theta_{4,n}(Z_n-1) \\ \sum \theta_{5,n}(Z_n-1) \\ \sum \theta_{6,n}(Z_n-1) \\ Z_c-1 \\ 0 \\ -1 \\ \sum \theta_{7,n}(Z_n-1) \end{bmatrix} \qquad (A\text{-}22)$$

$\bar{A}$ is a 10 by 10 matrix. The arrangement of the elements of $\bar{A}$ is inferred from $\bar{B}$ and $\bar{C}$ and is such that the elements containing γ will appear only in the last row and column of $\bar{A}$. The solution for the seven parameters and three undetermined multipliers is carried out on the computer in the same manner as described earlier for the 7 by 7 matrix; again all computations involving the matrix inversion being carried out in triple precision arithmetic.

Adjustment of BWR Constants to Fit Vapor Pressure of Liquid

For the BWR constants to predict correctly the vapor pressure at a temperature T, two conditions must be satisfied

$$P(\rho^L) = P(\rho^G) \tag{A-23}$$

$$f(\rho^L) = f(\rho^G) \tag{A-24}$$

The constants of the BWR equation of state may be adjusted to describe the vapor pressure curve throughout the liquid range by satisfying Equations (A-23) and (A-24). The method used here was to adjust only one constant. Which constant to adjust appears to be somewhat uncertain. This will be discussed further when examining the particular application to argon.

At constant temperature and pressure the differential of the fugacity function is written as

$$\delta(RT\ln f) = \left(\frac{\partial RT\ln f}{\partial \rho}\right)_{k_n} \delta\rho + \left(\frac{\partial RT\ln f}{\partial k_j}\right)_{\rho,k_{n-1}} \delta k_k \tag{A-25}$$

In Equation (A-25), k_j refers to the particular BWR constant being adjusted. The differential of pressure which must equal zero is

$$\delta P = \left(\frac{\partial P}{\partial \rho}\right)_{k_n} \delta\rho + \left(\frac{\partial P}{\partial k_j}\right)_{\rho,k_{n-1}} \delta k_j = 0 \tag{A-26}$$

Substituting Equation (A-26) into (A-25) results in

$$\frac{\delta RT\ln f}{\delta k_j} = -\left[\left(\frac{\partial P}{\partial k_j}\right)_{\rho,k_{n-1}}\right]\left[\left(\frac{\partial \rho}{\partial P}\right)_{k_n}\right]\left[\left(\frac{\partial RT\ln f}{\partial \rho}\right)_{k_n}\right]$$

$$+\left[\left(\frac{\partial RT\ln f}{\partial k_j}\right)_{\rho,k_{n-1}}\right] \tag{A-27}$$

Since it is desired to satisfy Equation (A-24)

$$RT\ln f(\rho^G) + \delta RT\ln f(\rho^G) = RT\ln f(\rho^L) + \delta RT\ln f(\rho^L) \qquad \text{(A-28)}$$

The change in the constants k_j required to produce this change in fugacity is then given approximately by

$$\delta k_j = [RT\ln f(\rho^L) - RT\ln f(\rho^G)] \Big/ \left[\frac{\delta RT\ln f(\rho^G)}{\delta k_j} - \frac{\delta RT\ln f(\rho^L)}{\delta k_j}\right] \qquad \text{(A-29)}$$

The numerator of Equation (A-29) represents the difference between the fugacity functions evaluated at T, P and the ρ^L and ρ^G given by a particular set of constants. The denominator of Equation (A-29) is evaluated from Equation (A-27) at ρ^G and ρ^L for the unadjusted constants. Thus the actual solution requires an iteration between Equation (A-29) and Equation (A-27) until Equation (A-24) is satisfied. Values of ρ^L amd ρ^G were calculated for each iteration from Equation (A-1). This insured that Equation (A-23) was satisfied.

Determination of BWR Constants for Hydrogen

The BWR constants for hydrogen were determined from PVT data of Goodwin et al.[31] for para-hydrogen and Michels et al.[53] for normal-hydrogen. The method used was that described previously in this appendix without restriction at the critical point. Two hundred fifty one selected PVT points were used in the fit. Of these, 169 were those of Goodwin et al.[31] covering the temperature range from 40° to 100° K and densities up to 31 gm moles/liter. The remaining 82 points were taken from Michels et al.[53] over the range 98.15° to 198.15° K and densities up to 28.5 gm moles/liter. The critical density of hydrogen is approximately 14.94[82] gm moles/liter.

Compressibility factors ranged from 0.49 to 1.79. Pressures ranged from 3.37 atm to 814.6 atm. The standard error of estimate is shown in Figure 27 as a function of γ. The best value of γ was taken to be 0.003. The values of the constants in liter-atm-^{o}K-gm mole are

$$A_o = 0.20432380$$
$$B_o = 0.21746707 \times 10^{-1}$$
$$C_o = 0.54767237 \times 10^{2}$$
$$a = -0.84030059 \times 10^{-3}$$
$$b = 0.58987532 \times 10^{-3}$$
$$c = 1.9138500$$
$$\alpha = -0.82694217 \times 10^{-4}$$

and $$\gamma = 0.0030$$

The values of a and α were negative for all values of γ tried for the particular set of data points described above. The negative values of a and α do not affect the calculation of the compressibility of pure hydrogen or mixtures of hydrogen, but the mixture rules do not give the correct result for the fugacity function. For this reason the suggestion of Ewbanks, as given by Motard and Organick,[58] was adopted. This consisted of changing the sign of a and α to plus and modifying b as follows:

$$b' = b + \frac{2|a|}{RT} \qquad \text{(A-30)}$$

This change does not affect the calculation of the compressibility factor and does give correct mixture rules for the fugacity function.

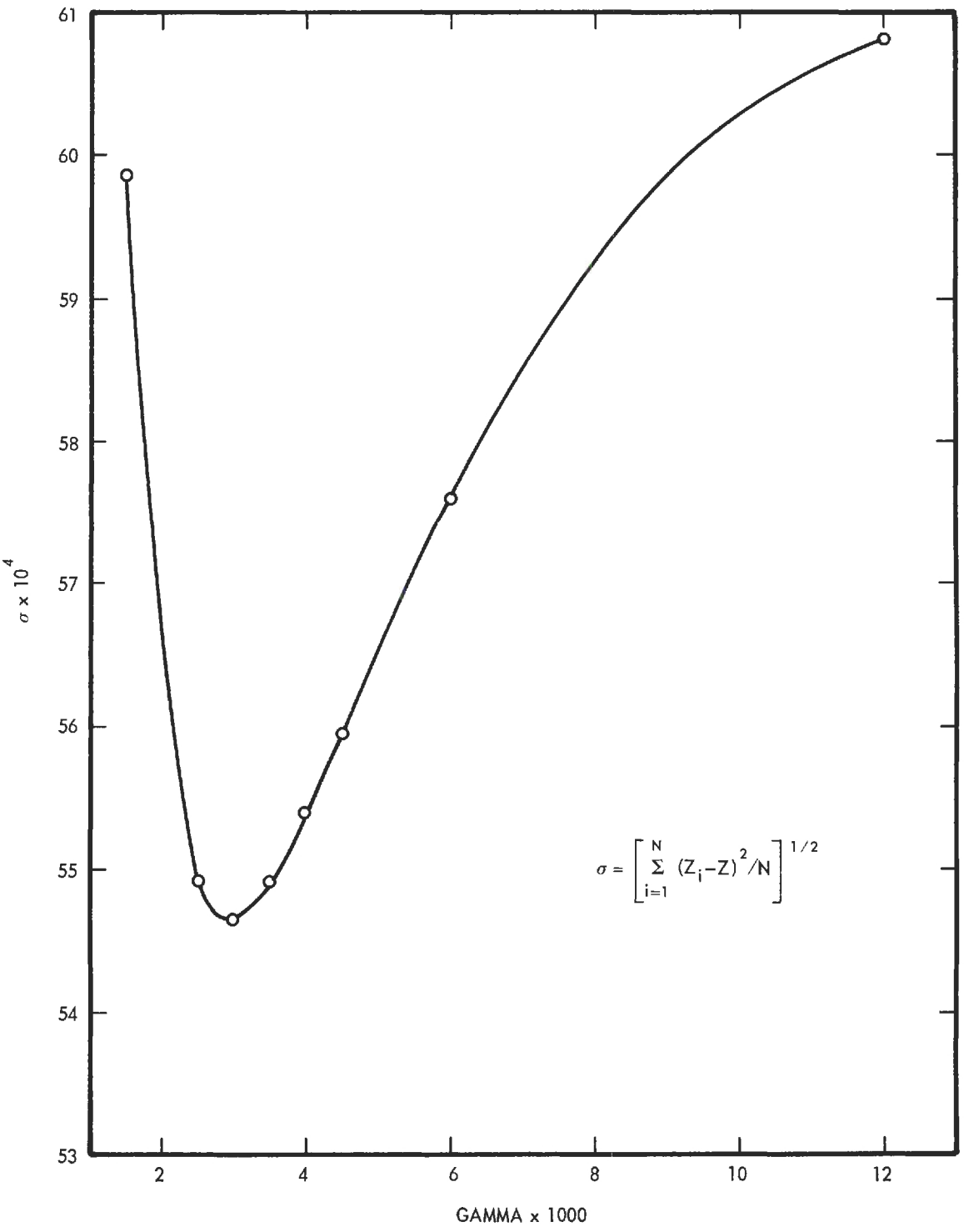

Figure 26. Determination of Optimum Gamma for BWR Constants of Hydrogen.

Determination of BWR Constants for Argon

The BWR constants for argon were determined from PVT data, the critical constants of Michels et al.,[54] and the vapor pressure data of Michels et al.[55] plus the selected normal boiling point and triple point of Ziegler et al.[84] First, 295 PVT points and the critical data of Michels were fit by the method of least squares to obtain the best set of parameters in a least squares sense constrained to fit the critical point. The PVT data covered the temperature range from 118° to 248° K, densities from 0.37 to 29.7 gm moles/liter, and pressures from 6.1 to 1028 atmospheres. This included 41 points in the pressurized liquid region. Values of the compressibility ranged from 0.0574 to 1.84. Values of the critical constants used were: T_c = 150.86° K; P_c = 48.34 atm; and ρ_c = 13.412 gm mole per liter. In Figure 27 is shown the variation of the standard error of estimate with gamma. The values of the constants from the least square fit are

A_o = 1.2874358	a = 0.017373414	α = 5.9791362 x 10^{-5}
B_o = 0.037352552	b = 0.0019170501	γ = 0.0036
C_o = 6505.1649	c = 664.67852	

The vapor pressure of Michels et al.[55] and the selected boiling point and triple point of Ziegler et al.[84] were then used to adjust a particular constant to predict the correct vapor pressure as described previously in this appendix. Each of the eight constants were independently adjusted to fit the vapor pressures. No good reason could be found for adjusting one rather than another and it was decided to

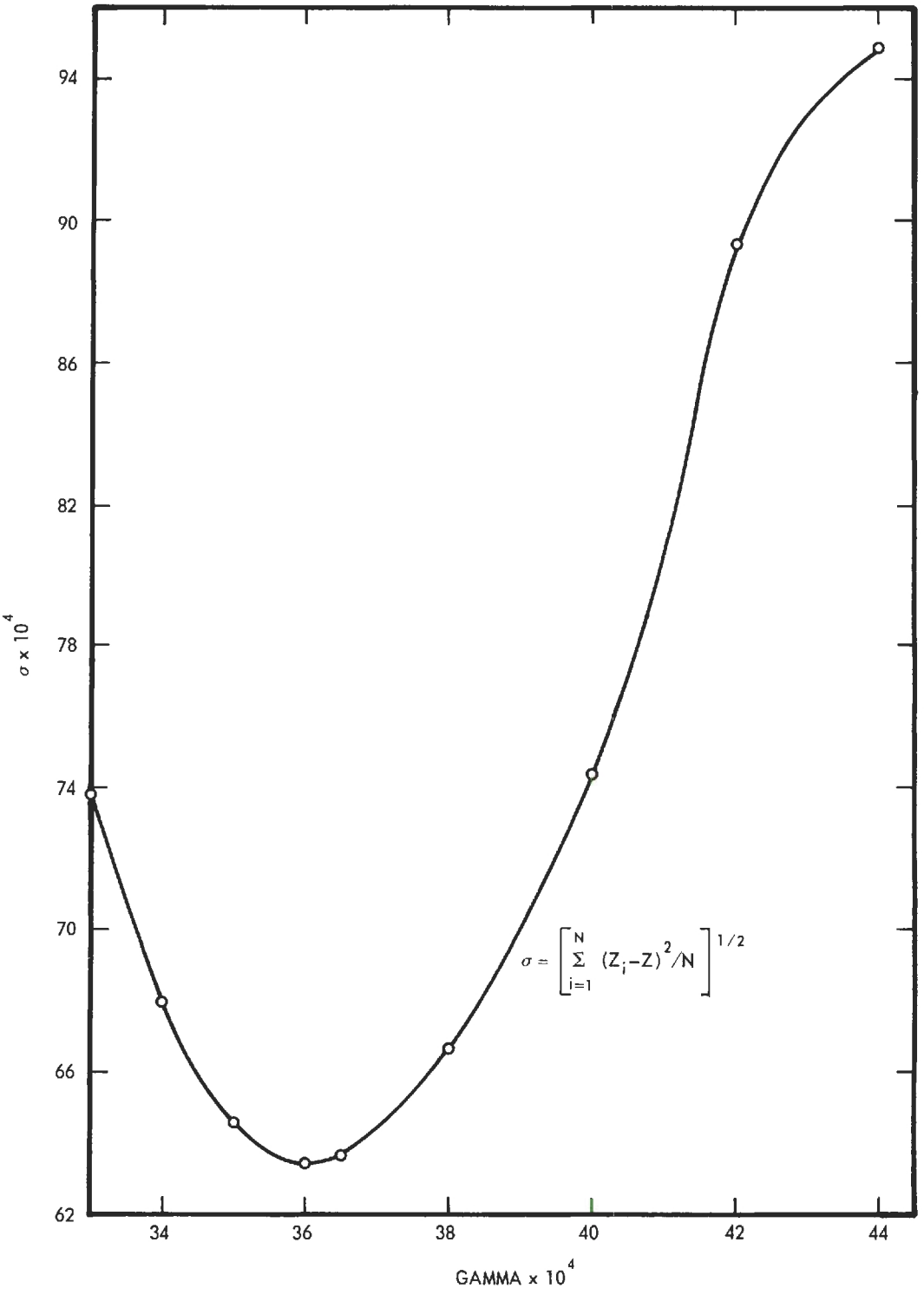

Figure 27. Determination of Optimum Gamma for BWR Constants of Argon.

conform with past investigators such as Stotler and Benedict,[75] and adjust C_o.

The adjusted values of C_o were approximately represented by the Equation (A-31).

For $T \leq 150.86^{\circ}$ K

$$C_o = \Big[1 - 7.5175653\,(T_c - T) \times 10^{-4} + 5.3958077\,(T_c - T)^2 \times 10^{-5} - 1.2521827\,(T_c - T)^3 \times 10^{-6} + 7.3843279\,(T_c - T)^4 \times 10^{-9}\Big] 6505.1649 \qquad \text{(A-31)}$$

The value of the standard error of estimate using the adjusted value of C_o from Equation (A-31) is 0.00623 compared to 0.00634 for the constant value of 6505.1649.

APPENDIX B

CALIBRATION OF GAS CHROMATOGRAPHS

General

Of the variables to be determined in the measurement of a binary system in equilibrium, usually the composition variables are the most difficult to determine. For this reason the calibration of the two chromatographs will be given in some detail. The chromatographs were calibrated on a peak height basis. The peak height read from the strip chart was first corrected for any drifts in the calibration. This was accomplished by multiplying the peak height by the ratio of the peak height of the "standard" mixture to the peak height of the "standard" mixture at the time of calibration. This corrected peak height, h, was then multiplied by the attenuation factor, s, on the chromatograph. This factor was then plotted as a function of h.s/y, where y is the mole fraction of the minor component. One of the calibration curves for the argon-helium system is shown in Figure 28. Had the peak height been exactly proportional to the composition, the calibration curve would have appeared as a vertical line, i.e., the value of h.s/y would be constant. This appears to be nearly the case at low concentrations for the systems studied here. A summary of the six different calibrations is given in Table 15.

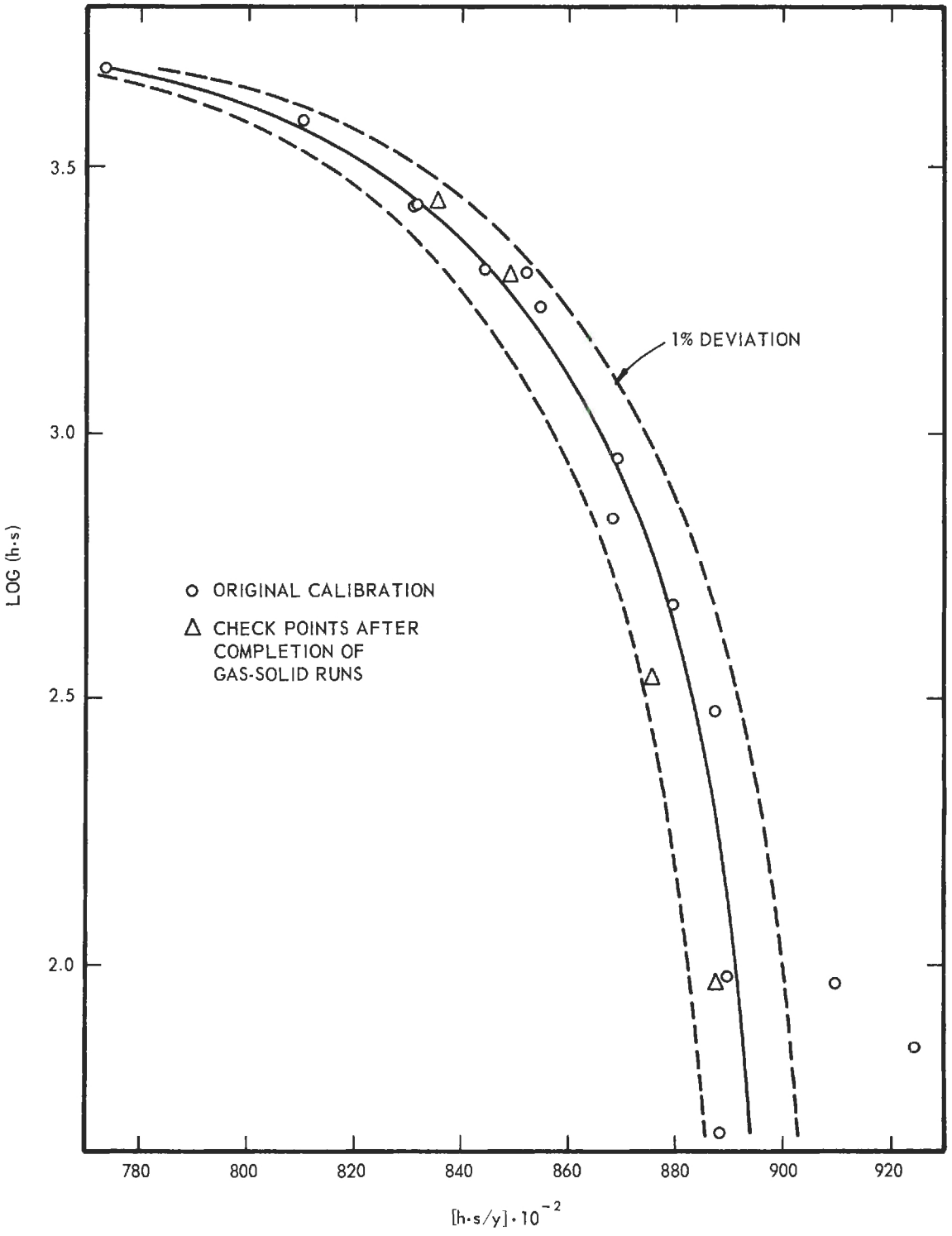

Figure 28. Calibration Curve for Argon in Helium on Vapor Fractometer 154B.

Table 15. Summary of Calibration Data for Chromatographs

System	Minor Component	Range, Mole Per Cent of Minor Comp.	No. of Points	Avg. Dev. %	Max. Dev. %	Sample Size* cc
A-He	A	0.054 - 6.2	19	0.6	3.2	5
A-He	A	1.00 - 15.2	10	0.3	0.6	2.5
A-He	He	0.15 - 11.5	12	0.5	1.2	10
A-H_2	A	0.34 - 3.6	14	0.3	0.5	10
A-H_2	A	1.95 - 32.0	12	0.1	0.3	0.5
A-H_2	H_2	1.3 - 20.0	13	0.25	0.6	10

*Atmospheric pressure and room temperature.

Calibration of the 154B for Argon-Helium Analysis

The first calibration was made on October 4, 1963 for the argon-helium system. The argon composition varied from 0.0546 to 6.227 mole per cent. This was the poorest calibration of the six different calibration curves. The difference was primarily the result of inexperience and the inability of the molecular sieve column to separate argon and oxygen at the temperature the columns were operated, 34° C. Small quantities of air leaked into the gas sampling valve, when evacuated. This leakage was monitored by observing the size of the nitrogen peak. The leak was essentially eliminated after the original calibration curve had been determined, but before the curve was used for analysis of samples. On November 11, 1963, after the completion of the gas phase determination of the argon-helium in solid-gas range four additional points were determined on the calibration curve as shown in Figure 28. These points were used to slightly change the shape of the curve, after which all the phase equilibrium points were recalculated.

Comments on Other Calibration Curves

In all cases except for the calibration of the model 154D for argon in helium, several points were checked on the calibration curve after the completion of all phase equilibrium runs involving that particular calibration curve. For the exception mentioned above, however, two of the "standard" mixtures were analyzed originally on the 154B and found to contain 4.02 and 0.891 per cent argon. These same bottles were analyzed to contain 4.03 and 0.890 per cent argon on the calibration curve obtained for the 154D.

One "standard" bottle analyzed to contain 3.23_9 per cent argon in hydrogen calibrated on the 154B was found to contain 3.24_5 per cent argon on the calibration obtained later for the 154D.

For the liquid compositions no overlap calibrations were obtained, but checks on the calibrations were made after the completion of the phase equilibrium determinations. The calibration curve for hydrogen in argon is shown in Figure 29.

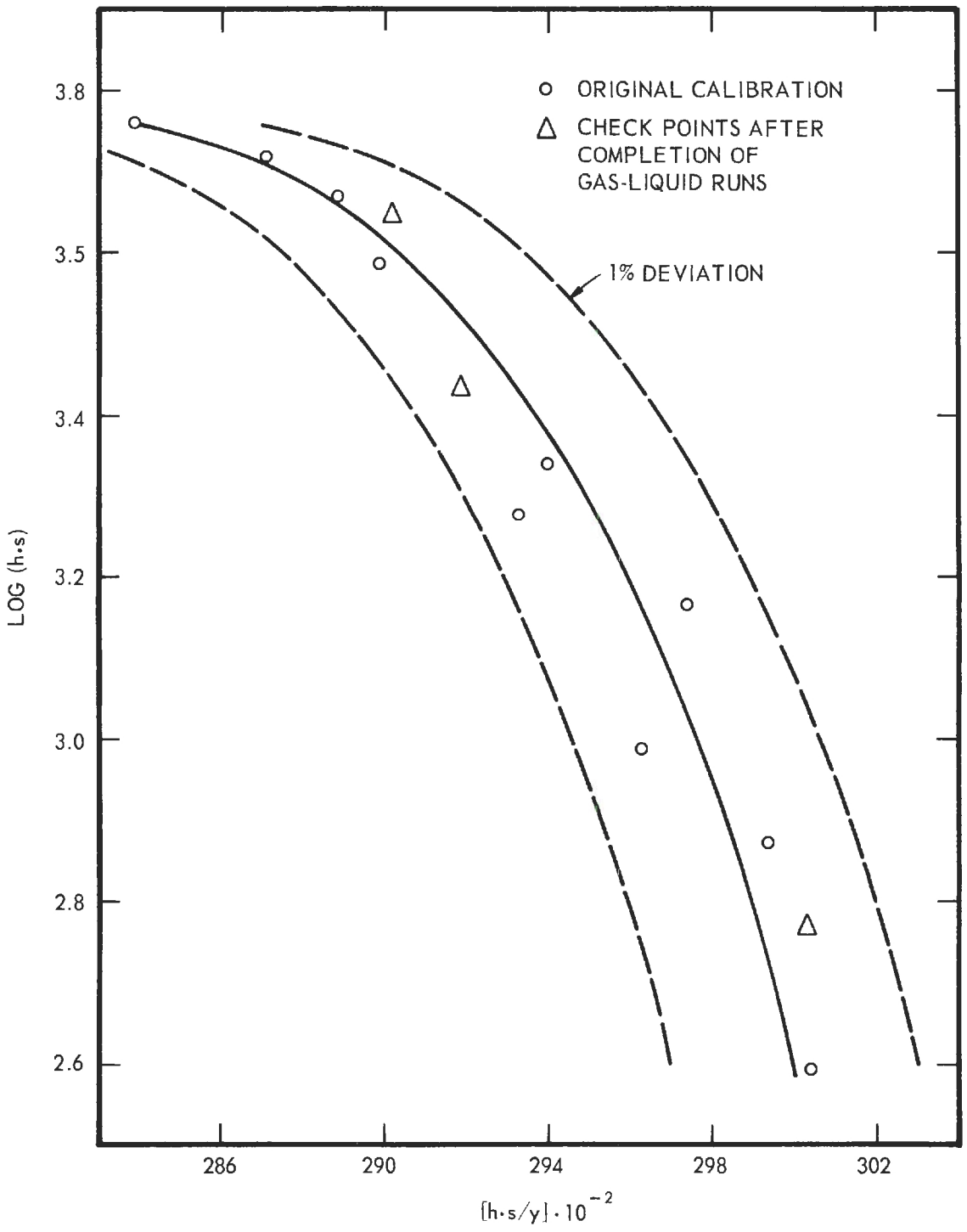

Figure 29. Calibration Curve for Hydrogen in Argon on Vapor Fractometer 154B.

APPENDIX C

SUMMARY OF PHASE EQUILIBRIUM DATA

In Tables 16 through 19 are summarized the gas-phase and liquid-phase data for the two binary systems argon-helium and argon-hydrogen. Tables 16 and 18 give the data for the gas-phase composition of the argon-helium and argon-hydrogen systems while Tables 17 and 19 give the results for the liquid phase of the same two systems.

In these tables the first column gives the code name for the sample number. The first letter designates the isotherm, the next number designates the particular setting of pressure and the next letter which is either G or L designates whether the sample was withdrawn through the gas or liquid sampling line. In the case of the gas-solid region, samples of the gas were taken from both sampling lines. The sequential number of the sample taken is the next integer and this is followed by a letter if more than one analysis was performed on the same sample. For example in A1G3A, A is the designation of the first isotherm run, 1 the first pressure setting on that isotherm, G designates that the gas was withdrawn from the gas sampling line, 3 designates it as the third sample under these conditions and A indicates the first analysis of the sample.

The enhancement factor is shown for each experimental gas composition in Tables 16 and 18 and a Henry's law constant for each liquid composition in Tables 17 and 19. The Henry's law constant used here is

defined by Equation (I-9). Values of the vapor pressure of argon were calculated from Equations (V-1) through (V-3).

A selected value is given for each experimental point. This was not necessarily an average value.

Table 16. Experimental Values of Equilibrium Gas Phase Compositions in the Argon-Helium System

Sample No.	T °K	P atm	P_{01} atm	$100y_1$ mole percent	Φ
A1G3A	80.002	120.48	0.3951	0.583	1.777
A1G3B	80.002	120.48	0.3951	0.582	1.774
A1G4A	80.009	120.48	0.3955	0.589	1.794
A1G4B	80.009	120.48	0.3955	0.590	1.797
A1L1A	80.060	120.48	0.3985	0.594	1.795
A1L1B	80.060	120.48	0.3985	0.592	1.789
SELECTED	80.03	120.48			1.788
A2G1A	80.057	101.16	0.3983	0.652	1.655
A2G1B	80.057	101.16	0.3983	0.656	1.666
A2G2A	80.057	101.16	0.3983	0.658	1.671
A2G2B	80.057	101.16	0.3983	0.662	1.681
A2L1A	80.118	101.16	0.4019	0.662	1.666
SELECTED	80.08	101.16			1.668
A3G3A	79.992	80.75	0.3945	0.753	1.541
A3G3B	79.992	80.75	0.3945	0.754	1.543
A3L2A	80.040	80.95	0.3973	0.752	1.532
A3L2B	80.040	80.95	0.3973	0.752	1.532
A3G4A	79.991	80.95	0.3944	0.752	1.543
A3G4B	79.991	80.95	0.3944	0.751	1.541
SELECTED	80.01	80.90			1.539
A4G1A	80.022	60.68	0.3962	0.918	1.405
A4G1B	80.022	60.68	0.3962	0.914	1.399
A4G1C	80.022	60.68	0.3962	0.918	1.405
A4L1A	80.111	60.68	0.4015	0.920	1.390
A4L1B	80.111	60.68	0.4015	0.916	1.384
SELECTED	80.06	60.68			1.395
A5G1A	80.049	41.57	0.3978	1.222	1.276
A5L1A	80.101	41.57	0.4009	1.224	1.269
A5L1B	80.101	41.57	0.4009	1.222	1.267
A5G2A	80.058	41.57	0.3984	1.217	1.269
SELECTED	80.07	41.57			1.271

(continued)

Table 16. Experimental Values of Equilibrium Gas Phase Compositions in the Argon-Helium System (continued)

Sample No.	^{o}T K	P atm	P_{01} atm	$100y_1$ mole percent	Φ
A6G1A	80.088	20.53	0.4002	2.216	1.136
A6L1A	80.117	20.53	0.4019	2.228	1.138
A6L1B	80.117	20.53	0.4019	2.239	1.143
A6G2A	80.120	20.53	0.4021	2.231	1.139
A6G2B	80.120	20.53	0.4021	2.264	1.156
A6G2C	80.120	20.53	0.4021	2.260	1.153
A6G3A	80.138	20.53	0.4031	2.257	1.149
SELECTED	80.10	20.53			1.144
B1G1A	73.918	115.88	0.1477	0.249	1.953
B1G2A	73.927	115.88	0.1479	0.250	1.958
B1G2B	73.927	115.88	0.1479	0.251	1.966
B1L1A	73.973	115.88	0.1491	0.277	2.152
B1L1B	73.973	115.88	0.1491	0.279	2.168
B1L2A	73.973	115.88	0.1491	0.263	2.043
B1G3A	73.951	115.88	0.1485	0.251	1.958
B1G3B	73.951	115.88	0.1485	0.251	1.958
B1L3A	73.986	115.88	0.1495	0.260	2.015
B1L3B	73.986	115.88	0.1495	0.260	2.015
B1G4A	73.972	115.88	0.1491	0.251	1.950
B1L4A	73.995	115.88	0.1497	0.261	2.020
B1L4B	73.995	115.88	0.1497	0.260	2.012
SELECTED	73.96	115.88			1.960
B2G1A	73.998	101.02	0.1498	0.270	1.821
B2L1A	74.035	101.02	0.1507	0.279	1.869
B2L1B	74.035	101.02	0.1507	0.281	1.883
B2L1C	74.035	101.02	0.1507	0.281	1.883
B2G2A	74.014	101.02	0.1502	0.270	1.816
B2G2B	74.014	101.02	0.1502	0.270	1.816
SELECTED	74.02	101.02			1.818
B3G4A	74.138	81.50	0.1535	0.321	1.704
B3G4B	74.138	81.50	0.1535	0.321	1.704
B3L2A	74.191	81.50	0.1549	0.319	1.678
B3G5A	74.177	81.50	0.1545	0.322	1.698
SELECTED	74.16	81.50			1.693

(continued)

Table 16. Experimental Values of Equilibrium Gas Phase Composition in the Argon-Helium System (continued)

Sample No.	T °K	P atm	P_{01} atm	$100y_1$ mole percent	Φ
B4G1A	74.016	61.43	0.1502	0.371	1.516
B4L1A	74.035	61.43	0.1507	0.366	1.491
B4G2A	74.023	61.43	0.1504	0.371	1.515
B4G3A	74.008	61.43	0.1500	0.364	1.490
B4G3B	74.008	61.43	0.1500	0.363	1.486
B4L2A	74.046	61.43	0.1510	0.366	1.488
B4G4A	74.043	61.43	0.1510	0.363	1.477
SELECTED	74.03	61.43			1.495
B5G1A	73.901	41.16	0.1472	0.475	1.327
B5L1A	73.920	41.16	0.1477	0.478	1.331
B5G3A	73.895	41.16	0.1471	0.475	1.329
SELECTED	73.91	41.16			1.329
B6G1A	73.907	19.96	0.1474	0.855	1.157
B6L1A	73.913	19.96	0.1476	0.856	1.157
B6G2A	73.898	19.96	0.1472	0.857	1.162
SELECTED	73.90	19.96			1.159
B7G4A	74.031	120.34	0.1506	0.248	1.981
B7G4B	74.031	120.34	0.1506	0.248	1.981
B7L2A	74.019	120.34	0.1503	0.245	1.961
B7L2B	74.019	120.34	0.1503	0.244	1.953
B7G5A	74.021	120.34	0.1504	0.246	1.968
B7G5B	74.021	120.34	0.1504	0.246	1.968
SELECTED	74.02	120.34			1.969
C1L3A	68.067	120.27	0.04844	0.0892	2.214
C1G8A	68.005	120.27	0.04782	0.0888	2.233
C1L4A	68.064	120.27	0.04841	0.0899	2.233
C1L4B	68.064	120.27	0.04841	0.0889	2.208
C1G9A	68.029	120.27	0.04806	0.0893	2.234
C1G9B	68.029	120.27	0.04806	0.0893	2.234
C1G0A	68.033	120.27	0.04810	0.0892	2.230
C1G0B	68.033	120.27	0.04810	0.0889	2.223
SELECTED	68.04	120.27			2.225

(continued)

Table 16. Experimental Values of Equilibrium Gas Phase Composition in the Argon-Helium System (continued)

Sample No.	T °K	P atm	P_{01} atm	$100y_1$ mole percent	Φ
C2G1A	68.090	100.07	0.04867	0.0969	1.992
C2G1B	68.090	100.07	0.04867	0.0973	2.000
C2L1A	68.125	100.07	0.04902	0.0973	1.986
C2L1B	68.125	100.07	0.04902	0.0981	2.002
C2G2A	68.079	100.07	0.04856	0.0974	2.007
C2G2B	68.079	100.07	0.04856	0.0982	2.023
SELECTED	68.10	100.07			2.002
C3G1A	68.062	79.73	0.04839	0.1093	1.801
C3G2A	68.025	79.73	0.04802	0.1075	1.784
C3G2B	68.025	79.73	0.04802	0.1081	1.794
C3G3A	68.058	79.73	0.04835	0.1085	1.789
C3L1A	68.079	79.73	0.04856	0.1086	1.783
C3L1B	68.079	79.73	0.04856	0.1091	1.791
C3L1C	68.079	79.73	0.04856	0.1090	1.789
C3G4A	68.058	79.73	0.04835	0.1090	1.797
C3G4B	68.058	79.73	0.04835	0.1089	1.795
SELECTED	68.07	79.73			1.792
C4G1A	68.065	60.00	0.04842	0.1274	1.578
C4G2A	68.070	60.00	0.04847	0.1274	1.577
C4G2B	68.070	60.00	0.04847	0.1276	1.579
C4L1A	68.102	60.00	0.04879	0.1279	1.572
C4L1B	68.102	60.00	0.04879	0.1281	1.575
SELECTED	68.08	60.00			1.576
C5G1A	68.061	40.07	0.04838	0.1685	1.395
C5G2A	68.065	40.07	0.04842	0.1685	1.394
C5G2B	68.065	40.07	0.04842	0.1699	1.406
C5L1A	68.080	40.07	0.04857	0.1687	1.391
C5L2A	68.076	40.07	0.04853	0.1708	1.410
C5L2B	68.076	40.07	0.04853	0.1699	1.402
C5L2C	68.076	40.07	0.04853	0.1696	1.400
SELECTED	68.07	40.07			1.398

(continued)

Table 16. Experimental Values of Equilibrium Gas Phase Composition in the Argon-Helium System (continued)

Sample No.	^{o}T K	P atm	P_{01} atm	$100y_1$ mole percent	Φ
C6G1A	68.075	20.22	0.04852	0.286	1.191
C6G1B	68.075	20.22	0.04852	0.286	1.191
C6G2A	68.075	20.22	0.04852	0.285	1.187
C6G2B	68.075	20.22	0.04852	0.285	1.187
C6L1A	68.095	20.22	0.04872	0.286	1.187
C6L1B	68.095	20.22	0.04872	0.285	1.182
C6G3A	68.088	20.22	0.04865	0.285	1.184
SELECTED	68.08	20.22			1.186
D1G2A	77.876	79.93	0.2851	0.559	1.567
D1L2A	77.903	79.93	0.2863	0.564	1.574
D1L2B	77.903	79.93	0.2863	0.564	1.574
D1G3A	77.880	79.93	0.2853	0.559	1.566
D1G3B	77.880	79.93	0.2853	0.559	1.566
D1G3C	77.880	79.93	0.2853	0.559	1.566
D1L3A	77.920	80.07	0.2871	0.563	1.570
D1L3B	77.920	80.07	0.2871	0.565	1.575
D1L3C	77.920	80.07	0.2871	0.564	1.573
SELECTED	77.90	80.00			1.570
D2G1A	77.886	60.14	0.2855	0.679	1.430
D2L1A	77.920	60.14	0.2871	0.682	1.428
D2G2A	77.884	60.14	0.2855	0.680	1.432
D2G2B	77.884	60.14	0.2855	0.679	1.430
SELECTED	77.90	60.14			1.430
E1G4	91.975	80.27	1.604	2.943	1.472
E1G5	91.973	80.20	1.604	2.955	1.477
E1G6	91.990	80.20	1.607	2.943	1.469
E1G7	91.990	80.20	1.607	2.943	1.469
E1G8	92.021	80.20	1.611	2.951	1.468
SELECTED	91.99	80.20			1.471
E2G2	91.992	60.20	1.607	3.62	1.356
E2G3	91.993	60.20	1.607	3.62	1.356
E2G4	91.998	60.41	1.608	3.62	1.360
SELECTED	91.99	60.30			1.357

(continued)

Table 16. Experimental Values of Equilibrium Gas Phase Compositions in the Argon-Helium System (continued)

Sample No.	^{o}T F	P atm	P_{01} atm	$100y_1$ mole percent	ϕ
E3G2	92.001	40.14	1.608	5.04	1.257
E3G3	92.006	40.14	1.609	5.04	1.257
SELECTED	92.00	40.14			1.257
E4G3	91.977	19.92	1.605	9.18	1.139
E4G4	91.910	19.92	1.594	9.14	1.141
E4G5	91.955	19.92	1.601	9.18	1.141
SELECTED	91.95	19.92			1.140
E5G2	91.962	119.80	1.602	2.248	1.680
E5G3	91.963	119.80	1.602	2.253	1.684
E5G4	91.965	119.80	1.603	2.261	1.689
SELECTED	91.96	119.80			1.684
E6G1	91.987	100.27	1.606	2.533	1.581
E6G2	92.005	100.27	1.609	2.541	1.583
E6G3	91.951	100.27	1.601	2.537	1.589
E6G4	91.960	100.27	1.602	2.529	1.582
SELECTED	91.98	100.27			1.584
F1G1	97.494	120.07	2.621	3.60	1.649
F1G2	97.482	120.07	2.618	3.58	1.641
F1G3	97.500	120.07	2.622	3.59	1.644
F1G4	97.507	120.07	2.623	3.58	1.638
F1G5	97.511	120.07	2.624	3.57	1.633
SELECTED	97.50	120.07			1.641
F2G1	97.496	100.07	2.621	4.02	1.534
F2G2	97.496	100.07	2.621	4.02	1.534
F2G3	97.499	100.07	2.622	4.03	1.538
F2G4	97.501	100.07	2.622	4.05	1.545
SELECTED	97.50	100.07			1.538
F3G1	97.516	80.00	2.625	4.69	1.429
F3G2	97.526	80.00	2.628	4.70	1.430
F3G3	97.508	80.00	2.624	4.71	1.436
F3G4	97.496	80.00	2.621	4.69	1.431
SELECTED	97.51	80.00			1.432

(continued)

Table 16. Experimental Values of Equilibrium Gas Phase Compositions in the Argon-Helium System (continued)

Sample No.	^{o}T K	P atm	P_{01} atm	$100y_1$ mole percent	Φ
F4G1	97.507	60.27	2.623	5.87	1.348
F4G2	97.507	60.27	2.623	5.88	1.350
F4G3	97.511	60.20	2.624	5.88	1.348
SELECTED	97.51	60.25			1.349
F5G1	97.510	40.00	2.624	8.28	1.262
F5G2	97.510	40.00	2.624	8.26	1.259
F5G3	97.512	40.00	2.625	8.20	1.249
F5G4	97.511	40.14	2.624	8.16	1.248
SELECTED	97.51	40.04			1.252
F6G1	97.514	20.02	2.625	14.81	1.129
F6G2	97.516	20.02	2.625	14.79	1.127
F6G3	97.518	20.02	2.626	14.77	1.126
SELECTED	97.52	20.02			1.127
F7G1	97.500	60.20	2.622	5.86	1.345
F7G2	97.507	60.20	2.623	5.84	1.340
SELECTED	97.50	60.20			1.342
G1G1	86.017	80.14	0.8710	1.652	1.519
G1G2	86.021	80.14	0.8714	1.648	1.515
G1G3	86.022	80.14	0.8715	1.650	1.517
G1G4	86.023	80.14	0.8716	1.650	1.517
SELECTED	86.02	80.14			1.517
G2G1	86.027	60.34	0.8720	2.013	1.392
G2G2	86.021	60.27	0.8714	2.021	1.397
G2G3	86.021	60.27	0.8714	2.005	1.386
SELECTED	86.02	60.30			1.392
G3G1	86.023	39.52	0.8716	2.797	1.268
G3G2	86.027	39.52	0.8720	2.810	1.273
G3G3	86.034	39.52	0.8727	2.814	1.274
SELECTED	86.03	39.52			1.271

(continued)

Table 16. Experimental Values of Equilibrium Gas Phase Compositions in the Argon-Helium System (continued)

Sample No.	T °K	P atm	P_{01} atm	$100y_1$ mole percent	ϕ
G4G1	86.029	19.95	0.8722	5.00	1.143
G4G2	86.014	19.95	0.8708	4.98	1.140
G4G3	86.015	19.95	0.8709	4.98	1.140
SELECTED	86.02	19.95			1.141
G5G2	86.022	120.07	0.8715	1.277	1.759
G5G3	86.020	120.07	0.8713	1.275	1.756
G5G4	86.021	120.07	0.8714	1.273	1.754
SELECTED	86.02	120.07		1.274	1.756
G6G5	86.009	120.20	0.8703	1.273	1.758
G6G6	86.012	120.27	0.8706	1.279	1.766
SELECTED	86.01	120.23		1.276	1.762
G7G1	86.003	100.34	0.8697	1.430	1.649
G7G2	86.006	100.41	0.8700	1.423	1.642
G7G3	86.006	100.41	0.8700	1.432	1.652
SELECTED	86.00	100.38			1.648
G8G3	86.000	120.03	0.8694	1.297	1.790
G8G4	85.993	120.00	0.8688	1.295	1.788
G8G5	85.997	119.93	0.8691	1.295	1.786
SELECTED	86.00	120.00			1.788
G9G2	86.023	120.00	0.8716	1.285	1.769
G9G3	86.023	120.00	0.8716	1.266	1.742
G9G4	86.023	120.00	0.8716	1.281	1.763
SELECTED	86.02	120.00			1.754
H1G1	108.000	120.00	5.769	7.71	1.603
H1G2	108.006	120.00	5.771	7.71	1.603
H1G3	108.025	120.00	5.779	7.70	1.598
H1G4	108.022	120.07	5.778	7.72	1.604
SELECTED	108.01	120.00			1.602

(continued)

Table 16. Experimental Values of Equilibrium Gas Phase Compositions in the Argon-Helium System (concluded)

Sample No.	^{o}T F	P atm	P_{01} atm	$100y_1$ mole percent	Φ
H2G1	108.013	100.07	5.774	8.76	1.518
H2G2	108.009	100.07	5.773	8.78	1.522
H2G3	108.021	100.07	5.777	8.77	1.519
SELECTED	108.01	100.07			1.520
H3G1	108.045	80.00	5.787	10.32	1.426
H3G2	108.043	80.00	5.786	10.36	1.432
H3G3	108.040	80.00	5.785	10.36	1.432
H3G4	108.039	80.00	5.784	10.34	1.430
SELECTED	108.04	80.00			1.430
H4G1	108.036	60.00	5.783	12.92	1.340
H4G2	108.038	60.00	5.784	12.84	1.331
H4G3	108.040	60.00	5.785	12.92	1.340
H4G4	108.043	60.00	5.786	12.92	1.339
SELECTED	108.04	60.00			1.338

Table 17. Experimental Values of Equilibrium Liquid Phase Compositions in the Argon-Helium System.

Sample No.	^{o}T K	P atm	$P-p_{01}$ atm	$100x_2$ mole percent	$\bar{K}.10^{-2}$ $(P-p_{01}/x_2)$
E1L1A	91.992	80.20	78.59	0.749	104.9
E1L1C	91.992	80.20	78.59	0.764	102.9
SELECTED	91.99	80.20	78.59	0.756	104.0
E2L1A	91.999	60.41	58.80	0.580	101.4
E2L1B	91.999	60.41	58.80	0.578	101.7
E2L1C	91.999	60.41	58.80	0.581	101.2
SELECTED	92.00	60.41	58.80	0.580	101.4
E3L1A	92.004	40.14	38.53	0.387	99.6
E3L1B	92.004	40.14	38.53	0.387	99.6
E3L1C	92.004	40.14	38.53	0.386	99.8
SELECTED	92.00	40.14	38.53	0.387	99.6
E4L1A	91.955	19.92	18.31	0.192	95.4
E4L1B	91.955	19.92	18.31	0.192	95.4
E4L1C	91.955	19.92	18.31	0.193	94.9
SELECTED	91.96	19.92	18.31	0.192	95.4
E5L1A	91.968	119.80	118.19	1.071	110.4
E5L1B	91.968	119.80	118.19	1.071	110.4
SELECTED	91.97	119.80	118.19	1.071	110.4
E6L1A	91.961	100.27	98.66	0.917	107.6
E6L1B	91.961	100.27	98.66	0.917	107.6
E6L1C	91.961	100.27	98.66	0.917	107.6
SELECTED	91.96	100.27	98.66	0.917	107.6
F1L1A	97.513	120.07	117.44	1.412	83.2
F1L1B	97.513	120.07	117.44	1.403	83.7
F1L1C	97.513	120.07	117.44	1.403	83.7
SELECTED	97.51	120.07	117.44	1.406	83.5

(continued)

Table 17. Experimental Values of Equilibrium Liquid Phase Compositions in the Argon-Helium System. (continued)

Sample No.	^{o}T K	P atm	$P-p_{01}$ atm	$100x_2$ mole percent	$\bar{K}.10^{-2}$ $(P-p_{01}/x_2)$
F2L1A	97.503	100.07	97.44	1.211	80.5
F2L1B	97.503	100.07	97.44	1.213	80.3
F2L1C	97.503	100.07	97.44	1.213	80.3
SELECTED	97.50	100.07	97.44	1.212	80.4
F3L1A	97.496	80.00	77.37	0.984	78.6
F3L1B	97.496	80.00	77.37	0.986	78.5
F3L1C	97.496	80.00	77.37	0.984	78.6
SELECTED	97.50	80.00	77.37	0.985	78.6
F4L1A	97.519	60.20	57.57	0.756	76.2
F4L1B	97.519	60.20	57.57	0.756	76.2
F4L1C	97.519	60.20	57.57	0.757	76.1
SELECTED	97.52	60.20	57.57	0.756	76.2
F5L1A	97.512	40.14	37.51	0.499	75.2
F5L1B	97.512	40.14	37.51	0.499	75.2
F5L1C	97.512	40.14	37.51	0.499	75.2
SELECTED	97.51	40.14	37.51	0.499	75.2
F6L1A	97.524	20.02	17.39	0.2404	72.3
F6L1B	97.524	20.02	17.39	0.2400	72.5
F6L1C	97.524	20.02	17.39	0.2389	72.8
SELECTED	97.52	20.02	17.39	0.240	72.5
F7L1A	97.513	60.20	57.57	0.756	76.2
F7L1B	97.513	60.20	57.57	0.741	77.7
F7L1C	97.513	60.20	57.57	0.746	77.2
SELECTED	97.51	60.20	57.57	0.748	77.0
G1L1A	86.015	80.14	79.26	0.550	144.1
G1L1B	86.015	80.14	79.26	0.551	143.9
G1L1C	86.015	80.14	79.26	0.549	144.4
SELECTED	86.02	80.14	79.26	0.550	144.1

(continued)

Table 17. Experimental Values of Equilibrium Liquid Phase Compositions in the Argon-Helium System. (continued)

Sample No.	^{o}T K	P atm	$P-p_{01}$ atm	$100x_2$ mole percent	$\bar{K}.10^{-2}$ $(P-p_{01}/x_2)$
G2L1A	86.024	60.27	59.39	0.419	141.8
G2L1B	86.024	60.27	59.39	0.419	141.8
G2L1C	86.024	60.27	59.39	0.417	142.4
SELECTED	86.02	60.27	59.39	0.418	142.1
G3L1A	86.033	39.52	38.64	0.282	137.0
G3L1B	86.033	39.52	38.64	0.282	137.0
G3L1C	86.033	39.52	38.64	0.284	136.1
SELECTED	86.03	39.52	38.64	0.283	136.6
G4L1A	86.004	19.97	19.10	0.142	134.5
G4L1B	86.004	19.97	19.10	0.143	133.6
G4L1C	86.004	19.97	19.10	0.143	133.6
SELECTED	86.00	19.97	19.10	0.143	133.6
G4L2A	86.012	19.97	19.09	0.143	133.6
G4L2B	86.012	19.97	19.09	0.143	133.6
G4L2C	86.012	19.97	19.09	0.143	133.6
SELECTED	86.01	19.97	19.09	0.143	133.6
G7L1A	86.010	100.41	99.53	0.677	147.0
G7L1B	86.010	100.41	99.53	0.675	147.5
G7L1C	86.010	100.41	99.53	0.673	147.9
SELECTED	86.01	100.41	99.53	0.675	147.5
H1L1A	108.019	120.07	114.29	2.220	51.5
H1L1B	108.019	120.07	114.29	2.214	51.6
H1L1C	108.019	120.07	114.29	2.214	51.6
SELECTED	108.02	120.07	114.29	2.216	51.6
H2L1A	108.027	100.07	94.29	1.879	50.2
H2L1B	108.027	100.07	94.29	1.879	50.2
H2L1C	108.027	100.07	94.29	1.879	50.2
SELECTED	108.03	100.07	94.29	1.879	50.2

(continued)

Table 17. Experimental Values of Equilibrium Liquid Phase Compositions in the Argon-Helium System. (concluded)

Sample No.	^{o}T K	P atm	$P-p_{01}$ atm	$100x_2$ mole percent	$\bar{K}.10^{-2}$ $(P-p_{01}/x_2)$
H3L1A	108.030	80.00	74.21	1.526	48.6
H3L1B	108.030	80.00	74.21	1.517	48.9
H3L1C	108.030	80.00	74.21	1.527	48.6
SELECTED	108.03	80.00	74.21	1.523	48.7
H4L1A	108.040	60.00	54.21	1.145	47.3
H4L1B	108.040	60.00	54.21	1.145	47.3
H4L1C	108.040	60.00	54.21	1.144	47.4
SELECTED	108.04	60.00	54.21	1.145	47.3

Table 18. Experimental Values of Equilibrium Gas Phase Compositions in the Argon-Hydrogen System

Sample No.	^{o}T K	P atm	P_{01} atm	$100y_1$ mole percent	Φ
I1G3	86.936	60.07	0.9618	5.05	3.153
I1G4	86.956	60.07	0.9639	5.05	3.147
I1G5	86.961	60.07	0.9644	5.06	3.151
SELECTED	86.95	60.07			3.15
I2G2	87.002	120.27	0.9686	6.85	8.51
I2G3	87.010	120.27	0.9694	6.85	8.50
I2G4	86.975	120.34	0.9658	6.85	8.53
I2G5	86.944	120.34	0.9626	6.85	8.56
SELECTED	86.97	120.30			8.52
I3G2	86.949	100.20	0.9632	6.03	6.27
I3G3	86.943	100.20	0.9625	6.03	6.28
I3G4	86.948	100.27	0.9631	6.04	6.29
SELECTED	86.94	100.20			6.28
I4G2	86.944	80.00	0.9626	5.41	4.495
I4G3	86.947	80.00	0.9630	5.41	4.494
SELECTED	86.94	80.00			4.495
I5G2	86.940	40.34	0.9622	5.23	2.192
I5G3	86.944	40.34	0.9626	5.22	2.187
I5G4	86.935	40.34	0.9617	5.20	2.181
SELECTED	86.94	40.34			2.186
I6G1	86.943	19.99	0.9625	7.10	1.474
I6G2	86.945	19.99	0.9627	7.10	1.474
SELECTED	86.94	19.99			1.474
J1G1	94.197	120.41	1.9693	10.48	6.41
J1G2	94.203	120.34	1.9703	10.50	6.41
J1G3	94.211	120.34	1.9717	10.48	6.40
J1G4	94.213	120.34	1.9721	10.43	6.36
J1G5	94.223	120.34	1.9738	10.46	6.38
SELECTED	94.21	120.34			6.38

(continued)

Table 18. Experimental Values of Equilibrium Gas Phase Compositions in the Argon-Hydrogen System (continued)

Sample No.	T °K	P atm	P_{01} atm	$100y_1$ mole percent	Φ
J2G1	94.194	100.34	1.9687	9.48	4.83
J2G2	94.194	100.34	1.9687	9.48	4.83
J2G3	94.200	100.34	1.9698	9.45	4.81
J2G4	94.198	100.34	1.9694	9.46	4.82
SELECTED	94.20	100.34			4.82
J3G1	94.204	80.00	1.9705	8.80	3.572
J3G2	94.207	80.00	1.9710	8.82	3.579
SELECTED	94.21	80.00			3.576
J4G1	94.204	60.00	1.9705	8.56	2.606
J4G4	94.211	60.00	1.9717	8.57	2.607
SELECTED	94.21	60.00			2.607
J5G1	94.213	39.80	1.9721	9.46	1.909
J5G2	94.209	39.80	1.9714	9.46	1.909
J5G3	94.209	39.80	1.9714	9.46	1.909
J5G4	94.213	39.80	1.9721	9.41	1.899
J5G5	94.212	39.80	1.9719	9.45	1.907
SELECTED	94.21	39.80			1.905
J6G1	94.189	20.12	1.9679	13.55	1.385
J6G2	94.216	20.12	1.9726	13.51	1.377
J6G3	94.208	20.13	1.9712	13.53	1.381
J6G4	94.222	20.13	1.9737	13.53	1.379
SELECTED	94.21	20.13			1.380
K1G1	99.953	60.34	3.2013	12.54	2.363
K1G2	99.943	60.41	3.1987	12.56	2.372
K1G3	99.948	60.41	3.2000	12.54	2.367
SELECTED	99.95	60.41			2.367
K2G1	99.945	40.00	3.1992	14.20	1.775
K2G2	99.952	40.00	3.2010	14.15	1.768
K2G3	99.954	40.00	3.2015	14.15	1.767
K2G4	99.951	40.00	3.2008	14.15	1.768
SELECTED	99.95	40.00			1.768

(continued)

Table 18. Experimental Values of Equilibrium Gas Phase Compositions in the Argon-Hydrogen System (continued)

Sample No.	^{o}T K	P atm	P_{01} atm	$100y_1$ mole percent	Φ
K3G1	99.953	20.00	3.2013	21.16	1.321
K3G2	99.963	20.02	3.2038	21.08	1.317
K3G3	99.967	20.02	3.2048	21.16	1.321
SELECTED	99.96	20.02			1.320
K4G2	99.931	119.73	3.1957	14.20	5.32
K4G3	99.943	119.73	3.1987	14.17	5.30
SELECTED	99.94	119.73			5.31
K5G1	99.941	100.41	3.1982	13.10	4.112
K5G2	99.941	100.34	3.1982	13.14	4.122
K5G3	99.943	100.34	3.1987	13.10	4.109
SELECTED	99.94	100.34			4.115
K6G1	99.953	80.00	3.2013	12.49	3.121
K6G2	99.951	80.00	3.2007	12.49	3.121
K6G3	99.945	80.00	3.1992	12.44	3.110
K6G4	99.950	80.00	3.2005	12.47	3.116
K6G5	99.960	80.00	3.2031	12.47	3.114
SELECTED	99.95	80.00			3.115
K7G1	99.953	60.68	3.2013	12.49	2.367
K7G2	99.953	60.68	3.2013	12.53	2.375
SELECTED	99.95	60.68			2.371
L1G1	105.016	60.20	4.688	16.97	2.179
L1G2	105.007	60.20	4.685	16.94	2.176
L1G3	105.004	60.20	4.684	16.94	2.177
SELECTED	105.01	60.20			2.177
L2G1	105.000	40.41	4.682	19.61	1.692
L2G2	105.002	40.41	4.683	19.61	1.692
L2G3	105.001	40.41	4.683	19.47	1.680
SELECTED	105.00	40.41			1.686
L3G1	105.019	20.26	4.689	29.44	1.272
L3G2	105.006	20.26	4.684	29.41	1.272
L3G3	105.010	20.26	4.686	29.30	1.266
SELECTED	105.01	20.26			1.269

(continued)

Table 18. Experimental Values of Equilibrium Gas Phase Compositions in the Argon-Hydrogen System (continued)

Sample No.	^{o}T K	P atm	P_{01} atm	$100y_1$ mole percent	Φ
L4G1	105.005	119.80	4.684	17.76	4.542
L4G2	105.006	119.80	4.684	17.74	4.537
L4G5	104.996	119.59	4.681	18.28	4.670
L4G6	105.005	119.59	4.684	18.35	4.685
L4G7	105.007	119.59	4.685	18.31	4.674
SELECTED	105.00	119.59			4.680
L5G1	105.019	100.27	4.689	17.09	3.654
L5G2	105.020	100.27	4.689	17.09	3.654
SELECTED	105.02	100.27			3.654
L6G1	105.004	79.93	4.683	16.53	2.821
L6G2	105.007	79.93	4.684	16.53	2.820
SELECTED	105.01	79.93			2.820
M1L3A	79.051	109.86	0.34216	3.399	10.91
M1L4A	79.056	109.86	0.34242	3.422	10.98
SELECTED	79.05	109.86			10.95
M2G2A	78.987	100.0	0.33882	3.160	9.33
M2L1A	79.026	100.0	0.34085	3.200	9.39
M2L1B	79.026	100.0	0.34085	3.204	9.40
M2G3A	78.996	100.0	0.33929	3.160	9.31
M2G3B	78.996	100.0	0.33929	3.160	9.31
M2L2A	79.031	100.0	0.34112	3.184	9.33
M2L2B	79.031	100.0	0.34112	3.180	9.32
SELECTED	79.01	100.0			9.33
M3G1A	78.961	80.27	0.33748	2.694	6.41
M3L1A	78.986	80.27	0.33877	2.754	6.53
M3G2A	78.974	80.27	0.33815	2.694	6.40
M3G2B	78.974	80.27	0.33815	2.694	6.40
M3L2A	79.003	80.27	0.33966	2.714	6.41
M3L2B	79.003	80.27	0.33966	2.710	6.40
SELECTED	78.98	80.27			6.42

(continued)

Table 18. Experimental Values of Equilibrium Gas Phase Compositions in the Argon-Hydrogen System (continued)

Sample No.	T °K	P atm	P_{01} atm	$100y_1$ mole percent	Φ
M4G2A	78.967	60.00	0.33779	2.360	4.19
M4L1A	79.004	60.00	0.33971	2.380	4.20
M4L1B	79.004	60.00	0.33971	2.388	4.22
M4G3A	78.981	60.00	0.33851	2.360	4.18
M4G3B	78.981	60.00	0.33851	2.364	4.19
SELECTED	78.98	60.00			4.20
M5G2A	78.981	40.00	0.33851	2.236	2.642
M5L1A	79.015	40.00	0.34028	2.251	2.646
M5L1B	79.015	40.00	0.34028	2.253	2.648
M5G3A	78.972	40.00	0.33805	2.234	2.643
M5G3B	78.972	40.00	0.33805	2.234	2.643
SELECTED	78.98	40.00			2.645
M6G1A	78.984	20.28	0.33867	2.742	1.641
M6G2A	78.997	20.28	0.33934	2.753	1.645
M6L1A	79.030	20.28	0.34106	2.769	1.646
M6L1B	79.030	20.28	0.34106	2.781	1.653
M6G3A	79.002	20.28	0.33960	2.765	1.651
M6G3B	79.002	20.28	0.33960	2.761	1.648
SELECTED	79.00	20.28			1.647
N1G1A	73.007	110.00	0.12565	1.870	16.37
N1L1A	73.040	110.00	0.12640	1.866	16.24
N1L1B	73.040	110.00	0.12640	1.870	16.27
N1G2A	72.992	110.00	0.12531	1.874	16.45
N1G2B	72.992	110.00	0.12531	1.870	16.42
SELECTED	73.02	110.00			16.35
N2L3A	73.073	90.14	0.12715	1.565	11.10
N2L4B	73.082	90.14	0.12735	1.560	11.04
N2G6A	73.086	90.14	0.12744	1.571	11.11
N2G6B	73.086	90.14	0.12744	1.575	11.14
SELECTED	73.08	90.14			11.06

(continued)

Table 18. Experimental Values of Equilibrium Gas Phase Compositions in the Argon-Hydrogen System (continued)

Sample No.	T °K	P atm	P_{01} atm	$100y_1$ mole percent	Φ
N3G1A	73.034	70.61	0.12625	1.290	7.21
N3L1A	73.058	70.61	0.12680	1.316	7.33
N3G2A	73.034	70.61	0.12626	1.284	7.18
N3G2B	73.034	70.61	0.12626	1.282	7.17
N3L2A	73.062	70.61	0.12689	1.290	7.18
SELECTED	73.04	70.61			7.20
N4G1A	73.021	50.34	0.12596	1.077	4.30
N4L1A	73.057	50.34	0.12678	1.083	4.30
N4L1B	73.057	50.34	0.12678	1.081	4.29
N4G2A	73.038	50.34	0.12635	1.077	4.29
N4G2B	73.038	50.34	0.12635	1.077	4.29
SELECTED	73.04	50.34			4.29
N5G1A	73.057	30.25	0.12678	1.017	2.426
N5L1A	73.077	30.25	0.12724	1.021	2.427
N5L1B	73.077	30.25	0.12724	1.021	2.427
N5G2A	73.054	30.25	0.12671	1.019	2.432
N5G2B	73.054	30.25	0.12671	1.021	2.437
SELECTED	73.06	30.25			2.43
N6G1A	73.058	20.25	0.12680	1.140	1.820
N6L1A	73.065	20.25	0.12696	1.145	1.826
N6L1B	73.065	20.25	0.12696	1.145	1.826
N6G2A	73.052	20.25	0.12666	1.138	1.819
N6G2B	73.052	20.25	0.12666	1.139	1.820
SELECTED	73.06	20.25			1.823
O1G5A	68.034	110.34	0.048107	1.094	25.09
O1L2A	68.048	110.34	0.048247	1.094	25.02
O1G6A	68.033	110.34	0.048097	1.098	25.19
O1L3A	68.067	110.34	0.048437	1.105	25.17
O1L3B	68.067	110.34	0.048437	1.105	25.17
O1G7A	68.048	110.34	0.048247	1.105	25.27
O1G7B	68.048	110.34	0.048247	1.105	25.27
SELECTED	68.05	110.34			25.20

(continued)

Table 18. Experimental Values of Equilibrium Gas Phase Compositions in the Argon-Hydrogen System (concluded)

Sample No.	T °K	P atm	P_{01} atm	$100y_1$ mole percent	Φ
02L3A	68.073	90.54	0.04849	0.906	16.91
02G4A	68.057	90.54	0.048337	0.903	16.91
02G4B	68.057	90.54	0.048337	0.905	16.95
02L4A	68.084	90.54	0.04860	0.903	16.82
02L4B	68.084	90.54	0.04860	0.904	16.84
SELECTED	68.07	90.54			16.87
03G1A	68.004	69.59	0.047808	0.691	10.06
03G2A	67.998	69.59	0.047749	0.691	10.07
03L1A	68.023	69.59	0.047997	0.700	10.15
03G3A	68.004	69.59	0.047808	0.690	10.04
03L2A	68.024	69.59	0.048007	0.695	10.07
03L2B	68.024	69.59	0.048007	0.696	10.09
03G4A	67.998	69.59	0.047749	0.693	10.10
03G4B	67.998	69.59	0.047749	0.693	10.10
SELECTED	68.01	69.59			10.10
04G1A	68.034	50.41	0.048107	0.539	5.65
04L1A	68.062	50.41	0.048387	0.542	5.65
04G2A	68.036	50.41	0.048127	0.538	5.64
04G2B	68.036	50.41	0.048127	0.542	5.68
04L2A	68.062	50.41	0.048387	0.542	5.65
04L2B	68.062	50.41	0.048387	0.544	5.67
SELECTED	68.05	50.41			5.66
05G2A	68.031	29.92	0.048077	0.460	2.862
05L1A	68.068	29.92	0.04844	0.467	2.884
05G3A	68.044	29.92	0.048207	0.461	2.861
05L2A	68.067	29.92	0.048437	0.458	2.829
05L2B	68.067	29.92	0.048437	0.458	2.829
05G4A	68.044	29.92	0.048207	0.459	2.848
05G4B	68.044	29.92	0.048207	0.461	2.861
SELECTED	68.05	29.92			2.85
06L1A	68.007	20.05	0.047838	0.485	2.032
06G2A	67.971	20.05	0.047481	0.481	2.031
06G3A	67.994	20.05	0.047709	0.481	2.021
06G3B	67.994	20.05	0.047709	0.482	2.025
06L2A	68.023	20.05	0.047997	0.485	2.026
SELECTED	68.00	20.05			2.025

Table 19. Experimental Values of Equilibrium Liquid Phase Compositions in the Argon-Hydrogen System

Sample No.	^{o}T K	P atm	$P-p_{01}$ atm	$100x_2$ mole percent	$\bar{K}.10^{-2}$ $(P-p_{01}/x_2)$
I1L1A	86.952	60.07	59.10	6.36	9.29
I1L1B	86.952	60.07	59.10	6.36	9.29
I1L1C	86.952	60.07	59.10	6.35	9.31
SELECTED	86.95	60.07	59.10	6.36	9.29
I3L1A	86.948	100.27	99.30	10.23	9.71
I3L1B	86.948	100.27	99.30	10.25	9.69
I3L1C	86.948	100.27	99.30	10.24	9.70
SELECTED	86.95	100.27	99.30	10.24	9.70
I4L1A	86.946	80.00	79.03	8.47	9.33
I4L1B	86.946	80.00	79.03	8.48	9.32
I4L1C	86.946	80.00	79.03	8.47	9.33
SELECTED	86.95	80.00	79.03	8.47	9.33
I5L1A	86.945	40.34	39.37	4.32	9.12
I5L1B	86.945	40.34	39.37	4.32	9.12
I5L1C	86.945	40.34	39.37	4.32	9.12
SELECTED	86.94	40.34	39.37	4.32	9.12
I6L1A	86.944	19.99	19.02	2.143	8.88
I6L1B	86.944	19.99	19.02	2.143	8.88
I6L1C	86.944	19.99	19.02	2.143	8.88
SELECTED	86.94	19.99	19.02	2.143	8.88
J1L1A	94.206	120.34	118.36	14.58	8.12
J1L1B	94.206	120.34	118.36	14.58	8.12
SELECTED	94.21	120.34	118.36	14.58	8.12
J2L1A	94.198	100.34	98.37	12.05	8.16
J2L1B	94.198	100.34	98.37	12.08	8.14
J2L1C	94.198	100.34	98.37	12.08	8.14
SELECTED	94.20	100.34	98.37	12.07	8.15

(continued)

Table 19. Experimental Values of Equilibrium Liquid Phase Compositions in the Argon-Hydrogen System (continued)

Sample No.	^{o}T K	P atm	$P-p_{01}$ atm	$100x_2$ mole percent	$\bar{K}.10^{-2}$ $(P-p_{01}/x_2)$
J3L1A	94.211	80.00	78.02	9.62	8.11
J3L1B	94.211	80.00	78.02	9.62	8.11
J3L1C	94.211	80.00	78.02	9.62	8.11
SELECTED	94.21	80.00	78.02	9.62	8.11
J4L1A	94.211	60.00	58.02	7.20	8.06
J4L1B	94.211	60.00	58.02	7.20	8.06
J4L1C	94.211	60.00	58.02	7.20	8.06
SELECTED	94.21	60.00	58.02	7.20	8.06
J5L1A	94.211	39.80	37.82	4.71	8.03
J5L1B	94.211	39.80	37.82	4.71	8.03
J5L1C	94.211	39.80	37.82	4.71	8.03
SELECTED	94.21	39.80	37.82	4.71	8.03
J6L1A	94.196	20.13	18.16	2.303	7.88
J6L1B	94.196	20.13	18.16	2.300	7.90
J6L1C	94.196	20.13	18.16	2.300	7.90
SELECTED	94.20	20.13	18.16	2.301	7.89
K2L1A	99.951	40.00	36.79	5.06	7.27
K2L1B	99.951	40.00	36.79	5.06	7.27
K2L1C	99.951	40.00	36.79	5.06	7.27
SELECTED	99.95	40.00	36.79	5.06	7.27
K3L1A	99.968	20.02	16.81	2.310	7.28
K3L1B	99.968	20.02	16.81	2.313	7.27
K3L1C	99.968	20.02	16.81	2.310	7.28
SELECTED	99.97	20.02	16.81	2.311	7.28
K4L1A	99.945	119.73	116.53	16.49	7.07
K4L1B	99.945	119.73	116.53	16.40	7.10
K4L1C	99.945	119.73	116.53	16.44	7.09
SELECTED	99.94	119.73	116.53	16.44	7.09

(continued)

Table 19. Experimental Values of Equilibrium Liquid Phase Compositions in the Argon-Hydrogen System (continued)

Sample No.	^{o}T K	P atm	$P-p_{01}$ atm	$100x_2$ mole percent	$\bar{K}.10^{-2}$ $(P-p_{01}/x_2)$
K5L1A	99.945	100.34	97.14	13.53	7.18
K5L1B	99.945	100.34	97.14	13.50	7.20
K5L1C	99.945	100.34	97.14	13.50	7.20
SELECTED	99.94	100.34	97.14	13.51	7.19
K6L1A	99.965	80.00	76.79	10.59	7.25
K6L1B	99.965	80.00	76.79	10.58	7.26
K6L1C	99.965	80.00	76.79	10.57	7.27
SELECTED	99.96	80.00	76.79	10.58	7.26
K7L1A	99.945	60.68	57.48	7.89	7.28
K7L1B	99.945	60.68	57.48	7.89	7.28
K7L1C	99.945	60.68	57.48	7.89	7.28
SELECTED	99.94	60.68	57.48	7.89	7.28
L1L1A	105.007	60.20	55.51	8.29	6.70
L1L1B	105.007	60.20	55.51	8.25	6.73
L1L1C	105.007	60.20	55.51	8.27	6.71
SELECTED	105.01	60.20	55.51	8.27	6.71
L2L1A	105.001	40.41	35.72	5.28	6.77
L2L1B	105.001	40.41	35.72	5.29	6.75
L2L1C	105.001	40.41	35.72	5.29	6.75
SELECTED	105.00	40.41	35.72	5.29	6.75
L3L1A	105.013	20.26	15.57	2.297	6.78
L3L1B	105.013	20.26	15.57	2.289	6.80
L3L1C	105.013	20.26	15.57	2.292	6.79
SELECTED	105.01	20.26	15.57	2.292	6.80
L4L1A	105.008	119.59	114.90	18.04	6.37
L4L1B	105.008	119.59	114.90	17.97	6.39
L4L1C	105.008	119.59	114.90	18.02	6.38
SELECTED	105.01	119.59	114.90	18.01	6.38

(continued)

Table 19. Experimental Values of Equilibrium Liquid Phase Compositions in the Argon-Hydrogen System (concluded)

Sample No.	^{o}T K	P atm	$P-p_{01}$ atm	$100x_2$ mole percent	$\bar{K}.10^{-2}$ $(P-p_{01}/x_2)$
L5L1A	105.021	100.27	95.58	14.73	6.49
L5L1B	105.021	100.27	95.58	14.71	6.50
L5L1C	105.021	100.27	95.58	14.75	6.48
SELECTED	105.02	100.27	95.58	14.73	6.49
L6L1A	105.011	79.93	75.24	11.38	6.61
L6L1B	105.011	79.93	75.24	11.38	6.61
L6L1C	105.011	79.93	75.24	11.38	6.61
SELECTED	105.01	79.93	75.24	11.38	6.61

APPENDIX D

EXPERIMENTAL VAPOR PRESSURE OF ARGON

At the conclusion of all other phase equilibrium measurements, a number of vapor pressure determinations were made for pure argon. These measurements tend to lend confidence to the measurement of temperature, the measurement of pressure, and the purity of the argon. The results of the measurements are given in Table 20 compared with the vapor pressures calculated from Equation (V-3). At the lower pressures the vapor pressures were measured on both the 0-3000 psig and on the 0-600 psig Ashcroft gauges. The agreement between the two gauges and with the equation of Michels et al.,[55] while not extremely good, was within the accuracy claimed for the temperature and pressure measurements in this work, namely ± 0.03° K and one half per cent of the reported pressure.

Table 20. Experimental Vapor Pressure of Argon

Temperature °K	Observed Vapor Pressure		Deviation from Eq.(V-3),OBS-CALC	
	High Pressure Gauge atm	Low Pressure Gauge atm	High Pressure Gauge atm	Low Pressure Gauge atm
147.45	42.64	-	0.28	-
144.98	38.80	-	0.37	-
140.03	31.69	31.41	0.33	0.05
135.05	25.50	25.19	0.24	-0.07
130.04	20.46	20.18	0.42	0.14
125.19	16.17	15.89	0.39	0.11
120.11	12.40	12.17	0.34	0 11

APPENDIX E

COMPUTATION OF PHASE EQUILIBRIA FROM THE BWR EQUATION OF STATE

A method of predicting phase equilibria in binary systems such as encountered here in the argon-hydrogen system is described for the BWR equation of state. The relations required in the calculation, in addition to those given in Chapter IV, are given below. The K factor of component i is given by

$$K_i = \left[\bar{f}_i^L(\rho_m^L, x_i)/x_i\right] / \left[\bar{f}_i^G(\rho_m^G, y_i)/y_i\right] = y_i/x_i \qquad \text{(E-1)}$$

In searching for values of density which are solutions of the BWR equation of state, the following relations obtained from Equation (IV-46) are utilized to determine the maximum, the minimum, and points of inflection of the equation.

$$\left(\frac{\partial P}{\partial \rho_m}\right)_{T,n} = RT[1 + 2B_m\rho_m + 3(b_m - a_m/RT)\rho_m^2] + 6a_m\alpha_m\rho_m^5 + \frac{c_m\rho_m^2}{T^2}[3 + 3\gamma_m\rho_m^2 - 2\gamma_m^2\rho_m^4]\exp(-\gamma_m\rho_m^2) \qquad \text{(E-2)}$$

$$\left(\frac{\partial^2 P}{\partial \rho_m^2}\right)_{T,n} = RT[2B_m - 6(b_m - a_m/RT)\rho_m] + 30a_m\alpha_m\rho_m^4 + \frac{c_m\rho_m}{T^2}[4\gamma_m^3\rho_m^6 - 18\gamma_m^2\rho_m^4 + 6\gamma_m\rho_m^2 + 6] \times \left[\exp(-\gamma_m\rho_m^2)\right] \qquad \text{(E-3)}$$

The partial molal volume of component i is calculated from the relation

$$\bar{V}_i = \left[\left(\frac{\partial P}{\partial n_i}\right)_{\rho_m,T,n_j} \right] \Big/ \left[\rho_m^{\,2} \left(\frac{\partial P}{\partial \rho_m}\right)_{P,T,n} \right] \qquad \text{(E-4)}$$

where

$$\begin{aligned}\left(\frac{\partial P}{\partial n_i}\right)_{T,\rho_m,n_j} &= RT\rho_m[1 + 2(x_i B_{ii} + x_j B_{ij})\rho_m + 3(b_m^{2/3} b_i^{1/3} \\ &\quad - a_m^{2/3} a_i^{1/3}/RT)\rho_m^{\,2}] + 3\,(a_m \alpha_m^{2/3} \alpha_i^{1/3} \\ &\quad + \alpha_m a_m^{2/3} a_i^{1/3})\rho_m^{\,6} + \rho_m^{\,3}\,[3c_m^{2/3} c_i^{1/3}(1 + \gamma_m \rho_m^{\,2}) \\ &\quad - 2c_m \gamma_m \gamma_m^{1/2} \gamma_i^{1/2} \rho_m^{\,4}] \exp\,(-\gamma_m \rho_m^{\,2}) \qquad \text{(E-5)}\end{aligned}$$

Values of the activity coefficient of component 1 and 2 in the liquid phase are calculated from the relations

$$\gamma_1' = \bar{f}_1^L\,(T,\rho_m^L,x_1)/x_1\;\bar{f}_1^L\,(T,\rho_1^L,x_1 = 1) \qquad \text{(E-6)}$$

$$\gamma_2' = \bar{f}_2^L\,(T,\rho_m^L,x_2)/x_2\;\bar{f}_2^L\,(T,\rho_1^L,x_2 = 0) \qquad \text{(E-7)}$$

The activity coefficient of component 1 is referred to pure component 1 at the system temperature and pressure, whereas the activity coefficient of component 2 is referred to the infinitely dilute state at the system temperature and pressure.

In describing the method of computation, reference is made to Figure 30 which shows two typical P versus ρ curves of the BWR equation of state, one curve below the critical temperature and the other above the critical temperature. If curve II were for a pure component, the solution for the vapor pressure at T would lie somewhere along the curve between P_{min} and P_{max}, e.g., P. The corresponding values of the

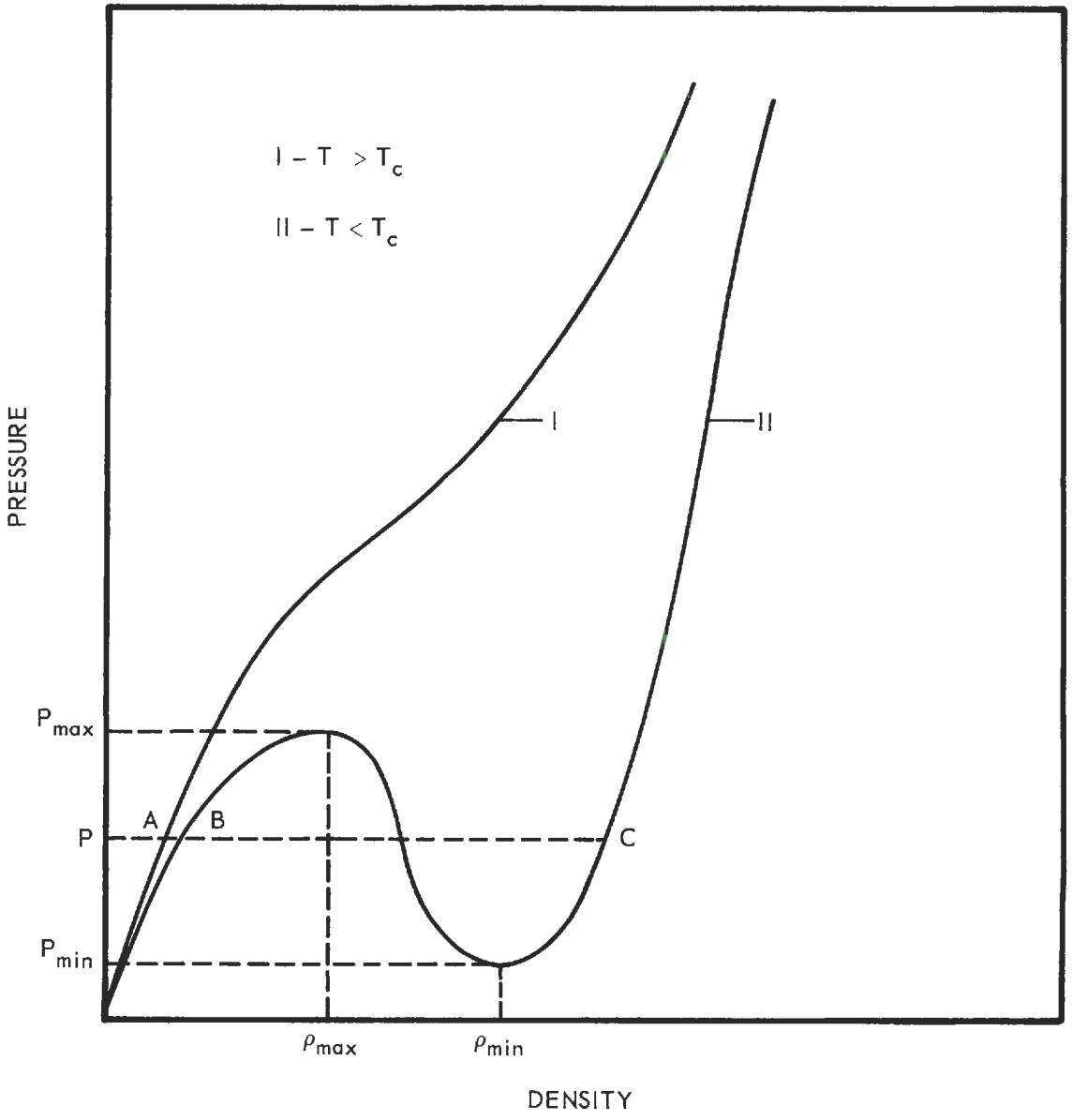

Figure 30. Typical Isotherms for BWR Equation of State of Constant Compositions Above and Below the Critical Temperature.

gas and liquid density in equilibrium, are at points B and C. This is not true if the curve represents a line of constant composition, unless it happens to be an azeotrope. It is convenient to characterize a curve by the values of P_{max}, P_{min}, ρ_{max}, ρ_{min} and the slope of the curve at its point of inflection. If the temperature is above the critical temperature, the slope at the inflection point is positive and there is no maximum or minimum. In systems such as the argon-hydrogen system, a trace of the liquid composition is of the kind represented by II whereas the gas phase in equilibrium may be of the type I, and the equilibrium values corresponding to P might be given by A and C.

A brief flow chart illustrating the method of computation is given in Figure 31. This does not accurately describe the actual program, which had a great deal more flexibility and therefore was considerably more complex. The flow chart is given to illustrate a relatively simple approach to the problem which will guarantee convergence if there is a solution of the three non-linear equations required to predict phase equilibria from the BWR equation along an isotherm. The calculations of the vapor pressure of pure component 1 and the corresponding values of ρ_1^L, ρ_1^G, f_1^L, and f_1^G were accomplished in a subprogram. This involved first finding solutions of the BWR equations of state for values of ρ_1^L and ρ_1^G and then calculation of f_1^L and f_1^G from these values for two initial values of the vapor pressure, $p_{01}^{(0)}$ and $p_{01}^{(1)} = 1.02\ p_{01}^{(0)}$. Further trial values of p_{01} were found by Aitken's method of polynomial interpolation.[57] The method was used to interpolate or extrapolate to

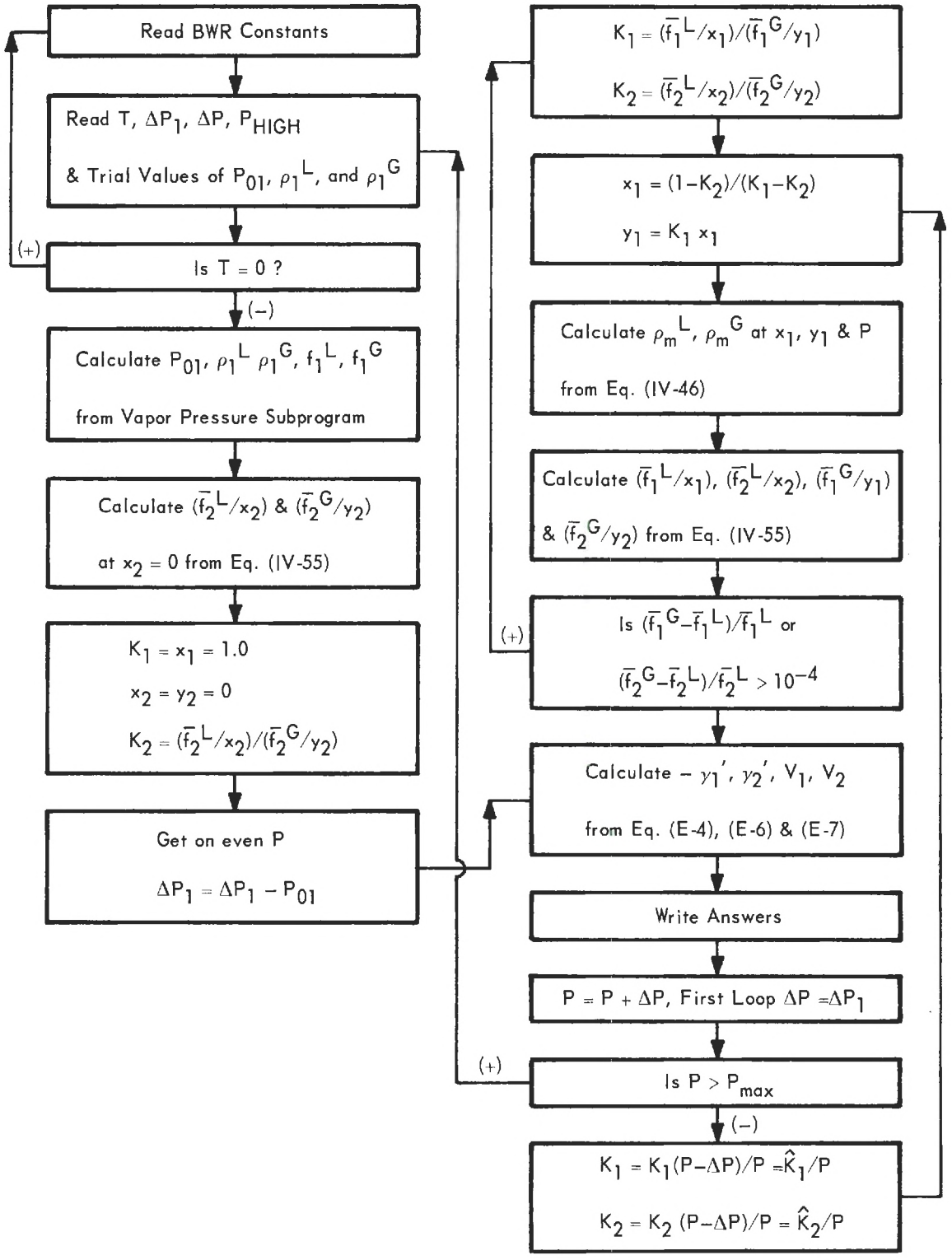

Figure 31. Schematic Diagram of a Method for Computing Phase Equilibria in Binary Systems from the BWR Equation of State.

obtain the n^{th} value of p_{01} corresponding to a fugacity error, $f_1^G - f_1^L$, of zero from the n-1 previous trials. The iteration is continued until $f_1^G - f_1^L / f_1^L \leq 10^{-4}$. If the BWR equation was originally fit to vapor pressure data, no convergence difficulties should occur at this point. One necessary condition, however, is that there exists solutions of ρ_1^G and ρ_1^L for each trial value of the vapor pressure. This is insured by requiring that each trial value of vapor pressure be between P_{max} and P_{min}.

After completing the solution of the vapor pressure and the corresponding values of ρ_1^G, ρ_1^L, f_1^L and f_1^G, the partial molal quantities of component two are calculated at infinite dilution. The value of $\overline{V}_2^{-\infty}$, $\overline{f}_2^G/y_2$ and $\overline{f}_2^L/x_2$ are calculated directly from Equations (E-4) and (IV-55) using the calculated values of density ρ_1^G and ρ_1^L. The computation of the first equilibrium mixture is then begun after stepping the pressure to the next desired even value above p_{01}. At this point it is necessary to have a good trial value for the liquid and gas composition in order to achieve convergence. This is done by assuming that the Henry's law constant defined by Equation (F-26) does not vary between P and P + ΔP. Convergence can be assured by making ΔP sufficiently small.

$$\hat{K}_i = P \, (\overline{f}_i^L/x_i)/(\overline{f}_i^G/y_i) \tag{E-8}$$

$$K_i = \frac{\hat{K}_i}{P} \tag{E-9}$$

From these initial values of K_1 and K_2, values of x_1 and y_1 are calculated. Referring now to Figure 30, the value of ρ_m^G corresponding to

a curve of type II would be found and also values of $\bar{f}_1^L/x_1$ and $\bar{f}_2^L/x_2$. From these fugacity coefficients new K values are calculated and the iteration continued until $(\bar{f}_i^G-\bar{f}_i^L)/\bar{f}_i^L < 10^{-4}$ for both components.

APPENDIX F

THERMODYNAMIC RELATIONS INVOLVING HENRY'S LAW CONSTANTS

A useful parameter for describing the composition of the liquid phase in systems such as the two bin ry systems studied in this work, i.e., where

$$T > T_{c2} \qquad (F\text{-}1)$$

$$T < T_{c1}$$

is the Henry's law constant. A common definition of Henry's law constant at constant temperature is given by Equation (F-2).

$$H = \bar{f}_2^G / x_2 \qquad (F\text{-}2)$$

The value of the constant at infinite dilution is given by Equation (F-3).

$$H^o = \lim_{x_2 \to 0} \frac{\bar{f}_2^G}{x_2} \qquad (F\text{-}3)$$

Thus, H is a function of temperature, pressure and composition, whereas H^o is a function of temperature, pressure and the properties of the pure solvent.

The activity coefficient, γ_i' for a non-ideal solution is normally defined by Equation (F-4) with an additional statement about the

limiting condition.*

$$\mu_i^L = \mu_i^* (P,T) + RT \ln x_i \gamma_i' \qquad \text{(F-4)}$$

For the type of system considered here, it is customary to refer the chemical potential of component 1 to pure component 1 under its vapor pressure, p_{01}. Thus, as $x_1 \rightarrow 1$, $\gamma_1' \rightarrow 1$, and

$$\mu_1^L = \mu_1^* (p_{01},T) \qquad \text{(F-5)}$$

This is not a satisfactory standard state for component 2 since it does not exist as a pure liquid at this temperature. For this reason the standard state for component 2 is usually referred to infinite dilution. As $x_2 \rightarrow 0$, $P \rightarrow p_{02}$ and $\gamma_2' \rightarrow 1$. Thus, $\mu_2^* (p_{02},T)$ corresponds to the extrapolated value of μ_2 on a line from infinite dilution at $\gamma_2' = 1$ over to $x_2 = 1$.

The fugacity of component 2 in the gas phase is defined by Equations (F-6) and (F-7).

$$\mu_2^G = \mu_2^o(T) + RT \ln \frac{\bar{f}_2^G}{f_2^o} \qquad \text{(F-6)}$$

$$\lim_{P \rightarrow 0} \frac{\bar{f}_2^G}{p_2} = 1 \qquad \text{(F-7)}$$

$\mu_2^o(T)$ is the value of μ_2^G when the fugacity of the gas is f_2^o, an arbitrary standard fugacity taken as the ideal gas at one atmosphere.

---

* A number of the relations used in this Appendix are given by Denbigh.[22]

At equilibrium

$$\mu_2^G = \mu_2^L \tag{F-8}$$

Substituting Equations (F-4) and (F-6) into (F-8) and rearranging, results in Equation (F-9).

$$RT \ln \frac{\bar{f}_2^G}{x_2 f_2^o} = RT \ln \gamma_2' + \mu_2^*(P,T) - \mu_2^o(T) \tag{F-9}$$

For f_2^o equal to unity this may be written as

$$\ln H = \ln \frac{\bar{f}_2^G}{x_2} = \ln \gamma_2' + [\mu_2^*(P,T) - \mu_2^o(T)]/RT \tag{F-10}$$

At infinite dilution, Equation (F-10) reduces to Equation (F-11).

$$\ln H^o = [\mu_2^*(p_{01},T) - \mu_2^o(T)]/RT \tag{F-11}$$

In order to develop the temperature and pressure dependence of H and H^o, it is necessary to develop several other relations. From the fundamental relation

$$dG = -SdT + VdP + \sum_{i=1}^{2} \mu_i dn_i \tag{F-12}$$

the pressure and temperature effects on the chemical potential are given by Equations (F-13) and (F-14).

$$\left(\frac{\partial \mu_i}{\partial P}\right)_{T,n} = \left(\frac{\partial V}{\partial n_i}\right)_{P,T,n_j} = \bar{V}_i \tag{F-13}$$

$$\left(\frac{\partial \mu_i}{\partial T}\right)_{P,n} = -\left(\frac{\partial S}{\partial n_i}\right)_{P,T,n_j} = -\bar{S}_i \tag{F-14}$$

Since

$$\bar{H}_i = \mu_i + T\bar{S}_i = \mu_i - T\left(\frac{\partial \mu_i}{\partial T}\right)_{P,n} \qquad \text{(F-15)}$$

Equation (F-14) may be rearranged to give Equation (F-16).

$$\left[\frac{\partial(\mu_i/T)}{\partial T}\right]_{P,n} = -\frac{\bar{H}_i}{T^2} \qquad \text{(F-16)}$$

Applying the results of Equation (F-16) to the standard state of component 2 at infinite dilution yields Equation (F-17).

$$\left[\frac{\partial(\mu_2^*(P,T)/T)}{\partial T}\right]_P = -\frac{\bar{H}_2^{-\infty}}{T^2} \qquad \text{(F-17)}$$

$\bar{H}_2^{-\infty}$ is the partial molal enthalpy of component 2 at infinite dilution. Similarly,

$$\left[\frac{\partial\, \mu_2^*(P,T)}{\partial P}\right]_T = \bar{V}_2^{-\infty} \qquad \text{(F-18)}$$

where $\bar{V}_2^{-\infty}$ is the partial molal volume of component 2 at infinite dilution.

Evaluation of Heats of Solution from Henry's Law Data

Equation (F-11) may be differentiated with respect to reciprocal temperature to obtain Equation (F-19).

$$\frac{d \ln H^o}{d(1/T)} = -T^2\left(\frac{\partial \ln H^o}{\partial T}\right)_P - T^2\left(\frac{\partial \ln H^o}{\partial P}\right)_T \frac{dP}{dT} \qquad \text{(F-19)}$$

Substituting the appropriate relations, Equation (F-17), (F-18) and (F-11), Equation (F-19) may be rewritten as Equation (F-20).

$$\frac{d \ln H^o}{d(1/T)} = \frac{\bar{H}_2^{-\infty} - h_2^o}{R} - \frac{\bar{V}_2^{-\infty}}{R}\frac{Tdp_{01}}{dT} \qquad \text{(F-20)}$$

In Equation (F-20) the pressure is the vapor pressure of component 1. In most cases this is small and the last term may be neglected. If this is so, experimental values of Henry's law constant at infinite dilution may be plotted against (1/T) and the value of the heat of solution of an ideal gas into an infinitely dilute solution may be calculated from the slope.

The Krichevsky-Karsanovsky Equation

Equation (F-10) and (F-11) may be combined to give

$$\ln H = \ln H^{o} + \ln \gamma_2' + \frac{\mu_2^*(P,T) - \mu_2^*(p_{01},T)}{RT} \qquad \text{(F-21)}$$

From Equations (F-18) and (F-21)

$$\ln H = \ln H^{o} + \ln \gamma_2' + \frac{1}{RT} \int_{p_{01}}^{P} \overline{V}_2^{-\infty} \, dP \qquad \text{(F-22)}$$

If the solution is ideal and $\overline{V}^{-\infty}$ is constant, Equation (F-22) reduces to the Krichevsky-Karsanovsky[47] equation.

$$\ln \frac{\overline{f}_2^{g}}{x_2} = \ln H^{o} + \frac{\overline{V}_2^{-\infty}}{RT} (P-p_{01}) \qquad \text{(F-23)}$$

Thus, if the Krichevsky-Karsanovsky equation is followed, a plot of $\ln (\overline{f}_2^{g}/x_2)$ versus $(P-p_{01})$ should be straight with the intercept equal to $\ln H^{o}$ and the slope $(\overline{V}_2^{-\infty}/RT)$.

Different Forms of Henry's Law Constant

For correlating solubility data it is quite often more convenient to define a Henry's law constant in two other different forms.

$$\overline{K} = \frac{P-p_{01}}{x_2} \qquad \text{(F-24)}$$

$$\lim_{x_2 \to 0} \bar{K} = \bar{K}^o \tag{F-25}$$

$$\hat{K} = \frac{Py_2}{x_2} \tag{F-26}$$

$$\lim_{x_2 \to 0} \hat{K} = \hat{K}^o \tag{F-27}$$

Equation (F-24) is very useful for correlating data from several sources since it requires no knowledge of the composition of the gas phase. The limiting value of Equation (F-24), Equation (F-25), is not easily related to the limiting form of Equation (F-10) given by Equation (F-11). Equation (F-26) requires a knowledge of the composition of the gas phase, but is easily converted to Equation (F-10) and (F-11). The fugacity coefficient is defined by

$$\bar{f}_i^G = x_i \, y_i \, P \tag{F-28}$$

$$\hat{K} = \frac{H}{x_2} \tag{F-29}$$

If the virial equation, Equation (IV-4), is used, x_2 is given by

$$\ln x_2 = - \ln Z_m + 2(y_2 B_{22} + y_1 B_{12})/V_m + 3[y_2^2 C_{222} + 2y_2 y_1 C_{122} + y_1^2 C_{112}]/2V_m^2 \tag{F-30}$$

At infinite dilution the value of x_2 is given by

$$\ln x_2 = - \ln Z_{01} + \frac{2 B_{12}}{V_{01}} + \frac{3}{2} \frac{C_{112}}{V_{01}^2} \tag{F-31}$$

APPENDIX G

DERIVATION OF THE VOLUME IMPLICIT RELATION FOR THE ENHANCEMENT FACTOR

Consider a binary system at a temperature, T, and pressure P, such that a gas and a condensed phase exist in equilibrium.

$$\mu_1^L = \mu_1^G \tag{G-1}$$

$$\mu_1^L = \mu_1^*(P,T) + RT \ln \gamma_1' x_1 \qquad \gamma_1' \to 1,\ x_1 \to 1 \tag{G-2}$$

Equation (G-2) defines the activity coefficient γ_1', based on the chemical potential of pure 1 at T and P. As $\gamma_1' \to 1$, $P \to p_{01}$ and

$$\mu_1^L = \mu_1^*(p_{01},T) \tag{G-3}$$

The effect of pressure on μ_1^* at constant temperature is given by

$$\left(\frac{\partial \mu_1^*}{\partial P}\right)_T = v_1 \tag{G-4}$$

$$\mu_1^*(P,T) = \mu_1^*(p_{01},T) + \int_{p_{01}}^{P} v_1 dP \tag{G-5}$$

The chemical potential of a pure condensed phase at saturation pressure, p_{01}, must be the same as for the pure gas at p_{01}.

$$\mu_1^*(p_{01},T) - g_1^\circ = \int_{V_{01}}^{\infty} \left[P - \frac{RT}{V}\right] dV + p_{01} V_{01} - RT \ln \frac{V_{01}}{RT} \tag{G-6}$$

Equation (G-6) may be derived from the following fundamental equation for the change in the molal free energy at constant T.

$$dg = VdP = d(PV) - PdV \tag{G-7}$$

$$\begin{aligned} g(V_{01},T)-g_1^{\circ} &= [g(V_{01},T)-g(V^{\infty},T)] + [g(V^{\infty},T)-g^{\circ}(V_{01},T)] \\ &\quad + [g^{\circ}(V_{01},T)-g^{\circ}(1\ \text{atm},T)] \\ &= \int_{\infty}^{V_{01}} d(PV)-PdV + \int_{\infty}^{V_{01}} \frac{RT}{V}\,dV + \int_{V_{01}}^{1\ \text{atm}} RT\,\frac{dV}{V} \\ &= p_{01}V_{01}-RT + \int_{V_{01}}^{\infty} (P-\frac{RT}{V})dV - RT\ \ln\frac{V_{01}}{RT} \end{aligned} \tag{G-8}$$

g_1° is the free energy of 1 mole of gas in the ideal state at one atmosphere pressure.

The chemical potential of component one in mixture may be written as

$$\begin{aligned} \mu_1^G(V_m,T) - g_1^{\circ} &= \int_{V_m}^{\infty} \left[\left(\frac{\partial P}{\partial n_1}\right)_{V,T,n_2} - \frac{RT}{V} \right] dV - RT\ \ln\frac{V_m}{RT} \\ &\quad + RT\ \ln y_1 \end{aligned} \tag{G-9}$$

Equation (G-9) may be derived from the following considerations:

$$\mu_1^G(V_m,T)-g_1^o = [\mu_1^G(V_m,T) - \mu_1^G(V^\infty,T)] + [\mu_1^G(V^\infty,T) - \mu_1^o(V_m,T)]$$
$$+ [\mu_1^o(V_m,T) - \mu_1^o(1 \text{ atm},T)] + [\mu_1^o(1 \text{ atm},T)$$
$$- g_1^o(1 \text{ atm},T)] \qquad \text{(G-10)}$$

The fundamental relation which expresses the change in chemical potential with volume at constant temperature and composition is

$$\left(\frac{\partial \mu_1^G}{\partial V}\right)_{T,n_1,n_2} = -\left(\frac{\partial P}{\partial n_1}\right)_{n_2,T,V} \qquad \text{(G-11)}$$

$$\mu_1^G(V_m,T) - g_1^o(1 \text{ atm},T) = \int_{V_m}^{\infty} \left(\frac{\partial P}{\partial n_1}\right)_{T,V,n_2} dV - \int_{V_m}^{\infty} \frac{RT}{V}\, dV$$
$$- \int_{1 \text{ atm}}^{V_m} \frac{RT}{V}\, dV + RT \ln y_1 \qquad \text{(G-12)}$$

Equation (G-9) follows directly from Equation (G-12). Combining Equations (G-1), (G-2), (G-5), (G-6) and (G-9) yields the final desired expression for the enhancement factor.

$$\ln \frac{Py_1}{p_{o1}} = Z_{o1}-1-\ln Z_{o1} + \frac{1}{RT} \int_{p_{o1}}^{P} v_1 dP + \frac{1}{RT} \int_{V_{o1}}^{\infty} [P-\frac{RT}{V_1}]dV_1$$
$$+ \ln Z_m - \frac{1}{RT} \int_{V_m}^{\infty} [(\frac{\partial P}{\partial n_1})_{V,T,n_2} - \frac{RT}{V_m}]dV_m$$
$$+ \ln \gamma_1' x_1 \qquad \text{(G-13)}$$

APPENDIX H

LEAST SQUARES SURFACE FIT USING ORTHOGONAL FUNCTIONS

Several times in the course of this investigation a method of fitting data on a thermodynamic surface was needed in order to obtain or compare values at other points on the surface. Since, in general, the data are not at evenly spaced intervals, and are not smoothed data, no simple interpolation scheme was suitable. The method used here is a modification of the method described by Bain,[1] who fitted P-V-T data for steam by a least squares approach in which the compressibility was represented by a double infinite series in density and inverse temperature.

Bain's method was slightly modified to permit a truncation of one independent variable. The method is then as follows. A set of $(M + 1)$ functions $\{\psi_k(x,y)\}$ are said to be orthogonal over a data set consisting of N data points (x_i, y_i, z_i) if the following equation is satisfied.

$$\sum_{i=1}^{N} \psi_j(x_i,y_i)\psi_k(x_i,y_i) = 0 \quad (j \neq k) \tag{H-1}$$

Given a set of functions, orthogonal with respect to a particular data set, the value of the dependent variable, z, can be represented as

$$z = \sum_{j=0}^{M} C_j \psi_j(x,y) \tag{H-2}$$

The C_j are weighting factors which are determined by the criteria used to fit z_i. In this case they were found by requiring that the sum of the squares of the residuals,

$$\sum_{i=1}^{N} R_i^2 = \sum_{i=1}^{N} \left[z_i - \sum_{j=0}^{M} C_j \psi_j (x_i, y_i) \right]^2 \qquad \text{(H-3)}$$

be minimized. Equating the partial derivatives with respect to each of the weighting factors, C_j, equal to zero, results in the following solution for each of the C_j.

$$C_j = \sum_{i=1}^{N} z_i \psi_j(x_i, y_i) \Big/ \sum_{i=1}^{N} \psi_j(x_i, y_i) \psi_j(x_i, y_i); \quad j=0,1,2,\ldots,M \qquad \text{(H-4)}$$

The set $\{\psi_j\}$ may be generated in a number of ways. One method used here is described as follows. Let p and q be the maximum powers of x and y, respectively, occurring in the set $\{\psi_j\}$. Further, let $p \geq q$. The set $\{\psi_j\}$ contains terms $x^m y^n$ such that $0 \leq m \leq p$ and $0 \leq n \leq q$. Let $\{g\}$ be a subset of $\{\psi_j\}$ such that $\{g\}$ consists of all the ψ_j's containing terms with a maximum power $(m+n)$ of g. The orthogonal functions are then generated in the following manner:

$$
\begin{aligned}
g = 0 \quad & \psi_o = 1.0 \\
g = 1 \quad & \psi_1 = x - \alpha_{0,1}\psi_o \\
& \psi_2 = y - \alpha_{0,2}\psi_o - \alpha_{1,2}\psi_1 \\
g = 2 \quad & \psi_3 = x^2 - \alpha_{0,3}\psi_o - \alpha_{1,3}\psi_1 - \alpha_{2,3}\psi_2 \\
& \psi_4 = xy - \alpha_{0,4}\psi_o - \alpha_{1,4}\psi_1 - \alpha_{2,4}\psi_2 - \alpha_{3,4}\psi_3 \\
& \psi_5 = y^2 - \alpha_{0,5}\psi_o - \alpha_{1,5}\psi_1 - \alpha_{2,5}\psi_2 - \alpha_{3,5}\psi_3 - \alpha_{4,5}\psi_4 \\
& \vdots \\
g = q \quad & \psi_r = x^q - \alpha_{0,r}\psi_o - \cdots \alpha_{r-1,r}\psi_{r-1}; \; r = g(g+1)/2 \\
& \psi_{r+1} = x^{q-1}y^1 - \alpha_{0,r+1}\psi_o - \cdots \alpha_{r,r+1}\psi_r \quad 0 \leqq g \leqq q \\
& \vdots \\
& \psi_{r+g} = y^q - \alpha_{0,r+g}\psi_o - \cdots \alpha_{r+g-1,r+g}\psi_{r+g-1} \\
& \vdots \\
g > q \quad & \psi_r = x^p - \alpha_{0,r}\psi_o - \cdots \alpha_{r-1,r}\psi_{r-1}; \; r = (q+1)(2g-q)/2 \\
& \psi_{r+1} = x^{p-1}y^1 - \alpha_{0,r+1}\psi_o - \cdots \alpha_{r,r+1}\psi_r \quad q \leqq g \leqq p \\
& \vdots \\
& \psi_{r+q} = x^{p-q}y^q - \alpha_{0,r+q}\psi_o - \cdots \alpha_{r+q-1,r+q}\psi_{r+q-1}
\end{aligned}
\qquad \text{(H-5)}
$$

The orthogonal coefficients, α_{ij}, are determined from the requirement of orthogonality. The coefficients for the first group, g = 1, are given below.

$$\alpha_{0,1} = \frac{\Sigma\, x_i\, \psi_o}{\Sigma\, \psi_o\, \psi_o}$$

$$\alpha_{0,2} = \frac{\Sigma\, y_i\, \psi_o}{\Sigma\, \psi_o\, \psi_o} \qquad \alpha_{1,2} = \frac{\Sigma\, y_i \psi_1(x_i)}{\Sigma\, \psi_1(x_i)\psi_1(x_i)} \qquad \text{(H-6)}$$

The advantages of using a fitting scheme as described above are several. In general, less error due to loss of significant figures is

incurred than is normally the case for schemes which require matrix inversion. Another advantage is that the power of the fitting function can be increased without recalculating any of the previously calculated C_j and α_{ij}. One disadvantage can occur if it is necessary to convert the coefficients and weighting factors of the orthogonal functions to the coefficients of the power series. Not only can this be quite involved, but a loss of accuracy may result.

APPENDIX I

PREDICTED ENHANCEMENT FACTORS FOR ARGON-HELIUM AND ARGON-HYDROGEN

The calculated enhancement factors for the various methods of prediction discussed in Chapters V and VI are summarized in the following tables. The calculations are reported at 10 atm intervals up to 120 atm for temperatures corresponding to the experimental isotherms. The calculations for the argon-helium system are limited to the "homogeneous" methods of prediction since no Benedict-Webb-Rubin constants were available for helium. For the equations used in the calculations for each particular method the reader is referred to Table 11. Calculations were not made for all experimental isotherms for several of the "hybrid" methods of prediction. Table 21 contains the calculated enhancement factors for the argon-helium system. Table 22 contains the enhancement factors calculated for the argon-hydrogen system by the "homogeneous" methods and Table 23 the values of the enhancement factors for the argon-hydrogen system calculated by the "hybrid" methods.

Table 21. Predicted Enhancement Factors for the Argon-Helium System

P, atm	Enhancement Factor, Φ				
	PPGL	LJCL	LJ2Q	KIH	KIHA
			- - - -68.07° K- - - -		
10	1.113	1.116	1.140	1.137	1.093
20	1.231	1.238	1.291	1.283	1.187
30	1.356	1.367	1.455	1.441	1.285
40	1.488	1.504	1.632	1.611	1.386
50	1.628	1.648	1.824	1.794	1.491
60	1.776	1.800	2.029	1.990	1.599
70	1.933	1.960	2.250	2.199	1.711
80	2.098	2.128	2.486	2.423	1.827
90	2.272	2.304	2.739	2.660	1.946
100	2.455	2.488	3.008	2.913	2.068
110	2.647	2.681	3.294	3.181	2.195
120	2.849	2.883	3.598	3.465	2.325
			- - - -74.05° K- - - -		
10	1.097	1.099	1.118	1.116	1.081
20	1.192	1.197	1.240	1.234	1.158
30	1.292	1.300	1.370	1.360	1.236
40	1.397	1.407	1.508	1.493	1.317
50	1.506	1.518	1.655	1.634	1.400

(continued)

Table 21. Predicted Enhancement Factors for the Argon-Helium System (continued)

P, atm	Enhancement Factor, Φ				
	PPGL	LJCL	LJ2Q	KIH	KIHA
		- - - -74.05° K- - - -			
60	1.621	1.635	1.810	1.783	1.485
70	1.741	1.755	1.975	1.940	1.572
80	1.866	1.881	2.149	2.105	1.661
90	1.997	2.011	2.332	2.279	1.752
100	2.133	2.147	2.525	2.462	1.845
110	2.275	2.287	2.728	2.653	1.940
120	2.424	2.432	2.942	2.854	2.038
		- - - -77.90° K- - - -			
10	1.090	1.092	1.109	1.108	1.077
20	1.175	1.179	1.217	1.213	1.146
30	1.264	1.269	1.331	1.323	1.215
40	1.356	1.363	1.451	1.440	1.287
50	1.452	1.460	1.578	1.562	1.359
60	1.551	1.560	1.712	1.690	1.434
70	1.655	1.664	1.852	1.824	1.509
80	1.763	1.771	2.000	1.965	1.586
90	1.875	1.882	2.154	2.112	1.665
100	1.992	1.996	2.316	2.266	1.745
110	2.113	2.114	2.485	2.426	1.827
120	2.239	2.235	2.662	2.594	1.910

(continued)

Table 21. Predicted Enhancement Factors for the Argon-Helium System (continued)

P, atm	Enhancement Factor, Φ				
	PPGL	LJCL	LJ2Q	KIH	KIHA
			- - - -80.06° K- - - -		
10	1.088	1.090	1.105	1.105	1.076
20	1.169	1.171	1.207	1.204	1.141
30	1.252	1.256	1.314	1.307	1.207
40	1.338	1.343	1.426	1.416	1.273
50	1.427	1.434	1.544	1.530	1.342
60	1.520	1.527	1.668	1.649	1.411
70	1.617	1.623	1.797	1.773	1.481
80	1.717	1.722	1.933	1.903	1.553
90	1.821	1.824	2.075	2.038	1.626
100	1.929	1.929	2.223	2.179	1.700
110	2.041	2.037	2.378	2.326	1.776
120	2.157	2.148	2.539	2.479	1.853
			- - - -86.02° K- - - -		
10	1.091	1.091	1.104	1.105	1.082
20	1.167	1.168	1.198	1.197	1.145
30	1.246	1.247	1.297	1.293	1.208
40	1.327	1.328	1.399	1.393	1.272
50	1.411	1.412	1.507	1.497	1.337
60	1.498	1.499	1.620	1.607	1.404
70	1.589	1.588	1.738	1.721	1.472

(continued)

Table 21. Predicted Enhancement Factors for the Argon-Helium System (continued)

P, atm	Enhancement Factor, Φ				
	PPGL	LJCL	LJ2Q	KIH	KIHA
			- - - -86.02° K- - - -		
80	1.684	1.680	1.862	1.840	1.541
90	1.782	1.775	1.991	1.965	1.611
100	1.885	1.873	2.126	2.094	1.684
110	1.991	1.974	2.268	2.230	1.757
120	2.102	2.078	2.416	2.371	1.832
			- - - -91.98° K- - - -		
10	1.092	1.091	1.100	1.102	1.085
20	1.162	1.161	1.186	1.186	1.144
30	1.232	1.232	1.274	1.272	1.201
40	1.305	1.304	1.364	1.360	1.258
50	1.379	1.377	1.458	1.452	1.316
60	1.457	1.452	1.556	1.547	1.375
70	1.537	1.530	1.659	1.647	1.435
80	1.620	1.609	1.765	1.750	1.496
90	1.706	1.691	1.876	1.857	1.558
100	1.796	1.775	1.991	1.968	1.621
110	1.889	1.861	2.111	2.084	1.685
120	1.985	1.950	2.236	2.204	1.750

(continued)

Table 21. Predicted Enhancement Factors for the Argon-Helium System (continued)

P, atm	Enhancement Factor, Φ				
	PPGL	LJCL	LJ2Q	KIH	KIHA
		- - - -97.51° K- - - -			
10	1.091	1.089	1.096	1.098	1.087
20	1.161	1.159	1.180	1.181	1.147
30	1.228	1.225	1.261	1.261	1.201
40	1.295	1.291	1.344	1.342	1.255
50	1.364	1.358	1.430	1.426	1.309
60	1.435	1.427	1.518	1.513	1.363
70	1.508	1.497	1.610	1.603	1.418
80	1.584	1.569	1.706	1.696	1.473
90	1.663	1.642	1.805	1.792	1.530
100	1.744	1.717	1.908	1.892	1.587
110	1.829	1.794	2.015	1.995	1.645
120	1.917	1.873	2.126	2.103	1.704
		- - - -108.02° K- - - -			
10	1.069	1.068	1.069	1.071	1.068
20	1.159	1.155	1.167	1.170	1.151
30	1.228	1.223	1.248	1.250	1.210
40	1.293	1.286	1.326	1.327	1.263
50	1.358	1.348	1.404	1.405	1.315
60	1.423	1.411	1.484	1.484	1.366

(continued)

Table 21. Predicted Enhancement Factors for the Argon-Helium System (concluded)

P, atm	Enhancement Factor, Φ				
	PPGL	LJCL	LJ2Q	KIH	KIHA
			- - - -108.02° K- - - -		
70	1.491	1.474	1.567	1.565	1.416
80	1.561	1.538	1.652	1.648	1.467
90	1.633	1.603	1.740	1.735	1.518
100	1.708	1.669	1.831	1.824	1.570
110	1.785	1.737	1.926	1.917	1.622
120	1.866	1.806	2.024	2.013	1.675

Table 22. Predicted Enhancement Factors for the Argon-Hydrogen System. Homogeneous Methods.

P, atm	Enhancement Factor, Φ				
	BWR	PPGL	LJCL	LJ3Q	KIH
			- - - -68.04° K- - - -		
10	1.385	1.399	1.394	1.419	1.407
20	1.930	1.971	1.966	2.038	2.001
30	2.696	2.789	2.802	2.962	2.872
40	3.755	3.957	4.033	4.353	4.156
50	5.181	5.606	5.849	6.458	6.054
60	7.043	7.904	8.534	9.665	8.865
70	9.397	11.056	12.516	14.612	13.054
80	12.281	15.317	18.495	22.499	19.416
90	15.715	21.021	27.824	36.421	29.625
100	19.705	28.652	44.387	-*	49.755
110	24.240	39.037	-*	-	-*
120	29.301	53.956	-	-	-
			- - - -73.05° K- - - -		
10	1.315	1.326	1.323	1.343	1.334
20	1.734	1.763	1.760	1.818	1.788
30	2.287	2.350	2.356	2.476	2.411
40	3.009	3.134	3.170	3.394	3.264

(continued)

Table 22. Predicted Enhancement Factors for the Argon-Hydrogen System. Homogeneous Methods. (continued)

P, atm	Enhancement Factor, Φ				
	BWR	PPGL	LJCL	LJ3Q	KIH
			- - - -73.05° K- - - -		
50	3.933	4.173	4.280	4.678	4.435
60	5.092	5.542	5.799	6.485	6.047
70	6.515	7.329	7.884	9.059	8.283
80	8.222	9.647	10.779	12.826	11.440
90	10.230	12.645	14.906	18.720	16.081
100	12.549	16.538	21.198	-*	23.737
110	15.181	21.673	-*	-	-*
120	18.128	28.739	-	-	-
			- - - -79.01° K- - - -		
10	1.258	1.264	1.262	1.278	1.272
20	1.582	1.600	1.599	1.644	1.623
30	1.989	2.028	2.033	2.122	2.077
40	2.497	2.569	2.591	2.751	2.666
50	3.122	3.252	3.311	3.579	3.431
60	3.880	4.112	4.243	4.683	4.433
70	4.788	5.192	5.459	6.175	5.759
80	5.859	6.546	7.066	8.255	7.554
90	7.107	8.251	9.257	11.376	10.106

(continued)

Table 22. Predicted Enhancement Factors for the Argon-Hydrogen System. Homogeneous Methods. (continued)

P, atm	Enhancement Factor, Φ				
	BWR	PPGL	LJCL	LJ3Q	KIH
			- - - -79.01° K- - - -		
100	8.543	10.417	12.453	-	14.255
110	10.176	13.231	-	-	-
120	12.016	17.073	-	-	-
			- - - -86.95° K- - - -		
10	1.199	1.199	1.198	1.210	1.206
20	1.436	1.443	1.444	1.476	1.463
30	1.720	1.735	1.741	1.804	1.776
40	2.057	2.086	2.104	2.211	2.162
50	2.454	2.507	2.548	2.720	2.638
60	2.918	3.011	3.093	3.362	3.231
70	3.455	3.614	3.768	4.187	3.980
80	4.072	4.338	4.619	5.284	4.954
90	4.774	5.209	5.722	6.856	6.288
100	5.565	6.267	7.249	-*	8.424
110	6.451	7.571	-*	-	-*
120	7.434	9.233	-	-	-

(continued)

Table 22. Predicted Enhancement Factors for the Argon-Hydrogen System. Homogeneous Methods. (continued)

P, atm	Enhancement Factor, Φ				
	BWR	PPGL	LJCL	LJ3Q	KIH
			- - - -94.21° K- - - -		
10	1.160	1.158	1.157	1.165	1.164
20	1.354	1.355	1.356	1.380	1.372
30	1.577	1.581	1.587	1.634	1.617
40	1.834	1.843	1.860	1.939	1.908
50	2.129	2.147	2.183	2.308	2.256
60	2.466	2.500	2.567	2.759	2.679
70	2.846	2.910	3.030	3.322	3.199
80	3.275	3.387	3.597	4.052	3.859
90	3.753	3.944	4.312	5.079	4.753
100	4.283	4.597	5.275	-*	-*
110	4.866	5.374	-*	-	-
120	5.503	6.318	-	-	-
			- - - -99.95° K- - - -		
10	1.129	1.128	1.127	1.132	1.132
20	1.302	1.300	1.301	1.319	1.315
30	1.493	1.492	1.498	1.535	1.523
40	1.708	1.709	1.724	1.787	1.766
50	1.951	1.956	1.988	2.087	2.052

(continued)

Table 22. Predicted Enhancement Factors for the Argon-Hydrogen System. Homogeneous Methods. (continued)

P, atm	Enhancement Factor, Φ				
	BWR	PPGL	LJCL	LJ3Q	KIH
			- - - -99.95° K- - - -		
60	2.223	2.237	2.296	2.448	2.392
70	2.527	2.558	2.660	2.892	2.807
80	2.863	2.924	3.100	3.463	3.331
90	3.232	3.345	3.650	4.281	4.049
100	3.635	3.830	4.393	-*	-*
110	4.069	4.397	-*	-	-
120	4.534	5.074	-	-	-
			- - - -105.01° K- - - -		
10	1.098	1.098	1.097	1.100	1.101
20	1.259	1.258	1.258	1.272	1.270
30	1.430	1.429	1.433	1.462	1.455
40	1.618	1.618	1.630	1.682	1.667
50	1.827	1.830	1.856	1.939	1.914
60	2.058	2.069	2.117	2.245	2.206
70	2.313	2.339	2.424	2.620	2.559
80	2.590	2.645	2.792	3.105	3.006
90	2.891	2.993	3.251	-*	-*
100	3.212	3.394	-*	-	-

Table 22. Predicted Enhancement Factors for the Argon-Hydrogen System. Homogeneous Methods. (concluded)

P, atm	Enhancement Factor, Φ				
	BWR	PPGL	LJCL	LJ3Q	KIH
			- - - -105.01° K- - - -		
110	3.552	3.863	-	-	-
120	3.906	4.432	-	-	-

*At this pressure the solution of the appropriate enhancement factor or equation of state failed to converge.

Table 23. Predicted Enhancement Factors for the Argon-Hydrogen System. Hybrid Methods

P, atm	Enhancement Factor, Φ								
	B1	B3	B4	B5	H1	H2	H3	H5	H6
				- - - -68.04° K- - - -					
10	1.399		1.416	1.405	1.400	1.399	1.405		1.416
20	1.971	-	2.021	1.984	1.974	1.971	1.984	-	2.021
30	2.782	-	2.891	2.805	2.791	2.782	2.805	-	2.891
40	3.911	-	4.122	3.947	3.937	3.912	3.947	-	4.123
50	5.443	-	5.819	5.494	5.503	5.445	5.496	-	5.821
60	7.457	-	8.087	7.530	7.583	7.463	7.537	-	8.095
70	10.018	-	11.019	10.128	10.261	10.038	10.147	-	11.042
80	13.173	-	14.689	13.344	13.608	13.222	13.392	-	14.747
90	16.947	-	19.148	17.223	17.683	17.055	17.326	-	19.276
100	21.346	-	24.421	21.787	22.534	21.558	21.992	-	24.679
110	26.357	-	30.511	27.045	28.200	26.741	27.423	-	30.989
120	31.954	-	37.400	32.994	34.715	32.603	33.642	-	38.226
				- - - -73.05° K- - - -					
10	1.326	-	1.341	1.332	-	-	1.332	-	1.341
20	1.763	-	1.807	1.778	-	-	1.778	-	1.807
30	2.344	-	2.435	2.372	-	-	2.372	-	2.435
40	3.105	-	3.271	3.152	-	-	3.152	-	3.272
50	4.084	-	4.365	4.156	-	-	4.157	-	4.366

(continued)

Table 23. Predicted Enhancement Factors for the Argon-Hydrogen System. Hybrid Methods (continued)

P, atm	Enhancement Factor, Φ								
	B1	B3	B4	B5	H1	H2	H3	H5	H6
				- - - -73.05° K- - - -					
60	5.315	-	5.764	5.424	-	-	5.427	-	5.768
70	6.830	-	7.516	6.991	-	-	7.000	-	7.525
80	8.652	-	9.659	8.889	-	-	8.909	-	9.685
90	10.799	-	12.228	11.143	-	-	11.187	-	12.282
100	13.280	-	15.246	13.774	-	-	13.862	-	15.356
110	16.096	-	18.728	16.795	-	-	16.960	-	18.936
120	19.243	-	22.678	20.215	-	-	20.504	-	23.047
				- - - -79.01° K- - - -					
10	1.263	-	1.277	1.270	1.266	1.263	1.270	-	1.277
20	1.599	-	1.636	1.615	1.604	1.599	1.615	-	1.636
30	2.022	-	2.095	2.051	2.032	2.022	2.051	-	2.095
40	2.549	-	2.677	2.597	2.571	2.549	2.597	-	2.677
50	3.197	-	3.404	3.272	3.241	3.198	3.272	-	3.405
60	3.984	-	4.302	4.095	4.064	3.985	4.097	-	4.303
70	4.924	-	5.393	5.086	5.063	4.927	5.090	-	5.398
80	6.030	-	6.702	6.262	6.259	6.039	6.271	-	6.714
90	7.314	-	8.250	7.640	7.677	7.335	7.662	-	8.276

(continued)

Table 23. Predicted Enhamcement Factors for the Argon-Hydrogen System. Hybrid Methods (continued)

P, atm	Enhancement Factor, Φ								
	B1	B3	B4	B5	H1	H2	H3	H5	H6
				- - - -79.01° K- - - -					
100	8.786	-	10.057	9.238	9.344	8.826	9.281	-	10.110
110	10.450	-	12.140	11.069	11.289	10.525	11.151	-	12.242
120	12.310	-	14.512	13.148	13.547	12.442	13.295	-	14.699
				- - - -86.95° K- - - -					
10	1.198	-	1.208	1.204	1.203	1.198	1.204	-	1.208
20	1.441	-	1.468	1.455	1.448	1.441	1.455	-	1.468
30	1.729	-	1.783	1.756	1.743	1.729	1.756	-	1.783
40	2.072	-	2.162	2.115	2.095	2.072	2.115	-	2.162
50	2.473	-	2.613	2.538	2.513	2.473	2.538	-	2.614
60	2.940	-	3.147	3.034	3.006	2.941	3.035	-	3.148
70	3.477	-	3.772	3.610	3.583	3.479	3.612	-	3.774
80	4.089	-	4.497	4.272	4.253	4.093	4.277	-	4.502
90	4.779	-	5.330	5.028	5.026	4.788	5.038	-	5.342
100	5.549	-	6.279	5.882	5.913	5.567	5.902	-	6.302
110	6.401	-	7.349	6.841	6.928	6.433	6.878	-	7.394
120	7.334	-	8.545	7.907	8.087	7.390	7.974	-	8.628
				- - - -94.21° K- - - -					
10	1.156	1.154	1.162	1.161	-	-	1.161	1.154	1.162
20	1.351	1.347	1.371	1.363	-	-	1.363	1.347	1.371

(continued)

Table 23. Predicted Enhancement Factors for the Argon-Hydrogen System. Hybrid Methods. (continued)

P, atm	Enhancement Factor, Φ								
	B1	B3	B4	B5	H1	H2	H3	H5	H6
				- - - -94.21° K- - - -					
30	1.574	1.569	1.614	1.597	-	-	1.597	1.569	1.614
40	1.830	1.822	1.896	1.866	-	-	1.866	1.822	1.896
50	2.121	2.109	2.223	2.176	-	-	2.176	2.110	2.223
60	2.450	2.434	2.599	2.529	-	-	2.529	2.434	2.599
70	2.819	2.797	3.027	2.928	-	-	2.929	2.798	3.028
80	3.230	3.198	3.511	3.377	-	-	3.380	3.201	3.514
90	3.682	3.639	4.055	3.878	-	-	3.884	3.644	4.062
100	4.176	4.119	4.661	4.432	-	-	4.444	4.128	4.675
110	4.711	4.635	5.330	5.040	-	-	5.062	4.652	5.356
120	5.283	5.184	6.061	5.702	-	-	5.741	5.213	6.107
				- - - -99.95° K- - - -					
10	1.124	-	1.127	1.127	-	-	1.127	-	1.127
20	1.294	-	1.308	1.304	-	-	1.304	-	1.308
30	1.482	-	1.513	1.502	-	-	1.502	-	1.513
40	1.693	-	1.745	1.724	-	-	1.724	-	1.745
50	1.928	-	2.008	1.975	-	-	1.975	-	2.008
60	2.189	-	2.304	2.256	-	-	2.256	-	2.304
70	2.476	-	2.636	2.568	-	-	2.569	-	2.637
80	2.789	-	3.004	2.912	-	-	2.914	-	3.006

(continued)

Table 23. Predicted Enhancement Factors for the Argon-Hydrogen System. Hybrid Methods. (concluded)

P, atm	Enhancement Factor, Φ								
	B1	B3	B4	B5	H1	H2	H3	H5	H6
	- - - -99.95° K- - - -								
90	3.128	-	3.410	3.289	-	-	3.294	-	3.415
100	3.491	-	3.853	3.699	-	-	3.708	-	3.863
110	3.875	-	4.331	4.139	-	-	4.155	-	4.350
120	4.277	-	4.842	4.607	-	-	4.634	-	4.875
	- - - -105.01° K- - - -								
10	1.092	-	1.093	1.094	1.098	1.092	1.094	-	1.093
20	1.249	-	1.258	1.256	1.260	1.249	1.256	-	1.258
30	1.414	-	1.437	1.430	1.432	1.414	1.430	-	1.437
40	1.596	-	1.636	1.622	1.622	1.596	1.622	-	1.636
50	1.795	-	1.858	1.835	1.833	1.795	1.835	-	1.858
60	2.012	-	2.104	2.070	2.067	2.013	2.070	-	2.104
70	2.248	-	2.375	2.326	2.326	2.248	2.327	-	2.376
80	2.500	-	2.671	2.605	2.609	2.502	2.607	-	2.673
90	2.768	-	2.991	2.905	2.918	2.771	2.909	-	2.995
100	3.049	-	3.333	3.224	3.251	3.055	3.231	-	3.341
110	3.341	-	3.695	3.558	3.606	3.351	3.571	-	3.709
120	3.637	-	4.070	3.905	3.982	3.654	3.926	-	4.095

BIBLIOGRAPHY

1. Bain, R. W., "Preparation of Steam Tables with the Aid of a Digital Computer," Journal Mechanical Engineering Science 3, 289-294 (1961).

2. Baly, E.C.C. and Donnan, F. G., "The Variation with Temperature of the Surface Energies and Densities of Liquid Oxygen, Nitrogen, Argon, and Carbon Monoxide," Journal of the Chemical Society (London) 81, 907-923 (1902).

3. Beattie, J. A. and Bridgeman, O. C., "A New Equation of State for Fluids," Proceedings of the American Academy of Arts and Sciences 63, 230-308 (1928).

4. Beattie, J. A. and Stockmayer, W. H., "The Thermodynamics and Statistical Mechanics of Real Gases," A Treatise on Physical Chemistry, Vol. 2, States of Matter, 3rd ed. by H. S. Taylor and Glasstone, New York: D. Van Nostrand Co., 1951, Chapter II, pages 187-352.

5. Bell, G. M., "General Discussion," Discussions of the Faraday Society 15, 290 (1953).

6. Benedict, M., Webb, George B., and Rubin, Louis C., "An Empirical Equation for Thermodynamic Properties of Light Hydrocarbons and Their Mixtures. I. Methane, Ethane, Propane, and n-Butane," Journal of Chemical Physics 8, 334-45 (1940).

7. Benedict, M., Webb, G. B., and Rubin, L. C., "An Empirical Equation for Thermodynamic Properties of Light Hydrocarbons and Their Mixtures. II. Mixtures of Methane, Ethane, Propane, and n-Butane," Journal of Chemical Physics 10, 747-758 (1942).

8. Benedict, M., Webb, G. B., and Rubin, L. C., "An Empirical Equation for Thermodynamic Properties of Light Hydrocarbons and Their Mixtures. Constants for Twelve Hydrocarbons," Chemical Engineering Progress 47, 419-422 (1951).

9. Benedict, M., Webb, G. B., and Rubin, L. C., "An Empirical Equation for Thermodynamic Properties of Light Hydrocarbons and Their Mixtures. Fugacities and Liquid-Vapor Equilibria," Chemical Engineering Progress 47, 449-54 (1951).

10. Bridgman, P. W., "The Melting Parameters of Nitrogen and Argon under Pressure, and the Nature of the Melting Curve," Physical Review 46, 930-933 (1934).

11. Buzyna, G., Macriss, R. A., and Ellington, R. T., "Vapor-Liquid Equilibrium in the Helium-Nitrogen System," Chemical Engineering Progress Symposium Series No. 44, 101-111 (1963).

12. Canfield, F. B., Leland, T. W., and Kobayashi, R., "Volumetric Behavior of Gas Mixtures at Low Temperatures by the Burnett Method: The Helium-Nitrogen System, 0° to -140° C," Advances in Cryogenic Engineering, Vol. 8, ed. by K. D. Timmerhaus, New York: Plenum Press, 1962, pages 146-157.

13. Cath, P. G. and Onnes, H. K., "Sur la mesure des temperatures tres basses. XXX. Comparaison des thermometres a helium, a argon, a neon, a oxygene et a azote au thermometre a hydrogene. Corrections pour ramener les indications de ces thermometres a l' echelle internationale Kelvin. Le deuxieme coefficient du viriel pour l' helium, l' argon, le neon, l' oxygene et l'azote au-dessous de 0° C," Communications from the Physical Laboratory of the University of Leiden No. 156a, 1-32.

14. Clusius, K., "Atomwarmen und Schmelzwarmen von Neon, Argon, und Krypton," Zeitschrift fur physikalische Chemie B31, 459-474 (1936).

15. Clusius, K. and Weigand, K., "The Melting Curves of the Gases A, Kr, CH_4, CH_3D, CD_4, C_2H_4, C_2H_6, COS and PH_3 to 200 Atm. Pressure," Zeitschrift fur physikalische Chemie B46, 1-37 (1940).

16. Connolly, J. F. and Kandalic, G. A., The Physics of Fluids 3, 463-467 (1960); Document No. 6307, Documentation Institute, Library of Congress, Washington, D. C.

17. Curl, R. F., Jr., and Pitzer, K. S., "Volumetric and Thermodynamic Properties of Fluids-Enthalpy, Free Energy, and Entropy," Industrial and Engineering Chemistry 50, 265-274 (1958).

18. Danon, F. and Pitzer, K. S., "Corresponding States Theory for Argon and Xenon," Journal of Physical Chemistry 66, 583-85 (1962).

19. Danon, F. and Pitzer, Kenneth S., "Volumetric and Thermodynamic Properties of Fluids. VI. Relationship of Molecular Properties to the Acentric Factor," Journal of Chemical Physics 36, 425-430 (1962).

20. De Boer, J. and Michels, A., "Contribution to the Quantum-Mechanical Theory of the Equation of State and the Law of Corresponding States. Determination of the Law of Force of Helium," Physica 5, 945-957 (1938).

21. De Boer, J. and Michels, A., "Quantum-Mechanical Calculation of the Second Virial-Coefficient of Helium at Low Temperatures," Physica 6, 409-420 (1939).

22. Denbigh, Kenneth, The Principles of Chemical Equilibrium, London: Cambridge University Press, 1957, 491 pages.

23. De Smedt, J. and Keesom, W. H., "The Crystal Structure of Argon. Researches on the Structure of Nitrogen and Oxygen at the Temperature of Liquid Hydrogen," Communication from the Physical Laboratory of the University of Leiden No. 178b, 19-21.

24. Dobbs, E. R., Figgins, B. F., Jones, G. O., Piercey, D. C., and Riley, D. P., "Density and Expansivity of Solid Argon," Nature 178, 483 (1956).

25. Dokoupil, Z., Van Soest, G., and Swenker, M.D.P., "On the Equilibrium Between the Solid Phase and the Gas Phase of the Systems Hydrogen-Nitrogen, Hydrogen-Carbon Monoxide, and Hydrogen-Nitrogen-Carbon Monoxide," Applied Scientific Research A5, 182-240 (1955). See also, Communications from the Physical Laboratory of the University of Leiden, No. 297 (1955).

26. Eubanks, L. S., Ph.D. Thesis, Rice Institute, Houston, Texas (May, 1957).

27. Faddeeva, V. N., Computational Methods of Linear Algebra, Translated by C. Benster, New York: Dover Publications, Inc., 1959, 252 pages.

28. Fender, B.E.F. and Halsey, G. D., Jr., "Second Virial Coefficients of Argon, Krypton, and Argon-Krypton Mixtures at Low Temperatures," The Journal of Chemical Physics 36, 1881-1888 (1962).

29. Flubacher, P., Leadbetter, A. J., and Morrison, J. A., "A Low Temperature Adiabatic Calorimeter for Condensed Substances. Thermodynamic Properties of Argon," Proceedings of the Physical Society (London) 78, 1449-1461 (1961).

30. Goodwin, Robert D., "Apparatus for Determination of Pressure-Density-Temperature Relations and Specific Heats of Hydrogen to 350 Atmospheres at Temperatures above 14° K," Journal of Research of the National Bureau of Standards 65C, 231-43 (1961).

31. Goodwin, Robert D., Diller, Dwain E., Roder, Hans M., and Weber, Lloyd A., "Pressure-Density-Temperature Relations of Fluid Para Hydrogen from 15 to 100° K at Pressures to 350 Atmospheres," Journal of Research of the National Bureau of Standards 67A, 173-192 (1963).

32. Gunn, R. D., Volumetric Properties of Non-Polar Gaseous Mixtures, MS Thesis, University of California, Berkeley, California, 1958.

33. Henshaw, D. G., "Atomic Distribution in Liquid and Solid Neon and Solid Argon by Neutron Diffraction," Physical Review 111, 1470-1475 (1958).

34. Hirschfelder, J. O., Curtiss, C. F., and Bird, R. B., Molecular Theory of Gases and Liquids, New York: John Wiley and Sons, 1954, 1219 pages.

35. Hiza, M. J. and Herring, R. N., "Solid-Vapor Equilibrium in the System Hydrogen-Methane," Advances in Cryogenic Engineering Vol. 10, ed. by K. D. Timmerhaus, New York: Plenum Press, 1965, (Accepted for Publication).

36. Karasz, Frank E., The Solubility of Helium and Neon in Liquid Argon, Ph.D. Thesis, University of Washington, 1958, 72 pages.

37. Karasz, F. E. and Halsey, G. D., Jr., "Solubility of Helium and Neon in Liquid Argon. An Approximation to the Entropy of Lattice Vacancy Formation in Liquid Argon," The Journal of Chemical Physics 29, 173-179 (1958).

38. Keesom, W. H., Helium, Amsterdam: Elsevier, 1942, 494 pages.

39. Kerr, E. C., Ph.D. Thesis, University of Michigan (1957).

40. Kihara, T., "Virial Coefficients and Models of Molecules in Gases," Reviews of Modern Physics 25, 831-43 (1953).

41. Kihara, T., "Virial Coefficients and Models of Molecules in Gases. B.," Reviews of Modern Physics 27, 412-423 (1955).

42. Kirk, B. S., Predicted and Experimental Gas Phase Compositions in Pressurized Binary Systems Containing an Essentially Pure Condensed Phase. Phase Equilibrium Data for the Methane-Hydrogen System from 66.88° to 116.53° K and up to 125 Atmospheres, Ph.D. Thesis, Georgia Institute of Technology, Atlanta, Georgia 1964, 265 pages.

43. Kirk, B. S. and Ziegler, W. T., "A Phase Equilibrium Apparatus for Gas-Liquid Systems and the Gas Phase of Gas-Solid Systems. Application to Methane-Hydrogen from 66.88° to 116.53° K and up to 125 Atmospheres," Advances in Cryogenic Engineering, Vol. 10, ed. by K. D. Timmerhaus, New York: Plenum Press, 1965, (Accepted for Publication).

44. Kirk, B. S., Ziegler, W. T. and Mullins, J. C., "A Comparison of Methods of Predicting Equilibrium Gas Phase Compositions in Pressurized Binary Systems Containing an Essentially Pure Condensed Phase," Advances in Cryogenic Engineering Vol. 6, ed. by K. D. Timmerhaus, New York: Plenum Press, 1961, pages 413-427.

45. Knaap, H.F.P., Knoester, M., Knobler, C. M., and Beenakker, J.J.M., "The Second Virial Coefficients of the Hydrogen Isotopes Between 20 and 70° K," Physica 28, 21-32 (1962).

46. Knobler, C. M., Beenakker, J.J.M., and Knaap, H.F.P., "The Second Virial Coefficient of Gaseous Mixtures at 90° K," Physica 25, 909-916 (1959).

47. Krichevsky, I. R. and Kasarnovsky, J. S., "Thermodynamical Calculations of Solubilities of Nitrogen and Hydrogen in Water at High Pressures," Journal of the American Chemical Society 57, 2168-2171 (1935).

48. Levelt, J.M.H., "The Reduced Equation of State, Internal Energy and Entropy of Argon and Xenon," Physica 26, 361-377 (1960).

49. Low Temperature Heavy Water Plant, Final Report to the U.S.A.E.C. by Hydrocarbon Research, Inc., Contract No. AT(30-1)810 NYO-889, March 16, 1951, pages 90-104.

50. Mathias, E., Onnes, H. K.,and Crommelin, C. A., "On the Rectilinear Diameter for Argon," Communications from the Physical Laboratory of the University of Leiden No. 131a, 1-14.

51. McCain, W. D., Jr., Vapor-Liquid Phase Equilibria of the Binary System Argon-Helium, Ph.D. Thesis, Georgia Institute of Technology, Atlanta, Georgia, 1964, 127 pages.

52. Michels, A., De Graaff, W., and Ten Seldam, C. A., "Virial Coefficients of Hydrogen and Deuterium at Temperatures Between -175° and +150° C. Conclusions from the Second Virial Coefficient with Regards to the Intermolecular Potential," Physica 26, 393-408.(1960)

53. Michels, A., De Graaff, W., Wassenaar, T., Levelt, J.M.H., and Louwerse, P., "Compressibility Isotherms of Hydrogen and Deuterium at Temperatures Between -175° C and +150° C at Densities up to 960 Amagat," Physica 25, 25-42 (1959).

54. Michels, A., Levelt, J. M., and De Graaff, W., "Compressibility Isotherms of Argon at Temperatures Between -25° C and -155° C, and at Densities up to 640 Amagat (Pressures up to 1050 Atmospheres)," Physica 24, 659-671 (1958).

55. Michels, A., Wassenaar, T., and Zwietering, Th., "The Vapour Pressure of Argon," Physica 17, 876-884 (1951).

56. Michels, A. and Wouters, H., "Isotherms of Helium Between 0° and 150° C up to 200 Amagat," Physica 8, 923-932 (1941).

57. Milne, W. E., Numerical Calculus, Princeton: Princeton University Press, 1949, 393 pages.

58. Motard, R. L. and Organick, E. I., "Thermodynamic Behavior of Hydrogen-Hydrocarbon Mixtures," A.I.Ch.E. Journal 6, 39-43 (1960).

59. Mullins, J. C. and Ziegler, W. T., The System Helium-Argon from 65° to 140° K up to Pressures of 120 Atm. Correlation of Available Phase Equilibrium Data, Technical Report No. 3, Project A-764, Engineering Experiment Station, Georgia Institute of Technology, January 10, 1965 (Contract No. CST-1154 National Standard Reference Data Program, National Bureau of Standards, Washington, D. C.).

60. Pitzer, K. S., "The Volumetric and Thermodynamic Properties of Fluids. I. Theoretical Basis and Virial Coefficients," Journal of The American Chemical Society 77, 3427-32 (1955).

61. Pitzer, K. S. and R. F. Curl, Jr., "The Volumetric Properties of Fluids. III. Empirical Equation for the Second Virial Coefficient," Journal of the American Chemical Society 79, 2369-2370 (1957).

62. Pitzer, K. S. and Hultgren, G. O., "The Volumetric and Thermodynamic Properties of Fluids. V. Two Component Solutions," Journal of the American Chemical Society 80, 4793-4796 (1958).

63. Pitzer, Kenneth S., Lippmann, David Z., Curl, R. F., Jr., Huggins, C. M., and Petersen, D. E., "The Volumetric and Thermodynamic Properties of Fluids. II. Compressibility Factor, Vapor Pressure and Entropy of Vaporization," Journal of the American Chemical Society 77, 3433-3440 (1955).

64. Prausnitz, J. M. and Gunn, R. D., "Volumetric Properties of Nonpolar Gaseous Mixtures," A.I.Ch.E. Journal 4, 430-435 (1958).

65. Prausnitz, J. M. and Keeler, R. N., "Application of the Kihara Potential to High Pressure Phase Equilibria," A.I.Ch.E. Journal 7, 399-405 (1961).

66. Prausnitz, J. M. and Myers, A. L., "Kihara Parameters and Second Virial Coefficients for Cryogenic Fluids and Their Mixtures," A.I.Ch.E. Journal 9, 5-11 (1963).

67. Price, A. R., Leland, T. W., and Kobayashi, R., "Evaluation of Benedict-Webb-Rubin Equation for Prediction of Phase Equilibrium of Light Hydrocarbon Mixtures at Low Temperatures," Chemical Engineering Progress Symposium Series 55, No. 21, 13-20 (1959).

68. Prigogine, I. and Defay, R., Chemical Thermodynamics, Translated and Revised in conjunction with authors by D. H. Everett, London: Longmans Green and Co., 1954, page 357.

69. Reuss, J. and Beenakker, J.J.M., "Determination of the Second Virial Coefficient B_{12} of Gas Mixtures," Physica 22, 869 (1956). See also, Communications from the Physical Laboratory of the University of Leiden, Supplement No. 110e, 1956.

70. Rodewald, N. C., Davis, J. A., and Kurata, F., "The Heterogeneous Phase Behavior of the Helium-Nitrogen System," A.I.Ch.E. Journal (Accepted for Publication).

71. Rowlinson, J. S., Sumner, F. H., and Sutton, J. R., "The Virial Coefficients of a Gas Mixture," Transactions of the Faraday Society 50, 1-8 (1954).

72. Schiller, F. C. and Canjar, L. N., "An Equation of State for Carbon Monoxide Vapor-Liquid Equilibria for N_2-CO system," Chemical Engineering Progress Symposium Series 49, No. 7, 67-72 (1953).

73. Simon, Franz, Ruhemann, Martin, and Edwards, W.A.M., "Die Schmelzkurven von Wasserstoff, Neon, Stickstoff und Argon," Zeitschrift fur physikalische Chemie B6, 331-342 (1929).

74. Simon, Franz and von Simson, Clara, "Die Kristallstruktur des Argons," Zeitschrift fur Physik 25, 160-164 (1924).

75. Stotler, H. H. and Benedict, M., "Correlation of Nitrogen-Methane Vapor-Liquid Equilibria by Equation of State," Chemical Engineering Progress Symposium Series 49, No. 6, 25-36 (1953).

76. Van Itterbeek, A. and Verbeke, O., "Density of Liquid Nitrogen and Argon as a Function of Pressure and Temperature," Physica 26, 931-938 (1960).

77. Van Itterbeek, A., Verbeke, O., and Staes, K., "Measurements on the Equation of State of Liquid Argon and Methane up to 300 kg cm^{-2} at Low Temperatures," Physica 29, 742-754 (1963).

78. Volk, H. and Halsey, G. D., Jr., "Solubility of Hydrogen and Deuterium in Liquid Argon," The Journal of Chemical Physics 33, 1132-39 (1960).

79. Whalley, E. and Schneider, W. G., "Intermolecular Potentials of Argon, Krypton, and Xenon," The Journal of Chemical Physics 23, 1644-1650 (1955).

80. White, D. and Johnston, H. L., The Thermodynamic Properties of Gaseous Hydrogen from Experimental Data of State, Tech. Report No. 26, Project RF-264, Cryogenic Laboratory, Department of Chemistry, The Ohio State University, Columbus, Ohio, November, 1953, (ASTIA AD No. 27-622) page 2. See also, Friedman, A. S., "Pressure-Volume-Temperature Relationships of Gases. Virial Coefficients," American Institute of Physics Handbook, Ed. by D. E. Gray, New York: McGraw Hill Book Co., 1957, Section 4i, Table 4i-8.

81. White, David, Rubin, Thor, Camky, Paul, and Johnston, H. L., "The Virial Coefficients of Helium from 20 to 300° K," Journal of Physical Chemistry 64, 1607-12 (1960).

82. Wilson, G. M., Silverberg, P. M., and Zellner, M. G., "Argon-Oxygen-Nitrogen Three Component System Experimental Vapor-Liquid Equilibrium Data," Advances in Cryogenic Engineering, Vol. 10, ed. by K. D. Timmerhaus, New York: Plenum Press, 1965, (Accepted for Publication).

83. Woolley, H. W., Scott, R. B., and F. G. Brickwedde, "Compilation of Thermal Properties of Hydrogen in its Various Isotopic and Ortho-Para Modifications," Journal of Research National Bureau of Standards 41, 379-475 (1948).

84. Ziegler, W. T., Mullins, J. C., and Kirk, B. S., Calculation of the Vapor Pressure and Heats of Vaporization and Sublimation of Liquids and Solids, Especially Below One Atmosphere Pressure. II Argon, Tech. Report No. 2, Project A-460, Engineering Experiment Station, Georgia Institute of Technology, June 15, 1962 (Contract No. CST-7238, National Bureau of Standards, Boulder, Colorado).

VITA

Joseph Chester Mullins was born December 5, 1931, in Thomaston, Georgia, to Ethel MacFarlin and Spencer Grady Mullins, Sr. He was reared in Thomaston where he attended the public schools. For the first two years of high school he attended Gordon Military College in Barnesville, Georgia and then received his high school diploma from R. E. Lee High School, in Thomaston, Georgia, in June, 1949. He attended Emory at Oxford Junior College in Covington, Georgia, for one year, prior to entering Georgia Institute of Technology in September, 1950. During his first year he worked while a student for the then Tennessee Products Chemical Corporation in Chattanooga, Tennessee and at the end of his first year at Georgia Tech received a four year scholarship in the Naval Reserve Officer Training Program. He elected to remain at Georgia Tech and received the degree Bachelor of Science in Chemical Engineering in June, 1955.

From June, 1955, to September, 1958, he served in the Supply Corps of the United States Navy as Supply Officer aboard the U.S.S. Guadalupe (AO-32) and as an assistant to the Supply Officer, U.S. Naval Air Station, Atlantic City, New Jersey.

He returned to Georgia Tech in September, 1958, and began work at the Engineering Experiment Station in November of that year. He received the degree Master of Science in Chemical Engineering in 1960. In July, 1964, he was promoted to Assistant Research Engineer.

Since January, 1965, to the present, he has been employed as an Assistant Professor of Chemical Engineering at Clemson University, Clemson, South Carolina.

He is married to the former Diane Victoria Hudson and has one son, Joseph Grady, and one daughter, Jessica Claire.